UNCLASSIFIED

SECURITY CLASSIFICATION OF THIS PAGE (When Data Entered)

AD-A210 731

REPORT DOCUMENTATION PAGE

READ INSTRUCTIONS BEFORE COMPLETING FORM

1. REPORT NUMBER: ARO 23120.3-MA	2. GOVT ACCESSION NO.: NA
3. RECIPIENT'S CATALOG NUMBER: NA	
4. TITLE (and Subtitle): NUMERICAL ANALYSIS OF A CLASS OF PROBLEMS IN THE MATHEMATICAL THEORY OF PLASTICITY AND DAMAGE	5. TYPE OF REPORT & PERIOD COVERED: FINAL REPORT April 15, '86 -April 14,'89
	6. PERFORMING ORG. REPORT NUMBER
7. AUTHOR(s): J. Tinsley Oden	8. CONTRACT OR GRANT NUMBER(s): DAAL03-86-K-0043
9. PERFORMING ORGANIZATION NAME AND ADDRESS: Texas Institute for Computational Mechanics, The University of Texas at Austin, Asutin, TX 78712-1085	10. PROGRAM ELEMENT, PROJECT, TASK AREA & WORK UNIT NUMBERS: NA
11. CONTROLLING OFFICE NAME AND ADDRESS: U. S. Army Research Office, P. O. Box 12211, Research Triangle Park, NC 27709-2211	12. REPORT DATE: June 14, 1989
	13. NUMBER OF PAGES
14. MONITORING AGENCY NAME & ADDRESS(if different from Controlling Office)	15. SECURITY CLASS. (of this report): UNCLASSIFIED
	15a. DECLASSIFICATION/DOWNGRADING SCHEDULE

16. DISTRIBUTION STATEMENT (of this Report)

Approved for public release; distribution unlimited.

17. DISTRIBUTION STATEMENT (of the abstract entered in Block 20, if different from Report)

NA

18. SUPPLEMENTARY NOTES

The view, opinions and/or findings contained in this report are those of the author(s) and should not be construed as an official Department of the Army position, policy, or decision, unless so designated by other documentation.

19. KEY WORDS (Continue on reverse side if necessary and identify by block number)

Plasticity
Damage

20. ABSTRACT (Continue on reverse side if necessary and identify by block number)

A fairly detailed study of many existing theories of damage was conducted. One conclusion, perhaps not surprising, is that there is poor agreement among researchers in this field as to what constitutes a physically correct measure of damage in both brittle and ductile materials. For anisotropic damage, scalar-, vector-, and tensor-valued damage variables have been proposed for materials that undergo elastic and elastoplastic deformation. Numerous deficiencies and inconsistencies, both physical and mathematical, exist

DD FORM 1 JAN 73 1473 EDITION OF 1 NOV 65 IS OBSOLETE 10 UNCLASSIFIED

SECURITY CLASSIFICATION OF THIS PAGE (When Data Entered)

20. ABSTRACT CONTINUED

in some of the more publicized theories. In general, the field is still quite immature and the general acceptance of basic principles and definition of terms have neither the experimental support nor the consensus of workers in the field to form the nucleus of a general mathematical theory.

The field of isotropic damage is in somewhat better shape. In the present study, a critical look at the subject was conducted and several new results were produced. In addition to providing arguments that some prevailing theories are based on mathematically-unsound assumptions, a consistent theory for isotropic damage was identified which with proper choices of parameters, could be used to produce results consistent with experimental data. An interesting and possibly new result of this study was the establishment of actual bounds on the moduli and Poisson's ration for damaged isotropic elastic solid.

In addition, existence and uniqueness theorems were proven for model boundary-value problems in isotropic damage theoery. These results were obtained using rather standard techniques. To extend them to more general theories of damage and plasticity appears to be far outside the reach of existing mathematical theories.

A second part of the study focused on developing numerical models of damage in elastic- and plastic materials and in developing test codes for numerical experimentation. In this phase of the work, finite element models of damage in two-dimensional structures were developed and several test problems were solved. The most challenging feature of this portion of the effort was the development of robust numerical schemes for integrating the evolution equations of damage and rate-dependency plasticity. Briefly, a new robust implicit scheme was developed which proved to be very effective in treating cyclic problems in damage simulations. Studies on error estimation and stability or these schemes for nonlinear problems remains a topic for future work.

NUMERICAL ANALYSIS OF A CLASS OF PROBLEMS IN THE MATHEMATICAL THEORY OF PLASTICITY AND DAMAGE

J. Tinsley Oden

Final Report

Contract (Research Agreement)
DAAL03-86-K-0043
Army Research Office

Texas Institute for Computational Mechanics
The University of Texas at Austin

June 14, 1989

TABLE OF CONTENTS

FOREWORD

This document is the Final Report on research on "The Numerical Analysis of a Class of Problems in the Mathematical Theory of Plasticity and Damage." The report summarizes work done on Contract DAAL03-86-K-0043 between the Army Research Office, Research Triangle Park, N.C. and The University of Texas at Austin. Principal Investigator of the work was Professor J. Tinsley Oden, Director of the Texas Institute for Computational Mechanics. This report provides 1) a list of publications and presentations that resulted from the work, 2) a list of students and faculty supported for varying periods of time by contract funds, and 3) chapters summarizing major theoretical and numerical results obtained during the course of the study.

1

SUMMARY OF WORK AND RESULTS

1 Scope and General Results of the Project

The success of the mathematical sciences in providing good and realistic models of material behavior has led to great expectations in the engineering community. Today, some theories of elasticity and plasticity have reached a level of maturity that admits the construction of a sound and rich mathematical basis and these theories, supported and confirmed by physical experiments, in turn form a basis for the numerical analysis of many problems of practical importance. Other theories of material behavior of more recent origin aim at characterizing more subtle or more complex mechanical phenomena and,while they are designed with the hope of modeling many fundamental aspects of material response, they are often founded on shaky mathematical assumptions which block further development and implementation.

Among theories of material behavior that fall into this class are the theories of damage that grew out of the work of Kachanov in the 1950's and which have fueled a growing percentage of the engineering literature on solid mechanics since the mid 1970's. Damage theory purports to model the evolution of damage of a material body subjected to forces up to the initiation of macro cracks and thus to provide models of materials just prior to crack initiation and fracture. There does not exist a uniformly accepted definition of damage in the literature (with the possible exception of isotropic damage) and, with the exception of results developed in the present study, no rigorous mathematical theory of damage appears to exist.

One characteristic of many damage theories is the inclusion of an evolution equation for the growth of damage in a material. This feature establishes a formal similarity of damage theory to modern theories of viscoplasticity and rate-dependent plasticity, even

though the physical mechanisms responsible for damage and plasticity are quite different. From the viewpoint of numerical analysis, many numerical techniques effective in integrating the ordinary differential equations of viscoplasticity are equally effective when applied to those of damage theory. Also, as was shown in this study, techniques can be developed which are applicable to problems of combined viscoplastic deformation and damage. One result of numerical experiments done in this study was the discovery that many (virtually all) numerical techniques proposed in the literature for handling cyclic viscoplasticity and damage are unstable or only marginally stable, and special steps must be taken to produce reliable numerical simulations.

It was these issues in mind that the present investigation was initiated. The major goals were:

1. the study and formulation of a physically sound and mathematically consistent theory of damage, and, in particular, to explore and develop the qualitative mathematical theory, and

2. the numerical analysis of the evolution equations of damage and rate-dependent plasticity.

Some new developments in each of these areas were contributed in the project.

2 General Results

A fairly detailed study of many existing theories of damage was conducted. One conclusion, perhaps not surprising, is that there is poor agreement among reearchers in this field as to what consititutes a physically correct measure of damage in both brittle and ductile materials. For anisotropic damage, scalar-, vector-, and tensor-valued damage variables have been proposed for materials that undergo elastic and elastoplastic deformation. Numerous deficiencies and inconsistencies, both physical and mathematical, exist in some of the more publicized theories. In general, the field is still quite immature and the general acceptance

of basic principles and definitions of terms have neither the experimental support nor the consensus of workers in the field to form the nucleus of a general mathematical theory.

The field of isotropic damage is in somewhat better shape. In the present study, a critical look at the subject was conducted and several new results were produced. In addition to providing arguments that some prevailing theories are based on mathematically-unsound assumptions, a consistent theory for isotropic damage was identified which with proper choices of parameters, could be used to produce results consistent with experimental data. An interesting and possibly new result of this study was the establishment of actual bounds on the moduli and Poisson's ratio for damaged isotropic elastic solid. Some of these results are summarized in Chapter 2 of this report.

In addition, existence and uniqueness theorems were proven for model boundary-value problems in isotropic damage theory. These results were obtained using rather standard techniques. To extend them to more general theories of damage and plasticity appears to be far outside the reach of existing mathematical theories.

A second part of the study focused on developing numerical models of damage in elastic- and plastic materials and in developing test codes for numerical experimentation. In this phase of the work, finite element models of damage in two-dimensional structures were developed and several test problems were solved. The most challenging feature of this portion of the effort was the development of robust numerical schemes for integrating the evolution equations of damage and rate-dependent plasticity. A summary of the work on this subject is reproduced in Chapter 3 of this report. Briefly, a new robust implicit scheme was developed which proved to be very effective in treating cyclic problems in damage simulations. Studies on error estimation and stability of these schemes for nonlinear problems remains a topic for future work.

3 Papers and Presentations

Several reports, journal articles, and presentations resulted from work on this project. These are listed as follows:

1. "A Critique and Remarks on Damage Theory," P.J. Rabier and J.T. Oden, TICOM Report 82-10, TICOM, Austin, 1987.

2. "Some Remarks on Damage Theory," P.J. Rabier, *International Journal of Engineering Science*,Volume 27, No. 1, pp. 29-54, 1989.

3. "Numerical Solution of the Evolution Equations of Damage and Rate-Dependent Plasticity," J.M. Bass and J.T. Oden, *International Journal of Engineering Science*, Vol. 26, No. 7, pp. 713-740, 1988.

4. "A Note on the Numerical Analysis of Material Damage Based on the Theory of Materials of Type N," S.J. Kim and J.T. Oden, *Computer Methods in Mathematics with Applications*, Vol. 15, No. 3, pp. 169-174, 1988.

5. "Thermo-Viscoplastic Analysis of Hypersonic Structure Subjected to Severe Aerodynamic Heating," Presented at the 30th Structures, Structural Dynamics, and Materials Conference, by E.A. Thornton, J.T. Oden, W. Tworzydlo, and S.K. Youn, Mobile, AL, April 3-5, 1989.

4 Students and Other Personnel

The following faculty and students were supported for varying periods of time on the project:

1. Dr. J.T. Oden, Principal Investigator

2. Dr. P.J. Rabier, Visiting Professor, Mathematics, University of Pittsburgh

3. Dr. P.B. Devloo, Post-Doctoral Research Fellow

4. Dr. J.A.C. Martins, Visiting Professor, Technical University of Portugal

5. Mr. L.O. Faria, Ph.D. student

6. Dr. P. Pattani, Post-Doctoral Research Fellow

The following students received some support from the project for a short period of time: Messrs. O. Hardy and T. Westermann and Drs. W. Rachowicz, C.Y. Huang, and S.K. Youn. Mr. Hardy completed requirements for the degree of Master of Science and L.O. Faria and W. Rachowicz completed requirements for the Ph.D. degree in Engineering Mechanics during this project. While their theses were not directly related to the theme of the project, they did contribute to some aspects of the study and they benefited from short-term support from the contract.

2

SOME REMARKS ON DAMAGE THEORY

Prologue

This Chapter reproduces the studies published in reports and papers 1, 2, and 4 listed in Section 1.2 of the previous chapter. It is intended to be a critique of several mathematical aspects of damage theories proposed in contemporary solid mechanics literature.

A critical look at this literature has led us to the conclusion that to date, damage theory suffers from both the lack of uniformity in its approach and the lack of rigor in its developments. It is one of the aims of this paper to somewhat remedy the second inconvenience and to show that, in turn, rigor greatly helps selecting prevailing points of view. This programme is carried out for the broad problem of anisotropic damage, and general directions for future research in various areas are indicated. In addition, in the case of isotropic damage, we have been able to establish a model that does not exhibit the weaknesses of the usual generalization of Kachanov's theory. In particular, softening of the material is translated by the modifications of both Young's modulus and Poisson's ratio, the change in volume due to voids expansion is properly accounted for, and the need for empirically determined thresholds for failure is eliminated. The model is valid for both the quasi-static and dynamic cases, in the assumption of small elasto-plastic deformations but without restriction to small damage. For simplicity, attention is confined to isothermal processes. The model is well suited for the mathematical treatment of P.D.E.'s. The final section is indeed devoted to some theoretical existence and uniqueness results.

1 Introduction: The Origin of Damage Theory

Despite that the macroscopic notion of a damaged material is familiar to everyone's most primitive intuition, the entire process through which an originally virgin (undamaged) solid becomes damaged is far from transparent. A simple but useful step towards the description of this process consists in making explicit the common understanding of damage. Usually, damage is acknowledged by the visual observation of cracks which were not present in the virgin material. At the same time, the relative size and the number of such cracks will automatically be taken as an empirical but instructive estimate on the level of damage.

While this is just a naive statement about the final consequences of damage which does not explain at all how such cracks have been able to develop, nevertheless it stresses that the origin of damage should be traced back to properties of the virgin material that are capable of generating such cracks. The analysis of these properties is not taken up by fracture mechanics, devoted to the study of evolution of pre-existing cracks, but which does not investigate the *structural changes* occuring between the original (virgin) and final (cracked) specimens.

By simply ruling out the existence of cracks, classical theories such as elasticity or elasto-plasticity equally ignore such structural changes. The reason fracture mechanics as well as elasticity or elasto-plasticity are unable to provide the desired information is that they are all macroscopic theories whereas damage originates in microphenomena occuring at the scale of grains. These phenomena are responsible for local modifications of the elasto-plastic properties of solids, in particular elastic moduli, during loading and unloading, up to eventual failure (crack initiation). By establishing principles appropriately corroborated by experiments, damage theory, existing or to be, is intended to provide the mathematical models of this transitional state.

For the three decades since the pioneering work by Kachanov [14], the starting

point of damage theory has been experimental evidence that any parcel of material contains a multitude of defects in the form of microvoids. During a loading-unloading process, these voids may undergo irreversible growth and new ones may nucleate. The ultimate coalescence of these voids results in macro-crack initiation. With Krajcinovic [17], we note that nucleation and growth of such microvoids is a mechanism distinct from propagation of dislocations responsible for plasticity. Just as in the macroscopic case, the number and size of voids in any unstressed configuration may be taken as an indication on the current level of damage. The crucial difference is that the smaller scale now under consideration enables one to use these measurable data as parameters representing damage at any given material point. Rather unfortunately however, no decisive argument has been made yet that dictates a specific way to measure damage. One of the many problems is the vague reference to some unstressed configuration that generally does not exit. This will be clarified below and, on the basis of a short critical review, we shall see that a point of view definitely seems to prevail.

2 The Measure of Damage

In what follows, *"damaged material"* refers to a certain specimen having undergone a certain loading/unloading process during a specified period of time. By *"virgin material"*, we mean the same specimen before any such process has started.

In his original one-dimensional model, Kachanov (loc. cit.) suggests that damage should be defined as the density of microvoids in any cross section of the material. More specifically, consider a rod submitted to uniform tractions and/or compressions in the direction of its axis, so that the deformation of the rod can accurately be described by a one-dimensional model. A mathematical point $\boldsymbol{X}$ is then associated with any cross section of the rod. The relative area of the voids in the cross section at $\boldsymbol{X}$ defines a scalar variable $D(\boldsymbol{X})$ $(0 \leq D(\boldsymbol{X}) \leq 1)$ representing damage.

In the three-dimensional case, one can attempt to construct a simple generalization

of this idea as follows: let $\boldsymbol{X}$ be a point of the three-dimensional material in its current configuration and consider a small volume element ΔV about $\boldsymbol{X}$. Since the geometry of the microvoids in ΔV is altered by the elastic part of the deformation, ΔV must first be put in a stress-free configuration, which can be done by separating ΔV from the remainder of the body and freed of external forces.[1] We shall henceforth denote by $\widetilde{\Delta V}$ the unstressed configuration of ΔV, unique to within rigid motions, and assume after suitable translation that the transformation $\Delta V \to \widetilde{\Delta V}$ leaves $\boldsymbol{X}$ invariant (this is done for notational convenience only). Each plane through $\boldsymbol{X}$ with normal $\boldsymbol{n}$ intersects $\widetilde{\Delta V}$ along a planar surface $\widetilde{\Delta A}$, depending on $\boldsymbol{n}$. The relative area of microvoids in $\widetilde{\Delta A}$, say $D(\boldsymbol{X}, \boldsymbol{n})$ can be taken as a measure of damage. If the distribution of voids is isotropic, $D(\boldsymbol{X}, \boldsymbol{n})$ is independent of $\boldsymbol{n}$ and becomes a variable $D(\boldsymbol{X})$ as in Kachanov's model. Mathematically, considering the limiting case of an infinitesimal volume element dV, the above procedure amounts to defining $D(\boldsymbol{X})$ as a density of microvoids.

Although this approach has been used even in recent work in the literature, this choice for the damage variable suffers several criticisms. First, although if it is reasonable to assume that the distribution of voids is isotropic in the virgin material, there is clear experimental evidence that this isotropy is destroyed as a result of planar voids (microcracks) nucleating and growing "in the direction perpendicular to the maximum tensile strain" (Krajcinovic and Fonseka [18], referring to experimental work by Hayhurst and Leckie). Isotropic damage can therefore be expected only as a result of isotropic stress fields, a situation of little practical importance. But there are a few exceptions to this rule and some materials, in particular some aluminum alloys, do exhibit essentially isotropic damage more or less independently of the stress field. In such cases, it is also clear from experimental observations that damage takes the form of nucleation and growth of nearly spherical microcavities. Because it nec-

[1] At the scale of the volume ΔV, it is reasonable to assume zero stress in absence of external forces; this follows from the postulate that material points retain no residual stress, unlike the whole body if plastic effects have taken place.

essarily goes along with modification of volume through the principle of conservation of mass (unlike damage due to microcracks) this phenomenon is better described in terms of the relative volume of the microcavities. As we shall later see, no purely mathematical argument can be made to link the two methods of measurement.

A third criticism is that, in the framework of the theory of small elasto-plastic deformations, the damage variable $D(\boldsymbol{X})$ defined above is used jointly with the notion of effective stress (stress relative to the effective area $1-D(\boldsymbol{X})$) to yield a questionable model in which softening of the material occurs without modification of Poisson's ratio.

In accordance with the foregoing arguments against the previous definition for the damage variable, one may arrive at the conclusion that the geometrical difference between planar voids (microcracks) and microcavities is reflected by two different aspects of damage: on the one hand, nucleation and growth of microcavities will be accompanied by changes in volume (and mass density) consistent with macroscopic measurements (porosity) and will not generate anisotropy in the material. Anisotropy will be accounted for by nucleation and growth of planar voids which, in turn, will not induce modification of volume. It is therefore both natural and desirable to represent these two aspects of damage by two complementary variables.

The obvious choice for defining a damage variable representing nucleation and growth of microcavities is their volume density, denoted by $\Omega(\boldsymbol{X})$ at each point $\boldsymbol{X}$ of the material. For practical measurements, this density can be identified with the relative volume of microcavities in the previous volume element $\widetilde{\Delta V}$ so that, again, $0 \leq \Omega(\boldsymbol{X}) \leq 1$. For a virgin material, $\Omega(\boldsymbol{X}) \equiv 0$,[2] i.e., is small enough to be negligible. As a result, if $\boldsymbol{x}$ denotes the position originally occupied by $\boldsymbol{X}$ in the virgin material and $\rho_o(\boldsymbol{x})$ is the mass density of the virgin material at $\boldsymbol{x}$, then the

[2]This assumption is not essential and the initial condition can be taken as an arbitrary function with values in $[0,1]$. If so, formula (2.1) must be modified accordingly.

mass density $\rho(\boldsymbol{X})$ of the damaged material at $\boldsymbol{X}$ would be given by

$$\rho(\boldsymbol{X}) = (1 - \Omega(\boldsymbol{X}))\rho_o(\boldsymbol{x}), \tag{2.1}$$

if the current configuration were stress-free.

The above method of measuring isotropic damage due to microcavities through the scalar variable Ω was introduced and used by Davison, Stevens and Kipp [8], and one can hardly imagine a drastically different and nonequivalent procedure. But the approach for measuring damage due to microcracks is far from being as self-evident.

The question here is to account for both the area of the cracks and their orientation. The importance of the orientation is obvious from the intention of relating microcracks to anisotropy. It has often been taken as a corollary to the direction dependence that the corresponding damage variable should not be a scalar: a vector representation has been proposed by Davison and Stevens [7] in which the direction of the vector is an average of the directions of the normals to the cracks lying in the volume element $\widetilde{\Delta V}$, and its magnitude is the projected area of the cracks onto the plane orthogonal to the average direction.

This definition is ambiguous, for it is not an easy task to average directions (these being equally represented by two opposite unit vectors). In particular, the only consistent way to define the average direction of cracks uniformally distributed is to choose it to be the zero vector (!) and there are other problems, such as obtaining a reasonably smooth vector field as a result of the operation of averaging directions. To partly circumvent these difficulties, the authors quoted above have suggested the use of not one but several vector fields, each one of them accounting for cracks with more or less similar orientation in the undamaged material. Aside from its rather empirical character, this approach prohibits taking the original damage to be zero and, more generally, does not allow for a correct evaluation of damage caused by nucleation of new cracks if their direction is not already included in the list of vector fields.

Serious concern should be expressed on the basis that nucleation appears to be a

dominant factor during most of the damaging process (Onat and Leckie [25]) whereas, as pointed out before, orientation of cracks depends on the applied forces. Another objection is made by Krajcinovic et al. [17,18] who observed that the model does not reduce to Kachanov's for uniaxial problems, the difference being the area of the planar voids entering the constitutive equations linearly (in [14]) instead of quadratically (in [8]). While an ad-hoc adjustment is proposed in [17,18] to reconcile both points of view, the very problem of definition of the vector-valued damage variable is prudently eluded by making rapid reference to "an appropriate averaging process. . . " with no further detail.

Undoubtedly, the surviving advocates of vector representations are only motivated by the desire of simplifying other existing *tensor* representations. Regarding these, we shall only mention that there are several points of view expressed in the literature, as to what the tensor's coefficients should represent and what its order should be. Not all of them are free of criticism either. The interested reader may find relevant references and additional comments in the aforementioned papers by Krajcinovic et al., but it is our feeling that some significant progress has recently been made by Onat and Leckie [25]. Their approach, with a technical difference in the method of measuring damage (cf. Remark 2.2 later) is as follows.

To begin with, let us move one step backwards and deny the existence of planar voids. This merely means that, no matter how flat it may look, a void has a positive volume or else is not a void. We are then ready to repeat the procedure leading to the density $D(\boldsymbol{X}, \boldsymbol{n})$ introduced earlier. This variable is still scalar valued but, for fixed $\boldsymbol{X}$, is a function of the direction $\boldsymbol{n}$. Equivalently, $D(\boldsymbol{X}, \cdot)$ identifies with an (even) function on the unit sphere S_2 and, as such, can be expressed as a generalized Fourier series by the means of spherical functions. Taking advantage of the evenness of $D(\boldsymbol{X}, \cdot)$ and after a suitable grouping of terms, one arrives at

$$D(\boldsymbol{X}, \boldsymbol{n}) = D_o(\boldsymbol{X}) + \sum_{i,j=1}^{3} f_{ij}(\boldsymbol{n}) D_{ij}(\boldsymbol{X}) + \sum_{i,j,k,l=1}^{3} f_{ijkl}(\boldsymbol{n}) D_{ijkl}(\boldsymbol{X}) + \cdots, \qquad (2.2)$$

namely, an expression involving even rank tensors of basis functions $(1, (f_{ij}(\boldsymbol{n}))$, $(f_{ijkl}(\boldsymbol{n}))$, ...) together with even rank tensors of coefficients $(1, (D_{ij}(\boldsymbol{X}))$, $(D_{ijkl}(\boldsymbol{X}))$, ...). The tensors of basis functions have explicit expressions in terms of the direction $\boldsymbol{n}$; for instance, in obvious notation

$$f_{ij}(\boldsymbol{n}) = n_i n_j - \tfrac{1}{3}\delta_{ij}, \quad 1 \leq i, j \leq 3,$$

and the tensors of coefficients can be obtained through integral formulae (in which integration is performed w.r.t. $\boldsymbol{n} \in S_2$), e.g.

$$\begin{aligned} D_o(\boldsymbol{X}) &= \tfrac{1}{4\pi} \int_{S_2} D(\boldsymbol{X}, \boldsymbol{n}), \\ D_{ij}(\boldsymbol{X}) &= \tfrac{15}{8\pi} \int_{S_2} D(\boldsymbol{X}, \boldsymbol{n}) f_{ij}(\boldsymbol{n}), \quad 1 \leq i, j \leq 3. \end{aligned} \tag{2.3}$$

From (2.3) it is clear that $D_o(\boldsymbol{X})$ represents the isotropic contribution since $D_o \equiv D$ whenever $D(\boldsymbol{X}, \boldsymbol{n})$ is independent of $\boldsymbol{n}$ while all other coefficients $D_{ij}(\boldsymbol{X})$, $D_{ijkl}(\boldsymbol{X})$, ..., vanish due to uniqueness of the decomposition (2.2). All the terms $D_{ij}(\boldsymbol{X})$, $D_{ijkl}(\boldsymbol{X})$, ..., in (2.2) therefore translate the anisotropy of the distribution of voids. Of course, for practical purposes, one needs to assume that only a few terms are significant in (2.2) throughout the loading/unloading process: starting with isotropic damage (e.g., zero) in the virgin material, one may assume that

$$D(\boldsymbol{X}, \boldsymbol{n}) = D_o(\boldsymbol{X}),$$

for materials complying with the isotropic damage assumption, the simplest case of anisotropic damage being handled through the choice

$$D(\boldsymbol{X}, \boldsymbol{n}) = D_o(\boldsymbol{X}) + \sum_{i,j=1}^{3} f_{ij}(\boldsymbol{n}) D_{ij}(\boldsymbol{X}). \tag{2.4}$$

Because of symmetry ($D_{ij} = D_{ji}$) and traceless property ($D_{11} + D_{22} + D_{33} = 0$) (cf. [15]) the above formula shows that the simplest model for anisotropic damage involves six scalar variables instead of three in a vector representation. Whether or not acceptable accuracy is achieved with (2.4) certainly depends on the material and the applied forces. If not, one knows immediately from (2.2) how to include terms providing a better approximation.

Remark 2.1: The above considerations do not justify the choice of the expansion (2.2) versus the usual series of spherical functions. The reason has to be found in the fact that each term in (2.2) involves an even rank tensor, say $2p$ with $p = 0, 1, \ldots,$ of coefficients. This tensor must be viewed as being p times covariant and p times contravariant. As such, we are prompted to introduce a state variable since the way this term complies with changes of coordinates is compatible with a state variable being independent of the coordinate frame. For more detail, see Fardshisheh and Onat [9]. By comparison, the series of spherical functions equivalent to (2.2) follows from the decomposition of the space of functions on S_2 into subspaces invariant under the action of the group of rotation (see Gel'fand and Shapiro [10]). As opposed to any of their particular bases, these spaces are the important intrinsic entities that capture anisotropy. However, they only yield a decomposition of $D(\boldsymbol{X}, \boldsymbol{n})$ as a series of *vectors* which are not appropriate state variables.

Remark 2.2: In [25], where the above approach is introduced, the choice for the damage variable is different. Its definition is based on the optical observation that in materials such as copper exhibiting anisotropic damage, microvoids nucleate and grow on grain boundaries. Assuming the grain boundaries to be planar and given a unit vector $\boldsymbol{n} \in S_2$, consider a surface element $\Delta S \subset S_2$ centered at $\boldsymbol{n}$. Picking $\boldsymbol{X}$ and ΔV as before, call $D(\boldsymbol{X}, \boldsymbol{n})$ the total volume of voids on grain boundaries orthogonal to some $\boldsymbol{n}' \in \Delta S$, *relative to* ΔS (i.e., divided by the area of ΔS) in the stress-free configuration $\widetilde{\Delta V}$ of ΔV. In the limiting case of an infinitesimal surface element dS, this defines $D(\boldsymbol{X}, \boldsymbol{n})$ as a density of voids volume on grain boundaries per unit area of S_2. However, a slight modification is needed if one wants to preserve the desirable property that the quantities D_o, D_{ij}, etc. ...in (2.3) are densities themselves. Indeed, in the present formulation, one has $\int_{S_2} D(\boldsymbol{X}, \boldsymbol{n}) = 2V_T$ where V_T is the total volume of voids in ΔV. Hence, $D_o(\boldsymbol{X}) = V_T/2\bar{n}$ is not a density, and difficulties arise when considering the limiting case of an infinitesimal volume element dV. But this is easily overcome: it suffices to replace $D(\boldsymbol{X}, \boldsymbol{n})$ above by

$D(\boldsymbol{X},\boldsymbol{n})/|\widetilde{\Delta V}|$ where $|\widetilde{\Delta V}|$ denotes the volume of $\widetilde{\Delta V}$ (so that $D(\boldsymbol{X},\boldsymbol{n})$ appears as a density per unit area of S_2 of a density of voids per unit volume!). In particular, $D_o(\boldsymbol{X})$ becomes $D_o(\boldsymbol{X}) = V_T/2\bar{n}|\widetilde{\Delta V}|$, indeed a density, and the same is true of the other coefficients D_{ij}, etc. .... This definition turns out to have also an advantage regarding *kinematical* considerations (see Section 4). Relating anisotropic damage to voids on grain boundaries leaves no other option than relating isotropic damage to voids nucleating and growing *within* the grain. This attitude seems to be in perfect agreement with theoretical and experimental results. For completeness, it must be mentioned that some materials (e.g., steel) exhibit both kinds of void distributions.

When damage is isotropic, it is tempting to try to relate $D(\boldsymbol{X},\boldsymbol{n}) = D(\boldsymbol{X})(= D_o(\boldsymbol{X})$ in (2.3)) to the other variable $\Omega(\boldsymbol{X})$ introduced for the same purpose. That this is not possible through purely mathematical arguments can be seen as follows: pick ΔV such that $\widetilde{\Delta V}$ is a spherical ball centered at $\boldsymbol{X}$ and consider any plane through $\boldsymbol{X}$ intersecting $\widetilde{\Delta V}$ along the disk $\widetilde{\Delta A}$. From the definitions of D and Ω, one has, modulo higher order terms,

$$D(\boldsymbol{X}) = \frac{\mathcal{A}}{|\widetilde{\Delta A}|}, \quad \Omega(\boldsymbol{X}) = \frac{\mathcal{V}}{|\widetilde{\Delta V}|},$$

where $\mathcal{A}$ and $\mathcal{V}$ denote the area and volume of voids in $\widetilde{\Delta A}$ and $\widetilde{\Delta V}$, respectively, and where $|\widetilde{\Delta A}|$ and $|\widetilde{\Delta V}|$ stand for the area and volume of $\widetilde{\Delta A}$ and $\widetilde{\Delta V}$, respectively. Clearly

$$\frac{9\pi}{16}\,\frac{D^3(\boldsymbol{X})}{\Omega^2(\boldsymbol{X})} = \frac{\mathcal{A}^3}{\mathcal{V}^2}\ .$$

Thus, if $\Omega(\boldsymbol{X})$ can be expressed as a function of $D(\boldsymbol{X})$, one finds, for a given value of $D(\boldsymbol{X})$, a formula for the calculation of $\mathcal{A}$ in terms of $\mathcal{V}$. To see that such a formula does not exist, consider two holes in $\widetilde{\Delta V}$ having volume $\mathcal{V}$, but one occupying a spherical ball centered at $\boldsymbol{X}$ and the other a spherical layer along the boundary of $\widetilde{\Delta V}$. In both cases, $\mathcal{A}$ is independent of the plane through $\boldsymbol{X}$ but $\mathcal{A} = |\widetilde{\Delta A}|\Omega(\boldsymbol{X})^{2/3}$ in the first case while $\mathcal{A} = |\widetilde{\Delta A}|(1-(1-\Omega(\boldsymbol{X}))^{2/3})$ in the second case. The impossibility of obtaining a formula for $\mathcal{A}$ in terms of $\mathcal{V}$ (or conversely) is easily traced back to the

fact that euclidian measure in spherical coordinates depends on the distance to the origin, and hence the position and geometry of the holes cannot be left unspecified in the calculation of their total volume from the knowledge of $\mathcal{A}$. Also, it is not hard to convince oneself that the counter-example given above represents the two extreme cases of any distribution of voids in $\widetilde{\Delta V}$. It follows that $D(\boldsymbol{X})$ can always be estimated from

$$1-(1-\Omega(\boldsymbol{X}))^{2/3} \leq D(\boldsymbol{X}) \leq \Omega(\boldsymbol{X})^{2/3}. \tag{2.5}$$

3 Damage and Elastic Properties

We shall begin with some notation: let U denote the original ($t = 0$) unstressed configuration of the *virgin* material, identified with an open subset of R^3 and let $\phi(U)$ be the configuration at some time $t = t_o > 0$. In the configuration $\phi(U)$, the body is in a certain state of stress and, during the time interval $[0, t_o]$, has undergone loading and unloading in a way that may have caused inelastic, permanent deformations.

Through nucleation and growth of microvoids, damage is responsible for at least part of these inelastic deformations. Therefore, unless damage has not evolved and no other plastic phenomenon has taken place in the time interval $[0, t_o]$, the deformation ϕ is not an elastic one. In standard plasticity theory, one would assume that the elastic properties of the material in the configuration $\phi(U)$ are the same as those of the material in configuration U. This means that the constitutive equation between stress and elastic strain is unaffected by the elastic deformation. In damage theory, the bottom line is that the elastic properties of the material have been modified as a result of damage. A major component of the study is then the establishment of sound models for these modifications.

In the assumption that damage is a state of the material,[3] damage theory naturally fits into the framework of elasto-plasticity with state variables developed since

[3]Some theories do not start with this assumption; see Section 4.

the mid-sixties for various purposes. Apparently, nothing has been done in the always difficult case of finite deformations. Even the more tractable problem of infinitesimal deformations is quite unsatisfactorily solved, mainly because the abundance of definitions for the damage variable makes impossible joint efforts in a uniformly accepted direction.

Although it is apparently always taken for granted, we believe that the preliminary step of investigating how the modifications of the elastic properties can be measured is worth a few comments. Certainly, the elastic properties of the material at a point $\boldsymbol{X}$ of the configuration $\phi(U)$ cannot be measured directly from this configuration. Neither can they be measured from a configuration obtained from $\phi(U)$ after unloading since, even if damage and plastic deformation are supposed to be unaffected by the unloading process, the unloaded configuration will generally not be free of residual stress. As was the case with the measure of damage, one must take advantage of the fact that the elastic properties of the body at $\boldsymbol{X}$ are not dependent on the entire configuration $\phi(U)$ but can (and must) be determined after an elementary volume ΔV about $\boldsymbol{X}$ has been separated from the remainder of the configuration $\phi(U)$ and freed of external forces so that it is now stress free in the configuration $\widetilde{\Delta V}$. Again, we have used the postulate that material points retain no residual stress.

The deformation between $\widetilde{\Delta V}$ and ΔV is an elastic one, at least under the reasonable assumption that unloading occurs with no change in plastic deformation (nor damage, but this is obvious from the very definition for the measure of damage made in Section 2). Assuming also this deformation to be infinitesimal, the stress at $\boldsymbol{X}$ in the configuration ΔV (i.e., $\phi(U)$) is a linear function of the strain tensor of $\widetilde{\Delta V} \rightharpoonup \Delta V$ at $\boldsymbol{X}$ (the configuration $\widetilde{\Delta V}$ being chosen, as before, so as to leave $\boldsymbol{X}$ invariant). Observe in passing that in the limiting case of an infinitesimal volume dV, this strain tensor coincides with the so-called elastic strain of the deformation ϕ at $\boldsymbol{X}$. As is well known, the determination of the elastic response of $\widetilde{\Delta V}$ depends on 21 constants. In this respect, it is an *implicit hypothesis* of damage theory that anisotropy

(resp. isotropy) of the distribution of voids in $\widetilde{\Delta V}$ is responsible for anisotropy (resp. isotropy) of the elastic response. The one and only difficulty is then to make the relationship explicit.

Even the isotropic case in which the problem reduces to finding the two Lamé constants is not agreed upon. For easy reference, we shall speak of "Lamé constants at $\boldsymbol{X}$" although the above arguments clearly show that they are not calculated in the configuration $\boldsymbol{\phi}(U)$. The model for isotropic damage based on an extension of Kachanov's approach discussed in the previous section assumes that both Lamé constants at $\boldsymbol{X} = \boldsymbol{\phi}(\boldsymbol{x})$, $\boldsymbol{x} \in U$, are obtained by multiplication of the Lamé constants at $\boldsymbol{x}$ [4] through the same factor $1 - D(\boldsymbol{X})$. The invariance of Poisson's ratio mentioned earlier follows immediately. The models based on vector representation of the damage variable lead to a five-constant constitutive equation (assuming there is only one damage field) reminiscent of those employed in the assumption of transverse isotropy. In these models, the Lamé constants are *unaffected* by damage which is only involved in the other three. The rigorous method used by Onat and Leckie to measure damage has still to be accompanied by a thorough examination of how the various (tensor) variables should enter the constitutive equation.

To be complete, let us mention that thermal effects cannot be ignored in a somewhat general theory of damage, although their study may reasonably be postponed until the isothermal case is better understood. Thermal effects are actually included in the work of Davison et al. [8] on isotropic damage, in which an interesting idea of how to calculate the Lamé constants at $\boldsymbol{X}$ is introduced. In the assumption of negligible thermal effects, we shall now expand on a generalization of this idea and derive some interesting and unexpected consequences.

The starting point is the simple observation that both the Lamé constants at $\boldsymbol{X}$ and the damage variable $\Omega(\boldsymbol{X})$ introduced in Section 2 are calculated from the same

[4] Here, the terminology applies in a strict sense since U is supposed to be a natural state

volume element ΔV about $\boldsymbol{X}$ in a stress-free configuration $\widetilde{\Delta V}$. The microvoids in $\widetilde{\Delta V}$ thus occupy the volume fraction $\Omega(\boldsymbol{X})$ and hence the volume fraction $1-\Omega(\boldsymbol{X})$ only consists of actual material. If now $\widetilde{\Delta V}$ is considered as a composite microvoids-material, there are several available procedures to estimate the Lamé constants of the composite. As in [8], we shall follow the self-consistent method of Budiansky [3] which yields, since the Lamé constants of a microvoid must obviously be taken equal to zero

$$K = K_o\left(1-\frac{3(1-\nu)}{2(1-2\nu)}\Omega\right), \tag{3.1}$$

$$\mu = \mu_o\left(1-\frac{15(1-\nu)}{7-5\nu}\Omega\right), \tag{3.2}$$

where K and K_o (resp. μ and μ_o) are the bulk moduli (resp. shear moduli) at $\boldsymbol{X}$ and $\boldsymbol{x}=\boldsymbol{\phi}^{-1}(\boldsymbol{X})$ respectively, $\nu=\nu(\boldsymbol{X})$ is Poisson's ratio at $\boldsymbol{X}$ (i.e., of the composite) and Ω stands for $\Omega(\boldsymbol{X})$. Naturally, ν is also related to K and μ through

$$\nu=\frac{3K-2\mu}{2(3K+\mu)}, \tag{3.3}$$

a formula complementing (3.1) and (3.2) and allowing for actual calculation of K and μ in terms of Ω. Note that (3.1)-(3.3) only yield implicit characterization of K and μ; note also that the conditions $\mu>0$ and $\lambda>0$ (with $K=\lambda+\frac{2}{3}\mu$) are *not* guaranteed by the above relations and depend on Ω which then should range in an interval $[0,\Omega_{\max})$ with $\Omega_{\max}\leq 1$.

Although its analog for arbitrary composite materials cannot be solved explicitly in general, the system (3.1)-(3.3) does admit an explicit solution. This can be seen as follows: setting

$$\theta = K/\mu, \tag{3.4}$$

one finds

$$\nu=\frac{3\theta-2}{2(3\theta+1)}. \tag{3.5}$$

For future use, it is also worth noticing that

$$\lambda > 0,\ \mu > 0 <=> \theta > \frac{2}{3},\ \mu > 0\ . \tag{3.6}$$

From (3.5), we get

$$\begin{cases} 1 - 2\nu = 3/(3\theta + 1), \\ 1 - \nu = (3\theta + 4)/2(3\theta + 1), \\ 7 - 5\nu = (27\theta + 24)/2(3\theta + 1). \end{cases} \tag{3.7}$$

With $\theta_o = K_o/\mu_o$, it follows from (3.5) and (3.7) that

$$\theta = \theta_o \frac{(4 - 3\theta\Omega - 4\Omega)(9\theta + 8)}{4(9\theta + 8 - 15\theta\Omega - 20\Omega)}\ . \tag{3.8}$$

Hence, θ can be recovered from θ_o and Ω by solving a quadratic equation, namely

$$(36 - 60\Omega + 27\theta_o\Omega)\theta^2 + (32 - 80\Omega - 36\theta_o + 60\theta_o\Omega)\theta + 32\theta_o(\Omega - 1) = 0 \tag{3.9}$$

It is easily checked that this equation has exactly one positive root for $\Omega \in [0, 1]$ if $\theta_o \geq 8/9$.

Let $g(\Omega)$ denote the positive root of (3.9). Substituting $\theta = g(\Omega)$ into (3.7) and from (3.1) and (3.2), one finds the desired expression for K and μ as functions of Ω. Of course, they are too complicated to be of any use in theoretical arguments. However, to corroborate the intuitive idea that the material becomes softer and softer as the damage Ω grows, it is natural to expect K and μ to be decreasing functions of Ω. Also, it would be of interest to determine the value $\Omega_{\max}$ beyond which either λ or μ becomes negative, thus ceasing to represent an actual material. These questions can, in fact, be answered with practically no calculation if one uses (3.8) to derive the expression of Ω in terms of θ and θ_o, which is easily seen to be

$$\Omega = f(\theta) \equiv \frac{4}{3}\ \frac{(\theta_o - \theta)(9\theta + 8)}{(\theta + 4/3)[(9\theta_o - 20)\theta + 8\theta_o]}. \tag{3.10}$$

A key observation is that, *irrespective* of $\theta_o \neq 4/3$, not only the substitution $\theta = \theta_o$ in (3.10) yields $\Omega = 0$ but the substitution $\theta = 4/3$ yields $\Omega = 1/2$. In addition, it is

immediate to check that for $\theta = 4/3$ and $\Omega = 1/2$, both constants K and μ vanish. This suggests that the study of $\Omega = f(\theta)$ as given by (3.10), but restricted to the interval $I = [\theta_o, 4/3]$ if $\theta_o < 4/3$, $I = [4/3, \theta_o]$ if $\theta_o > 4/3$, will provide the desired information.

To begin with, note that f is well defined on I since ($\theta_o \neq 4/3$ is always implicit in what follows)

$$8\theta_o/(9\theta_o - 20) < \theta_o \text{ if } \theta_o < 4/3,$$
$$8\theta_o/(9\theta_o - 20) > \theta_o \text{ if } 4/3 < \theta_o < 20/9,$$
$$8\theta_o/(9\theta_o - 20) < 0 \text{ if } \theta_o > 20/9,$$

and there is no problem if $\theta_o = 20/9$. It is equally straightforward to check that $f(I) \subset [0, 1/2]$ irrespective of θ_o, hence

$$f(I) = [0, 1/2],$$

from $f(\theta_o) = 0$, $f(4/3) = 1/2$ and the intermediate value theorem. Moreover, for every $\theta \in I$ and $\Omega = f(\theta)$, θ is uniquely characterized to be the unique positive root $g(\Omega)$ of equation (3.9). This shows that f and g are the inverse of each other. Actually, this has been shown for $\theta_o \geq 8/9$ only, the only case for which equation (3.9) has exactly one positive root for every $\Omega \in [0, 1]$. But since the interval of interest is $[0, 1/2]$ instead of $[0, 1]$ as would have been expected at the beginning, and since it is straightforward to check that equation (3.9) has a unique positive root irrespective of $\Omega \in [0, 1/2]$ for every $\theta_o \geq 0$, the restriction $\theta_o \geq 8/9$ is not necessary. From the fact that f and g are inverse of each other, it follows that f is a bijection from I to $[0, 1/2]$. Continuity being obvious, we infer that f is monotone on I and, finally, that $g = f^{-1}$ is monotone on $[0, 1/2]$ [5].

Suppose first that g is increasing. Using (3.1) and (3.7), we see that

$$K(= K(\Omega)) = K_o(1 - \tfrac{3}{4}(g(\Omega) + 1)\Omega), \tag{3.11}$$

which immediately shows that K is a decreasing function of $\Omega \in [0, 1/2]$. In particular $K(\Omega) > 0$ for $\Omega \in [0, 1/2)$ since $K(1/2) = 0$ is already known.

[5] Trying to give a direct proof of monotonicity of f and g for every $\theta_o \neq 4/3$ is rather inextricable.

Next, from (3.4) we find

$$\mu = \mu(\Omega) = K(\Omega)/g(\Omega).$$

Since $K \geq 0$ and $g > 0$ on $[0, 1/2]$, K is decreasing and g is increasing, it follows that μ is decreasing. In particular, $\mu(\Omega) > 0$ for $\Omega \in [0, 1/2)$ since $\mu(1/2) = 0$ is already known. From the equivalence (3.5) and recalling that $\theta_o > 2/3$ in physically relevant situations, hence $g(\Omega) \geq \min(\theta_o, 4/3) > 2/3$ for every $\Omega \in [0, 1/2]$, we obtain

$$\Omega_{\max} = 1/2,$$

irrespective of $\theta_o \neq 4/3$.

Suppose now that g is decreasing. Using (3.2) and (3.7), we see that

$$\mu(= \mu(\Omega)) = \mu_o \left[1 - \left(\frac{5}{3} + \frac{20/3}{9g(\Omega) + 8}\right)\Omega\right], \tag{3.12}$$

which immediately shows that μ is a decreasing function of $\Omega \in [0, 1/2]$. In particular, $\mu(\Omega) > 0$ for $\Omega \in [0, 1/2)$ since $\mu(1/2) = 0$ is already known. Next, from (3.4) we find

$$K(= K(\Omega)) = \mu(\Omega)g(\Omega).$$

Since $\mu \geq 0$ and $g > 0$ on $[0, 1/2]$ and μ and g are both decreasing, it follows that K is decreasing. Assuming again $\theta_o > 2/3$, the conclusion

$$\Omega_{\max} = 1/2,$$

is reached through the same arguments as above.

For $\Omega = 1/2$, we know that the corresponding value of θ is $\theta = 4/3$. With (3.5), we deduce the corresponding value of Poisson's ratio

$$\nu = \frac{1}{5}.$$

The above analysis is valid under the assumption $\theta_o \neq 4/3$. For $\theta_o = 4/3$ (i.e. $\nu_o = 1/5$ if ν_o denotes Poisson's ratio of the virgin material), equation (3.9) has

$\theta = 4/3$ as its unique positive root regardless of $\Omega \in [0,1]$ (so that the relation between θ and Ω is not invertible and the previous approach does not go through). Substituting $\theta = 4/3$ into (3.7), relations (3.1) and (3.2) become

$$K = K_o(1 - 2\Omega), \quad \mu = \mu_o(1 - 2\Omega),$$

and, again, we find

$$D_{\max} = 1/2.$$

Because $\theta = 4/3$ is independent of Ω, no modification of Poisson's ratio ($= 1/5$) is observed in this limiting case.

Remark 3.1: More generally, as a result of (3.5), it follows that $\nu = \nu(\Omega)$ is decreasing (resp. increasing) when g is decreasing (resp. increasing). As $\nu(1/2) = 1/5$ irrespective of initial conditions, it follows that g is decreasing if $\nu_o > 1/5$ (i.e., $\theta_o > 4/3$), increasing if $\nu_o < 1/5$ (i.e., $\theta_o < 4/3$).

The value $\Omega_{\max} = 1/2$ instead of the expected value 1 is, after all, not surprising. Let us, for instance, decide to view $\phi(U)$ as a union of identical microcubes, each of them containing the same spherical hole. It is obvious that the structure will be unable to support any stress when the volume of the spherical hole is maximum, namely when it occupies $\pi/6(\simeq 0.52)$ of the volume of the cube. The relation $\Omega_{\max} = 0.5$ can roughly be explained on this basis.

Let us point out that considering the damaged material as a composite to which the rules dictated by self-consistent methods apply is not the only possible attitude. The proposed model may require modifications for values of damage approaching 1/2, based either on refinements of the theory or empirical observations. But the fact that it is self-sufficient to predict vanishing of the Lamé constants before the maximum possible value 1 for the damage variable is important. This phenomenon, interpreted as failure (crack initiation) is indeed well known but is not included in simpler models which must appeal to experimentally determined thresholds. In [20] Lemaitre indicates the values 0.2 to 0.8 for the range of critical values relative to the

variable $D(\boldsymbol{X})$, depending on the material. Existence of such thresholds is *not* in contradiction with the relation $\Omega_{\max} = 1/2$ regardless of the material. Indeed, recall that there is no mathematical correlation between $D(\boldsymbol{X})$ and $\Omega(\boldsymbol{X})$, except for the estimate (2.5). In practice, this means that two materials showing isotropic damage may perfectly exhibit *different* maximum values $D_{\max}$ of the variable D despite that their values of $\Omega_{\max}$ is the same. This is because the average size of each individual void may be *typically* different in the two materials for specimens of equal total volume.

As a matter of fact, it is not even certain that $D_{\max}$ is independent of the experiment for a given material. Substituting $\Omega(\boldsymbol{X}) = \Omega_{\max} = 1/2$ into (2.5) yields the bracket $[0.37, 0.63]$ for $D_{\max}$ This bracket is narrower than $[0.2, 0.8]$ previously reported. However, it is not clear that the latter has actually been established with materials that all show isotropic damage, which could explain the discrepancy.

Earlier in this section, we have established that both $K(\Omega)$ and $\mu(\Omega)$ are decreasing functions of Ω. This was done to corroborate the fact that the material was indeed softening as damage increases. Later, in connection with the *dissipative* aspect of damage evolution, we shall need the following less intuitive and stronger result:

Proposition: *Set*

$$\begin{aligned} \hat{K}(\Omega) &= (1-\Omega)^{-1/3} K(\Omega), \\ \hat{\mu}(\Omega) &= (1-\Omega)^{-1/3} \mu(\Omega). \end{aligned}$$

Then, $\hat{K}(\Omega)$ *and* $\hat{\mu}(\Omega)$ *are descreasing functions* of $\Omega \in [0, 1/2]$.

Proof: Again, we shall distinguish the two cases when the function $g(\Omega)$ giving the unique positive root of equation (3.9) is either increasing or decreasing on $[0, 1/2]$ (recall that there is no other option).

Suppose then that g is increasing. From (3.11) and a straightforward calculation,

one finds

$$\hat{K}'(\Omega) \leq 0 <=> -\tfrac{3}{4}(g'(\Omega)\Omega + g(\Omega) + 1)(1-\Omega) + \tfrac{1}{3}[1 - \tfrac{3}{4}(g(\Omega)+1)\Omega] \leq 0.$$

The second inequality can be rewritten as

$$\tfrac{1}{3}[1 - \tfrac{3}{4}(g(\Omega)+1)\Omega] \leq \tfrac{3}{4}(g'(\Omega)\Omega + g(\Omega) + 1)(1-\Omega),$$

and, since $g'(\Omega) \geq 0$, will certainly be satisfied if

$$\tfrac{1}{3}[1 - \tfrac{3}{4}(g(\Omega)+1)\Omega] \leq \tfrac{3}{4}(g'(\Omega)+1)(1-\Omega) <=>$$
$$\tfrac{1}{3} \leq (g(\Omega)+1)(\tfrac{3}{4} - \tfrac{1}{2}\Omega)$$

As $\Omega \in [0, 1/2]$, this inequality follows from

$$\tfrac{1}{3} \leq \tfrac{1}{2}(g(\Omega)+1),$$

which is obvious because $g \geq 0$. Hence, $\hat{K}(\Omega)$ is a decreasing function of Ω.

To show that $\hat{\mu}(\Omega)$ is decreasing too, let us simply observe that $\hat{K}(\Omega)/\hat{\mu}(\Omega) = K(\Omega)/\mu(\Omega) = g(\Omega)$, so that $\hat{\mu}(\Omega) = \hat{K}(\Omega)/g(\Omega)$. The result is immediate from $\hat{K}$ being decreasing and nonnegative and g being increasing and nonnegative.

Suppose now that g is decreasing. With (3.12), one finds

$$\hat{\mu}(\Omega) \leq 0 <=> N'(\Omega)(1-\Omega) + \tfrac{1}{3}N(\Omega) \leq 0, \tag{3.13}$$

where

$$N(\Omega) \equiv 1 - \left(\frac{5}{3} + \frac{20/3}{9g(\Omega)+8}\right)\Omega.$$

Since g is decreasing, so is the function

$$\Omega \mapsto -\frac{20/3}{9g(\Omega)+8}\Omega,$$

and hence

$$N'(\Omega) \leq -\tfrac{5}{3}.$$

The second inequality in (3.13) is then true provided that

$$N(\Omega) \leq 5(1-\Omega).$$

But this is immediate for it is obvious that $N(\Omega) \leq 1$ while $5(1-\Omega) \geq 5/2$ for $\Omega \in [0, 1/2]$. Hence, $\hat{\mu}(\Omega)$ is a decreasing function of Ω Writing as before $\hat{K}(\Omega)/\hat{\mu}(\Omega) = g(\Omega)$, namely $\hat{K}(\Omega) = \hat{\mu}(\Omega)g(\Omega)$, one finds that $\hat{K}(\Omega)$ is decreasing as the product of two decreasing nonnegative functions and the proof is complete.

4 Kinematics

From now on, $\boldsymbol{x}$ will denote an arbitrary point of the reference configuration U and $\boldsymbol{X} = \boldsymbol{\phi}(\boldsymbol{x})$ represents the same material point in the current configuration. This is consistent with notation used in previous sections. If the problem were considered in the framework of elasto-plasticity theory, the deformation gradient $\nabla\boldsymbol{\phi}(\boldsymbol{x})$ would be decomposed according to one of several available procedures into "elastic" and "plastic" parts. Most commonly, one would use the multiplicative decomposition of Lee [19] to write

$$\nabla\boldsymbol{\phi}(\boldsymbol{x}) = \boldsymbol{E}(\boldsymbol{x})\boldsymbol{P}(\boldsymbol{x}), \tag{4.1}$$

where $\boldsymbol{E}$ and $\boldsymbol{P}$ denote elastic and plastic components, respectively. Because dislocations merely introduce negligible variations of volume, it is required that

$$\det \boldsymbol{P}(\boldsymbol{x}) = 1. \tag{4.2}$$

The decomposition (4.1) thus does not allow for the inelastic dilatation typical of isotropic damage. Incidentally, note that this observation alone justifies that damage be considered a phenomenon distinct from plasticity.

In [8], Davison et al. have made use of a modification of the decomposition (4.1) first introduced by Kratochvil for other (but somewhat related) purposes, and written $\nabla\boldsymbol{\phi}(\boldsymbol{x})$ in the form

$$\nabla\boldsymbol{\phi}(\boldsymbol{x}) = \boldsymbol{E}(\boldsymbol{x})\boldsymbol{M}(\boldsymbol{x})\boldsymbol{P}(\boldsymbol{x}), \tag{4.3}$$

where now the tensor $\boldsymbol{M}(\boldsymbol{x})$ accounts for the effect of damage. It is fairly simple to determine the structure of the tensor $\boldsymbol{M}(\boldsymbol{x})$. For this, it is helpful to refer once again to the volume element ΔV about $\boldsymbol{X} = \boldsymbol{\phi}(\boldsymbol{x})$ and its stress free configuration $\widetilde{\Delta V}$ (see Section 3). Clearly, considering the limiting case of an infinitesimal volume element dV, one sees that $\boldsymbol{E}(\boldsymbol{x})$ coincides with the gradient of the (elastic) deformation between $\widetilde{dV}$ and dV. To determine $\boldsymbol{M}(\boldsymbol{x})$, consider the volume element $\Delta v = \boldsymbol{\phi}^{-1}(\Delta V)$ about $\boldsymbol{x}$. Except for a plastic deformation which does not affect its volume, $\widetilde{\Delta V}$ differs from Δv through the dilatation introduced by evolution of damage. Since Δv and $\widetilde{\Delta V}$ contain the same volume of material, which represents only the fraction $1-\Omega(\boldsymbol{X})$ in $\widetilde{\Delta V}$, one has (assuming zero damage in the reference configuration) modulo higher order terms

$$|\widetilde{\Delta V}| = \frac{|\Delta v|}{1-\Omega(\boldsymbol{X})}.$$

Considering the limiting case of infinitesimal elements, we find that, necessarily

$$\det \boldsymbol{M}(\boldsymbol{x}) = (1-\Omega(\boldsymbol{X}))^{-1}, \quad \boldsymbol{X} = \boldsymbol{\phi}(\boldsymbol{x}). \tag{4.4}$$

As the distribution of microvoids is isotropic and $\boldsymbol{M}(\boldsymbol{x})$ depends only on this distribution, no direction must be privileged in $\boldsymbol{M}(\boldsymbol{x})$ (i.e., the first order difference between Δv and $\widetilde{\Delta V}$ consists of a stretch equal in all directions). It follows that $\boldsymbol{M}(\boldsymbol{x})$ is a multiple of identity and, together with (4.4), we find

$$\boldsymbol{M}(\boldsymbol{x}) = (1-\Omega(\boldsymbol{X}))^{-1/3}\boldsymbol{I}, \quad \boldsymbol{X} = \boldsymbol{\phi}(\boldsymbol{x})\,. \tag{4.5}$$

From now on, it will be more convenient to introduce the damage variable

$$\omega(\boldsymbol{x}) = \Omega(\boldsymbol{\phi}(\boldsymbol{x})), \quad \boldsymbol{x} \in U, \tag{4.6}$$

expressed in the reference configuration. Combining (4.3) and (4.5), we arrive at

$$\nabla\boldsymbol{\phi}(\boldsymbol{x}) = (1-\omega(\boldsymbol{x}))^{-1/3}\boldsymbol{E}(\boldsymbol{x})\boldsymbol{P}(\boldsymbol{x}). \tag{4.7}$$

Setting

$$\begin{cases} \boldsymbol{\phi}(\boldsymbol{x}) = \boldsymbol{x} + \boldsymbol{u}(\boldsymbol{x}), \\ \boldsymbol{E}(\boldsymbol{x}) = \boldsymbol{I} + \boldsymbol{e}(\boldsymbol{x}), \\ \boldsymbol{P}(\boldsymbol{x}) = \boldsymbol{I} + \boldsymbol{p}(\boldsymbol{x}), \end{cases} \tag{4.8}$$

an equivalent form of (4.7) is

$$\nabla \boldsymbol{u}(\boldsymbol{x}) = [(1-\omega(\boldsymbol{x}))^{-1/3} - 1]\boldsymbol{I} + (1-\omega(\boldsymbol{x}))^{-1/3}(\boldsymbol{e}(\boldsymbol{x}) + \boldsymbol{p}(\boldsymbol{x}) + \boldsymbol{e}(\boldsymbol{x})\boldsymbol{p}(\boldsymbol{x})).$$

In the case of infinitesimal elastic and plastic deformations, this relation reduces to (omitting $\boldsymbol{x}$ - dependence)

$$\nabla \boldsymbol{u} = [(1-\omega)^{-1/3} - 1]\boldsymbol{I} + (1-\omega)^{-1/3}(\boldsymbol{e} + \boldsymbol{p}).$$

Therefore, using the standard notations

$$\begin{cases} \boldsymbol{\varepsilon}(\boldsymbol{u}) = \frac{1}{2}(\nabla \boldsymbol{u} + \nabla \boldsymbol{u}^T), \\ \boldsymbol{\varepsilon}^e = \frac{1}{2}(\boldsymbol{e} + \boldsymbol{e}^T), \\ \boldsymbol{\varepsilon}^p = \frac{1}{2}(\boldsymbol{p} + \boldsymbol{p}^T), \end{cases} \tag{4.9}$$

we find

$$\boldsymbol{\varepsilon}(\boldsymbol{u}) = [(1-\omega)^{-1/3} - 1]\boldsymbol{I} + (1-\omega)^{-1/3}(\boldsymbol{\varepsilon}^e + \boldsymbol{\varepsilon}^p) \tag{4.10}$$

or, equivalently

$$\boldsymbol{\varepsilon}^e = (1-\omega)^{1/3}\boldsymbol{\varepsilon}(\boldsymbol{u}) - [1-(1-\omega)^{1/3}]\boldsymbol{I} - \boldsymbol{\varepsilon}^p \ . \tag{4.11}$$

Relation (4.2) is taken into account by requiring

$$Tr\boldsymbol{\varepsilon}^p = 0. \tag{4.12}$$

If anisotropic damage were to be considered, the decomposition (4.3) would still be appropriate, but the tensor $\boldsymbol{M}(\boldsymbol{x})$ should also represent the anisotropy of the distribution of voids, hence could no longer be a multiple of identity in general. However, repeating previous arguments, its determinant should still relate to the total volume of voids. This demonstrates a significant advantage in the choice of the

density of voids volume on grain boundaries per unit area of the unit sphere as a measure of damage (cf. Remark 2.2). Indeed, recall that the corresponding quantity $D_o(\boldsymbol{X})$ in (2.2) relates to the total volume V_T of voids in $\widetilde{\Delta V}$ through the simple relation

$$D_o(\boldsymbol{X}) = V_T/2\pi|\widetilde{\Delta V}| \,.$$

Hence

$$\det \boldsymbol{M}(\boldsymbol{x}) = (1 - 2\pi D_o(\boldsymbol{X}))^{-1}.$$

If the damage variable $D(\boldsymbol{X}, \boldsymbol{n})$ is defined as in Section 2, an experimentally determined correlation between $D_o(\boldsymbol{X})$ and V_T must be used, assuming of course that such a correlation exists for a given material. In this respect, recall that no purely mathematical argument can be made to establish the desired correlation. In any case, $\boldsymbol{M}(\boldsymbol{x})$ will depend on the damage variables accounting for the anisotropy of the distribution of voids. The difficulty in relating $\boldsymbol{M}(\boldsymbol{x})$ to these variables is greatly dependent on the clarity of their geometrical interpretation (but the problem is nevertheless not expected to be trivial). In this respect too, the variables introduced through the approach of Onat and Leckie seem to be the most appropriate.

Remark 4.1: In the event that anisotropy in the distribution of voids can be attributed to the plastic slip alone, the tensor $\boldsymbol{M}(\boldsymbol{x})$ remains a multiple of identity. Such an assumption may only apply to materials for which damage is isotropic when it occurs in the elastic range. We have found no information in the literature as to whether these materials form a broader class than those for which damage is always isotropic. For the elements of this class and for them only, anisotropy is entirely translated by the nature of the elastic response (constitutive equation). For the record, we note that it has generally been overlooked that anisotropy must also be involved in the kinematical aspect of the problem.

To complete this section, we shall briefly mention how the decomposition (4.3) can be used as a starting point for a totally different approach to damage theory.

Let us begin with the assumption that, due to damage, the tensor $\nabla\phi(\boldsymbol{x})$ has the decomposition (4.3) instead of (4.1). For a virgin material, $\boldsymbol{M}(\boldsymbol{x}) = \boldsymbol{I}$. This suggests writing $\boldsymbol{M}(\boldsymbol{x}) = \boldsymbol{I} + \boldsymbol{m}(\boldsymbol{x})$ and hence, omitting $\boldsymbol{x}$-dependence.

$$I + 2\boldsymbol{\varepsilon}(\boldsymbol{u}) + \nabla\boldsymbol{u}^T\nabla\boldsymbol{u} = \boldsymbol{I} + 2\boldsymbol{\varepsilon}^e + 2\boldsymbol{\varepsilon}^m + 2\boldsymbol{\varepsilon}^p + \text{higher order terms}, \tag{4.13}$$

where

$$\boldsymbol{\varepsilon}^m = \frac{1}{2}(\boldsymbol{m} + \boldsymbol{m}^T),$$

appears as a damage strain. Assuming infinitesimal strains, relation (4.13) becomes

$$\boldsymbol{\varepsilon}(\boldsymbol{u}) = \boldsymbol{\varepsilon}^e + \boldsymbol{\varepsilon}^m + \boldsymbol{\varepsilon}^p. \tag{4.14}$$

Decomposition (4.14) above is used e.g. by Nicholson [24]. Evolution of damage is next translated through a suitable differential equation for the damage strain $\boldsymbol{\varepsilon}^m$, just as plastic phenomena require the establishment of an appropriate differential equation for the plastic strain $\boldsymbol{\varepsilon}^p$. This approach does not require a specific damage variable to be introduced, but has the concomitant disadvantage of not relating damage to its physical origin (on the positive side is the fact that one does not have to deal with anisotropy, as a result of the voids not being explicitly involved

in the formulation of the problem). Such a theory however can hardly be used to investigate the modifications of the elastic properties due to damage. These modifications must then be negligible for the validity of the theory. In turn, negligible modification of the elastic properties enforces the hypothesis of small damage.

5 A Model for Isotropic Damage

The loading and unloading of the initially virgin material will be taken into account by time-dependent body force densities $\boldsymbol{b}$ (per unit mass) and surface traction densities $\boldsymbol{t}$ (per unit area) defined in the current configuration $\phi(U)$. During this process, supposed to be *isothermal*, the body is clamped along the part $\Gamma_o \subset \Gamma \equiv \partial U$ of the

reference configuration U. In particular, the surface tractions $\boldsymbol{t}$ are prescribed on $\phi(\Gamma_1)$ where $\Gamma_1 \equiv \Gamma \backslash \Gamma_o$. The total body force acting at $\boldsymbol{X} \in \phi(U)$ is the sum

$$\text{Div}^{\phi}(\boldsymbol{T}^{\phi}) + \rho \boldsymbol{b},$$

where $\boldsymbol{T}^{\phi}(= \boldsymbol{T}^{\phi}(\boldsymbol{X}))$ is the Cauchy stress tensor at $\boldsymbol{X}$, Div^{ϕ} is the divergence operator in the coordinate frame of the deformed configuration and ρ denotes mass density at $\boldsymbol{X}$. For $\boldsymbol{X} \in \phi(\Gamma_1)$, the total surface traction vanishes, i.e.,

$$(\boldsymbol{T}^{\phi}\nu^{\phi} + \boldsymbol{t})dA^{\phi} = \boldsymbol{0},$$

with ν^{ϕ} and dA^{ϕ} being the unit outward normal vector and the infinitesimal area element at $\boldsymbol{X}$, respectively. Using the Piola transformation, i.e., setting

$$\boldsymbol{T}(\boldsymbol{x}) = \det \nabla\phi(\boldsymbol{x}) \boldsymbol{T}^{\phi}(\phi(\boldsymbol{x})) \nabla\phi(\boldsymbol{x})^{-T}, \quad \boldsymbol{x} = \phi^{-1}(\boldsymbol{X}), \tag{5.1}$$

allows one to derive corresponding expressions in the reference configuration U through the identity (cf. Ciarlet [4]).

$$\text{Div}\, \boldsymbol{T}(\boldsymbol{x}) = \det \nabla\phi(\boldsymbol{x})\ \text{Div}^{\phi}(\boldsymbol{T}^{\phi})(\phi(\boldsymbol{x})), \quad \boldsymbol{x} \in U,$$
$$\boldsymbol{T}(\boldsymbol{x})\boldsymbol{\nu}(\boldsymbol{x})dA = \boldsymbol{T}^{\phi}(\phi(\boldsymbol{x}))\boldsymbol{\nu}^{\phi}(\phi(\boldsymbol{x}))dA^{\phi},$$

where Div is the divergence operator in the coordinate frame of the reference configuration and $\boldsymbol{\nu}(\boldsymbol{x})$ and dA are the unit outward normal vector and infinitesimal area element at $\boldsymbol{x}$, respectively. Thus, the total body force at $\boldsymbol{X} = \phi(\boldsymbol{x})$ is (using $\rho_o(\boldsymbol{x}) = \rho(\boldsymbol{X}) \det \nabla\phi(\boldsymbol{x})$)

$$[\det \nabla\phi(\boldsymbol{x})]^{-1}[\ \text{Div}\, \boldsymbol{T}(\boldsymbol{x}) + \rho_o(\boldsymbol{x})\boldsymbol{b}(\phi(\boldsymbol{x}))], \quad \boldsymbol{x} \in U, \tag{5.2}$$

while balance of surface tractions reads

$$-\boldsymbol{T}(\boldsymbol{x})\boldsymbol{\nu}(\boldsymbol{x})dA = \boldsymbol{t}(\phi(\boldsymbol{x}))dA^{\phi} = \boldsymbol{0}, \quad \boldsymbol{x} \in \Gamma_1. \tag{5.3}$$

In the hypothesis of *dead loading*, the body force density $\boldsymbol{b}(\phi(\boldsymbol{x}))$ and the surface traction densities are independent of ϕ, i.e.,

$$\boldsymbol{b}(\phi(\boldsymbol{x})) = \boldsymbol{b}(\boldsymbol{x}), \quad \boldsymbol{t}(\phi(\boldsymbol{x}))dA^{\phi} = \boldsymbol{t}(\boldsymbol{x})dA.$$

In this case, it easily follows from (5.2) and (5.3) that balance of linear momentum yields (omitting $\boldsymbol{x}$-dependence)

$$\begin{cases} \text{Div } \boldsymbol{T} + \rho_o \boldsymbol{b} = \rho_o \ddot{\boldsymbol{u}} & \text{in } U, \\ \boldsymbol{u} = \boldsymbol{0} & \text{on } \Gamma_o, \\ \boldsymbol{T}\boldsymbol{\nu} = \boldsymbol{t} & \text{on } \Gamma_1, \end{cases} \tag{5.4}$$

where we have used $\boldsymbol{\phi} = \boldsymbol{I} + \boldsymbol{u}$.

We shall limit ourselves to considering the case of infinitesimal elasto-plastic deformations. In the notation of Section 3, the elastic part of the deformation can be viewed as the deformation between the volume elements $\widetilde{\Delta V}$ and ΔV. For an infinitesimal elastic deformation, this means that

$$\boldsymbol{T}^{\boldsymbol{\phi}} = \boldsymbol{A}(\omega)\boldsymbol{\varepsilon}^e, \tag{5.5}$$

where ω is defined in (4.6) and, since the natural configuration $\widetilde{\Delta V}$ is isotropic and isothermal conditions are assumed, the fourth-order tensor $\boldsymbol{A}(\omega)$ is defined by

$$\boldsymbol{A}(\omega)\boldsymbol{\varepsilon} = \lambda(\omega)(Tr\boldsymbol{\varepsilon})\boldsymbol{I} + 2\mu(\omega)\boldsymbol{\varepsilon}, \tag{5.6}$$

for every 3 x 3 (symmetric) tensor $\boldsymbol{\varepsilon}$. Of course, the Lamé constants $\lambda(\omega)$ and $\mu(\omega)$ will be taken according to the procedure of Section 3.

Using (5.1) together with the hypothesis of infinitesimal elasto-plastic deformations in (4.7) and (4.8), the system (5.4) may then be rewritten as (neglecting higher order terms)

$$\begin{cases} \text{Div } [(1-\omega)^{-2/3}\boldsymbol{A}(\omega)\boldsymbol{\varepsilon}^e] + \rho_o \boldsymbol{b} = \rho_o \ddot{\boldsymbol{u}} \text{ in } U, \\ \boldsymbol{u} = \boldsymbol{0} \text{ on } \Gamma_o, \\ (1-\omega)^{-2/3}\boldsymbol{A}(\omega)\boldsymbol{\varepsilon}^e = \boldsymbol{t} \text{ on } \Gamma_1 \ . \end{cases}$$

In turn, recalling (4.11), this becomes

$$\begin{cases} \text{Div } \left[\boldsymbol{B}(\omega)(\boldsymbol{\varepsilon}(\boldsymbol{u}) - (1-\omega)^{-1/3}\boldsymbol{\varepsilon}^p)\right] - \nabla\pi(\omega) + \rho_o \boldsymbol{b} = \rho_o \ddot{\boldsymbol{u}} \text{ in } U, \\ \boldsymbol{u} = \boldsymbol{0} \text{ on } \Gamma_o, \\ \left[\boldsymbol{B}(\omega)(\boldsymbol{\varepsilon}(\boldsymbol{u}) - (1-\omega)^{-1/3}\boldsymbol{\varepsilon}^p)\right]\boldsymbol{\nu} = \pi(\omega)\boldsymbol{\nu} + \boldsymbol{t} \text{ on } \Gamma_1, \end{cases} \tag{5.7}$$

where

$$\boldsymbol{B}(\omega) = (1-\omega)^{-1/3}\boldsymbol{A}(\omega), \tag{5.8}$$

and where the pressure π depends only on damage through the relation

$$\pi(\omega) = 3K(\omega)(1-\omega)^{-1/3}[(1-\omega)^{-1/3} - 1], \tag{5.9}$$

with $K(\omega) \equiv \lambda(\omega) + (2/3)\mu(\omega)$. In particular, $\pi(\omega)$ *vanishes at failure* ($\omega = 1/2$), since $K(\omega)$ does (cf. Section 3). This should be expected from the fact that $\pi(\omega)\boldsymbol{I}$ is essentially the residual stress (Remark 5.2).

Remark 5.1: It is important to observe that despite the assumption of infinitesimal elasto-plastic deformations, the strain tensor $\boldsymbol{\epsilon}(\boldsymbol{u})$ need *not* be small. This has indeed not been required in the foregoing analysis and such an assumption would contradict relation (4.10) since the coefficient of $\boldsymbol{I}$ can be as large as 0.26 (for $\omega = 1/2$). Besides, on the basis of (4.10) again, requiring $\boldsymbol{\epsilon}(\boldsymbol{u})$ to be small would immediately limit damage to be small, too. This shows the importance of not having such a restriction.

Remark 5.2: Suppose that motion has occurred only in the elastic regime (i.e., $\boldsymbol{\epsilon}^p \equiv 0$) and the forces have been constant long enough for the body to be in equilibrium in the configuration $\phi(U)$. Then, the system (5.8) reduces to

$$\begin{cases} -\text{ Div } (\boldsymbol{B}(\omega)\boldsymbol{\epsilon}(\boldsymbol{u})) = \boldsymbol{b} - \nabla\pi(\omega) & \text{in } U, \\ \boldsymbol{u} = \boldsymbol{0} \quad \text{on } \boldsymbol{\Gamma_o}, \\ (\boldsymbol{B}(\omega)\boldsymbol{\epsilon}(\boldsymbol{u}))\boldsymbol{\nu} = \pi(\omega)\boldsymbol{\nu} + \boldsymbol{t} & \text{on } \Gamma_1. \end{cases}$$

This system is consistent with a model of linear elasticity in which the reference configuration U is isotropic but is *not a natural state* under zero external forces, unless $\pi(\omega) \equiv 0$, i.e., $\omega = 0$ or $1/2$ at *each* point. This agrees with the physical argument that void nucleation and growth demands an increase of volume for a natural state (if any exists at all) and the body cannot be confined to the volume available in U without the action of a residual stress. Consistency with isotropy follows from the fact this this residual stress is here the pressure $\pi(\omega)\boldsymbol{I}$. Naturally, except when $\Gamma_o = \Gamma$, the reference configuration U is not an actual configuration of the material in general.

For our model to be complete, we must introduce suitable evolution equations for the plastic strain $\boldsymbol{\epsilon}^p$ and for the damage variable ω. A differential equation of the

form

$$\dot{\omega} = F^{\phi}(\omega, \boldsymbol{T}^{\phi}), \tag{5.10}$$

where F^{ϕ} is a function to be determined from experiments, is of common use in the literature. This is what is done e.g., by Trampczynski, Hayhurst and Leckie [27], Davison et al. [8]. The former work uses a damage variable ω defined from D (cf. Section 2) instead of Ω, namely $\omega(\boldsymbol{x}) = D(\boldsymbol{\phi}(\boldsymbol{x}))$.[6] But one must be aware that a formulation like (5.10) cannot be valid without severe limitations, because it is not compatible with the basic postulate that damage is not affected by (at least appropriate) unloading. Recall that this postulate enters the very definition of the damage variable (cf. Section 2). Rather, one should say that (5.10) holds when loading occurs, while $\dot{\omega} = 0$ during unloading. The ambiguity is of course to define loading versus unloading, which can be done only in the case of proportional loading. Therefore, it appears that a relation such as (5.10) can be valid only for *monotone proportional* (or nearly proportional, although "monotone" must then be understood in some empirical sense) *loading*. This limited framework is nevertheless relevant in many practical situations.

In [8], where no distinction among stresses needs to be made in view of the completely linear model adopted (in particular, ignoring the residual stress), the function F^{ϕ} in (5.10) is derived from a model for nucleation and growth of microvoids developed by Barbee, Seaman, Crewdson and Curran [2]. In this respect, let us point out that it is indeed worthwhile taking the hint from the materials science approach to derive an appropriate formula for the rate $\dot{\omega}$. However, individual void growth is often measured through parameters which do not directly relate to the density ω (see e.g. Cocks and Ashby [6]) and some difficulties arise in establishing an appropriate correlation. Also, an important ingredient in the determination of F^{ϕ} which is omitted by studies on individual void growth is coalescence of two or more voids: the rapid yielding of the ligament between two adjacent voids resulting in coalescence will make

[6] As has been the case throughout this paper, time-dependence is implicit.

the damage rate $\dot{\omega}$ larger than what it would be in a situation when voids grow in a relatively independent fashion, at least when coalescence is significant. Obviously, the possibility of coalescence increases with the number of voids. This agrees with the premise that nucleation is dominant at the beginning of damage while growth takes over during later stages, as noted by Onat and Leckie [25].

Remark 5.3: Coalescence of two voids is often referred to as "rupture" or "failure" by materials science specialists. This definition is somewhat questionable since coalescence of two voids merely provides a bigger void, whose size is however at the same scale as the size of the original two. In our definition, failure occurs when the voids density ω is large enough to make the elastic moduli vanish ($\omega = 1/2$ if the approach of Section 3 is taken). This makes failure relate to a property of the material, with no concern as to how the critical value of ω is reached (nucleation, individual growth, coalescence or any combination of these).

Summarizing the preceding comments, the function F^{ϕ} should then be taken as the sum of the three rates

$$\text{nucleation} \; + \; \text{individual growth} \; + \; \text{coalescence} \, . \tag{5.11}$$

For the first term, one may refer to the work by Goods and Brown [11] (see also Argon, Im and Safoglu [1]). Individual growth from the point of view of materials science has already been mentioned above. Both the first two terms are considered in Barbee et al. (loc. cit.) who do treat void growth through the volume density ω. But their theory is admittedly limited to small damage and underestimates the actual void volume by a factor of 2 for larger values of ω. We strongly suspect that this is due to not considering the third term in (5.11), for which further investigation is needed. It should be negligible for small damage and dominant as ω approaches $1/2$.

We observe that an expression that agrees with (5.11) has been used by Tvergaard [28], although not in a damage model in the sense of this paper, and according to

other approaches (see the references in [28]). These approaches lead to a function F^{ϕ} in (5.10) which also depends on the stress rate $\dot{T}^{\phi}$. As we shall later see, such expressions are useful to deal with nonproportional or cyclic loading. Allowing F^{ϕ} in (5.10) to depend on ε^p, possible dependence on the plastic strain rate $\dot{\varepsilon}^p$ can also be incorporated in the hypothesis of rate-independent plasticity, namely assuming

$$\dot{\varepsilon}^p = G^{\phi}(\omega, T^{\phi}, \varepsilon^p) \tag{5.12}$$

where $TrG = 0$ is required in view of (4.12). The validity of (5.12) demands the same limitations on the loading process as the validity of (5.10).

Although the above comments are sufficient to demonstrate that much work must be done before a consensus can be reached, and that a formula for F^{ϕ} based on the average measurements dictated by the very definition of ω (e.g., a commonly used power law) is likely to be much too simplistic to encompass all the phenomena involved, some concern must also be expressed regarding T^{ϕ}-dependence of F^{ϕ}. Indeed, the experiments by Trampczynski et al. (loc. cit.) on aluminum alloys agree with a choice of F^{ϕ} depending only on the second invariant J_2 of the deviatoric stress. In contrast, the work of Barbee et al. (loc. cit.) also on aluminum alloys , emphasizes a choice of F^{ϕ} depending only on the hydrostatic pressure $p = (1/3)TrT^{\phi}$. Such a discrepancy can only be explained by the difference in the experimental procedure: steady loading in [27] versus impact in [2]. As a result, it clearly appears that the appropriate form for F^{ϕ} depends on the loading process. At the least, a marked difference must be made between quasistatic and quasi instantaneous loading. This is because the latter is accompanied by a shock wave, the effect of which on nucleation and growth of microvoids is yet to be analyzed.

Remark 5.4: For all the purposes enumerated above, one must bear in mind that nucleation, growth and coalescence of voids *within* the grains only is relevant in isotropic damage (cf. Remark 2.2). This considerably restricts the relevance of the various considerations found in the literature.

A final but important step in the establishment of our model consists in checking its compatibility with the second law of thermodynamics. Doing so will introduce some limitations in the choice of the functions F^{ϕ} and G^{ϕ} (assuming that evolution of the plastic strain is governed by equation (5.12)). The starting point is the system (5.7) which also reads

$$\begin{cases} \text{Div } \boldsymbol{\sigma} + \rho_o \hat{\boldsymbol{b}} = \rho_o \ddot{\boldsymbol{u}} & \text{in } U, \\ \boldsymbol{u} = \boldsymbol{0} & \text{on } \Gamma_o, \\ \boldsymbol{\sigma}\boldsymbol{\nu} = \hat{\boldsymbol{t}} & \text{on } \Gamma_1, \end{cases} \tag{5.13}$$

upon setting

$$\begin{aligned} \boldsymbol{\sigma} &= \boldsymbol{B}(\omega)[\boldsymbol{\epsilon}(\boldsymbol{u}) - (1-\omega)^{-1/3}\boldsymbol{\epsilon}^p], \\ \hat{\boldsymbol{b}} &= \boldsymbol{b} - (1/\rho_o)\nabla\pi(\omega), \\ \hat{\boldsymbol{t}} &= \boldsymbol{t} + \pi(\omega)\boldsymbol{\nu}. \end{aligned}$$

It should be noted that for $\boldsymbol{x} \in U$, $\boldsymbol{\sigma}(\boldsymbol{x})$ appears to be the *total stress* in the reference configuration

$$\boldsymbol{\sigma}(\boldsymbol{x}) = \boldsymbol{T}(\boldsymbol{x}) + \pi(\omega(\boldsymbol{x}))\boldsymbol{I}, \tag{5.14}$$

namely the sum of the first Piola-Kirchhoff and residual stresses at $\boldsymbol{x}$. Relation (5.14) easily follows from (5.5) and (5.1) and the assumption of infinitesimal elastic and plastic strains allowing one to write

$$\boldsymbol{T}(\boldsymbol{x}) = (1-\omega(\boldsymbol{x}))^{-2/3}\boldsymbol{T}^{\phi}(\boldsymbol{\phi}(\boldsymbol{x})) \tag{5.15}$$

upon neglecting higher order terms in $\boldsymbol{\epsilon}^e$ and $\boldsymbol{\epsilon}^p$.

Introducing the energy density $\psi = \psi(\boldsymbol{x}; \omega, \boldsymbol{S}^e)$ where $\boldsymbol{S}^e$ denotes an arbitrary symmetric 3 x 3 tensor, defined by

$$\psi(\boldsymbol{x}; \omega, \boldsymbol{S}^e) = \frac{1}{2\rho_o(\boldsymbol{x})}\boldsymbol{B}(\omega)\boldsymbol{S}^e : \boldsymbol{S}^e, \tag{5.16}$$

one finds

$$\boldsymbol{\sigma} = \rho_o \frac{\partial \psi}{\partial \boldsymbol{S}^e}, \tag{5.17}$$

provided that $\boldsymbol{S}^e$ is taken to be

$$\boldsymbol{S}^e = \boldsymbol{\varepsilon}(\boldsymbol{u}) - (1-\omega)^{-1/3}\boldsymbol{\varepsilon}^p. \tag{5.18}$$

In these notations, the system (5.13) is readily seen to be equivalent to the variational equality

$$-\int_U \rho_o \frac{\partial \psi}{\partial \boldsymbol{S}^e} : \boldsymbol{\varepsilon}(\boldsymbol{v}) + \int_U \rho_o \hat{\boldsymbol{b}} \cdot \boldsymbol{v} = \int_U \rho_o \ddot{\boldsymbol{u}} \cdot \boldsymbol{v},$$

for every admissible motion $\boldsymbol{v}$ (i.e., satisfying $\boldsymbol{v} = \boldsymbol{0}$ on Γ_o). Since the process is isothermal, the corresponding version of the Clausius-Duhem inequality reads

$$\boldsymbol{\sigma} : \dot{\boldsymbol{\varepsilon}}(\boldsymbol{u}) - \rho_o \frac{\partial \psi}{\partial \boldsymbol{S}^e} - \rho_o \dot{\omega} \frac{\partial \psi}{\partial \omega} \geq 0.$$

Equivalently, using (5.17) and (5.18), one finds

$$\boldsymbol{\sigma} : \dot{\boldsymbol{S}}^p - \rho_o \dot{\omega} \frac{\partial \psi}{\partial \omega} \geq 0, \tag{5.19}$$

with

$$\boldsymbol{S}^p \equiv (1-\omega)^{-1/3}\boldsymbol{\varepsilon}^p. \tag{5.20}$$

In order for (5.19) to be satisfied, it suffices that

$$\boldsymbol{\sigma} : \dot{\boldsymbol{S}}^p \geq 0, \tag{5.21}$$

$$-\dot{\omega} \frac{\partial \psi}{\partial \omega} \geq 0. \tag{5.22}$$

From (5.16), an elementary calculation yields

$$\frac{\partial \psi}{\partial \omega}(\boldsymbol{x}; \omega, \boldsymbol{S}^e) = \frac{1}{2\rho_o(\boldsymbol{x})} \left\{ \hat{K}'(\omega)(Tr\boldsymbol{S}^e)^2 + 2\hat{\mu}'(\omega)\boldsymbol{S}^e_D : \boldsymbol{S}^e_D \right\} \tag{5.23}$$

where $\boldsymbol{S}^e_D$ denotes the deviatoric part of $\boldsymbol{S}^e$ and

$$\hat{K}(\omega) = (1-\omega)^{-1/3}K(\omega), \quad \hat{\mu}(\omega) = (1-\omega)^{-1/3}\mu(\omega),$$

with $K(\omega)$ and $\mu(\omega)$ being the bulk and shear moduli respectively. As $\omega(\boldsymbol{x}) = \Omega(\phi(\boldsymbol{x}))$ by definition, $\hat{K}(\omega)$ and $\hat{\mu}(\omega)$ coincide with $\hat{K}(\Omega)$ and $\hat{\mu}(\Omega)$ of Section 3

upon substituting $\Omega = \omega$ and hence are decreasing functions of $\omega \in [0, 1/2]$. With (5.23) we infer that

$$\frac{\partial \psi}{\partial \omega} \leq 0, \quad 0 \leq \omega \leq 1/2,$$

so that relation (5.22) will be satisfied if $\dot{\omega} \geq 0$, namely (cf. (5.10)) if $F^{\phi}(\omega, \boldsymbol{T}^{\phi}) \geq 0$ for $\omega \in [0, 1/2]$. From (5.14) and (5.15), we may define the function $F(\omega, \boldsymbol{\sigma})$ by

$$F(\omega, \boldsymbol{\sigma}) \equiv F^{\phi}(\omega, \boldsymbol{T}^{\phi}). \tag{5.24}$$

It follows that the condition

$$F(\omega, \boldsymbol{\sigma}) \geq 0, \quad 0 \leq \omega \leq 1/2, \tag{5.25}$$

is equivalent to relation (5.22). In words, (5.25) means that the voids density ω *can only increase.* Similarly, set

$$\boldsymbol{G}(\omega, \boldsymbol{\sigma}, \boldsymbol{\varepsilon}^p) \equiv \boldsymbol{G}^{\phi}(\omega, \boldsymbol{T}^{\phi}, \boldsymbol{\varepsilon}^p). \tag{5.26}$$

It is immediate from (5.20) that condition (5.21) holds if and only if

$$\boldsymbol{\sigma} : (\tfrac{1}{3}\dot{\omega}\boldsymbol{\varepsilon}^p + (1-\omega)\dot{\boldsymbol{\varepsilon}}^p) \geq 0, \quad 0 \leq \omega \leq 1/2.$$

Recalling (5.10) and (5.12) and from (5.24) and (5.26) above, this amounts to saying that

$$\boldsymbol{\sigma} : (\tfrac{1}{3}F(\omega, \boldsymbol{\sigma})\boldsymbol{\varepsilon}^p + (1-\omega)\boldsymbol{G}(\omega, \boldsymbol{\sigma}, \boldsymbol{\varepsilon}^p)) \geq 0, \quad 0 \leq \omega \leq 1/2\ . \tag{5.27}$$

Thus, with the choice of $\boldsymbol{S}^e$ as in (5.18) and ω as internal variables, the proposed model is compatible with the second law of thermodynamics provided that inequalities (5.25) and (5.27) hold.

As mentioned earlier, neither relation (5.10) or (5.12) can be used for the evolution of damage or plastic strain under nonproportional or cyclic loading. It has been known for long that invariance of the plastic strain upon unloading can conveniently be handled by the introduction of a *yield surface* for the evolution of $\boldsymbol{\varepsilon}^p$. The same

idea can then be applied to the evolution of the damage ω. The dissipative nature of the damaging process suggests the introduction of a flow potential $P = P(\omega, \xi)$ where ξ denotes the variable conjugate to the damage variable, namely (see also (5.23))

$$\xi = -\frac{\partial \psi}{\partial \omega}(\boldsymbol{x}; \omega, \boldsymbol{S}^e) = -\frac{1}{2\rho_o(\boldsymbol{x})}\boldsymbol{B}'(\omega)\boldsymbol{S}^e : \boldsymbol{S}^e, \tag{5.28}$$

and $\boldsymbol{S}^e$ is given by (5.18). Evolution of the damage variable is then accounted for by the equation (assuming smoothness of the potential P)

$$\dot{\omega} = \begin{cases} -[(\partial P/\partial \xi)(\omega, \xi)/(\partial P/\partial \omega)(\omega, \xi)]\dot{\xi} & \text{if } P(\omega, \xi) = 0 \text{ and } (\partial P/\partial \xi)(\omega, \xi)\dot{\xi} \geq 0, \\ 0 \text{ otherwise.} \end{cases} \tag{5.29}$$

The condition $(\partial P/\partial \xi)(\omega, \xi)\dot{\xi} \geq 0$ must be interpreted as a loading criterion. Monotonicity of damage thus requires that

$$(\partial P/\partial \omega)(\omega, \xi) < 0$$

if $P(\omega, \xi) = 0$ and $(\partial P/\partial \xi)(\omega, \xi)\dot{\xi} \geq 0$. Observing that both ω and ξ are nonnegative ($\xi \geq 0$ follows from (5.28) and (5.23) and the growth properties of the functions $\hat{K}$ and $\hat{\mu}$), a sufficient condition for $\dot{\omega} \geq 0$ is then that

$$\{\omega \geq 0, \quad \xi \geq 0, \quad P(\omega, \xi) = 0\} \Rightarrow \left\{\frac{\partial P}{\partial \omega}(\omega, \xi) < 0, \quad \frac{\partial P}{\partial \xi}(\omega, \xi) > 0\right\}. \tag{5.30}$$

If so, the loading condition reduces to

$$\dot{\xi} \geq 0 \tag{5.31}$$

and the inequality

$$\xi\dot{\omega} \geq 0$$

ensuring dissipation (compliance with the Clausius-Duhem inequality) is automatically satisfied. The above formalism, which is compatible with damage being unaffected along appropriate unloading paths, was suggested by Krajcinovic [17].

It is rather unlikely that the potential P can be determined on the basis of energy release measurements since dissipation due to damage cannot be distinguished from

dissipation due to the plastic strain. However, existence of the potential P rather than its explicit form is important for the theory. Indeed, suppose that P exists such that (5.30) is fulfilled. It is easily checked that in view of the loading criterion (5.31), the equation (5.29) can be rewritten as

$$\dot{\omega}_t = \begin{cases} -[(\partial P/\partial \xi)(\omega_t, \xi_t)/(\partial P/\partial \omega)(\omega_t, \xi_t)]\dot{\xi}_t & \text{if } \dot{\xi}_t \geq 0 \text{ and } \xi_t = \max(\max_{s\in[0,t]} \xi_s, \bar{\xi}), \\ 0 \text{ otherwise.} \end{cases} \tag{5.32}$$

where the subscript "t" relates to the value of the variable at time t, and where $\bar{\xi}$ denotes the unique real root of $P(0, \bar{\xi}) = 0$. Uniqueness of $\bar{\xi}$ follows from the condition $(\partial P/\partial \xi)(0, \xi) > 0$ whenever $P(0, \xi) = 0$. Existence of $\bar{\xi}$ is guaranteed if $P(0,0) < 0$ and $\lim_{\xi\to\infty} P(0, \xi) > 0$. Now, it is easily seen from (5.16) and (5.17) that another expression for the variable ξ introduced in (5.28) is

$$\xi = -\frac{1}{2\rho_o(\boldsymbol{x})} \boldsymbol{B}'(\omega)(\boldsymbol{B}^{-1}(\omega)\boldsymbol{\sigma} : \boldsymbol{B}^{-1}(\omega)\boldsymbol{\sigma}).$$

Therefore, relation (5.32) is equivalent to a differential equation of the form

$$\dot{\omega}_t = \begin{cases} \boldsymbol{F}(\omega_t, \boldsymbol{\sigma}_t) : \dot{\boldsymbol{\sigma}}_t & \text{if } \dot{\xi}_t \geq 0 \text{ and } \xi_t = \max(\max_{s\in[0,t]} \xi_s, \bar{\xi}). \\ 0 \text{ otherwise.} \end{cases}$$

Of course, the vector-valued function $\boldsymbol{F}$ depends on the potential P. But, unlike $P(\omega, \xi)$, the expression $\boldsymbol{F}(\omega, \boldsymbol{\sigma}) : \dot{\boldsymbol{\sigma}}$ directly relates to void growth and nucleation and hence should be more easily accessible to experimental determination. We note that similar expressions already used in the literature (see Tvergaard [28] and the references therein) agree with the stress rate $\dot{\boldsymbol{\sigma}}$ entering linearly. Regarding the Clausius-Duhem inequality, a formula for $\boldsymbol{F}(\omega, \boldsymbol{\sigma}) : \dot{\boldsymbol{\sigma}}$ qualifies if and only if

$$\boldsymbol{F}(\omega_t, \boldsymbol{\sigma}_t) : \dot{\boldsymbol{\sigma}}_t \geq 0 \text{ whenever } \dot{\xi}_t \geq 0 \text{ and } \xi_t = \max(\max_{s\in[0,t]} \xi_s, \bar{\xi}),$$

where the number $\bar{\xi}$ also is to be determined from experiments.

For the evolution of the plastic strain, namely that of the variable $\boldsymbol{S}^p$ (cf. (5.20)), the same procedure applies: the evolution of $\boldsymbol{S}^p$ may be governed by a flow potential

Q and the associated flow rule. Typically, $Q = Q(\omega, \boldsymbol{\sigma}, \boldsymbol{\chi})$ where $\boldsymbol{\chi}$ denotes a family of suitable hardening parameters. For this, the reader is referred to the standard literature on plasticity theory, except that the contribution of damage to the potential Q remains to be determined. Apparently, there is no contradiction with basic principles in introducing two different potentials P and Q. This approach is consistent with damage and plastic slip resulting from distinct phenomena (voids nucleation and growth versus dislocations). Of course, using two different potentials induces two different notions for loading and unloading, but there is nothing wrong with that either: one merely needs a "compatibility condition" between P and Q

ensuring that unloading paths exist that are indeed unloading paths for both P and Q, a very mild restriction in practice.

6 Mathematical Aspects

This section is intended to show that the model for isotropic damage developed earlier leads to mathematically tractable boundary value problems. For simplicity, we shall limit ourselves to the *quasistatic* problem when $\boldsymbol{u}(t, \cdot)$ is an equilibrium position for all t. This means that the forces are varied sufficiently slowly for the acceleration term in (5.7) to be negligible and the equations thus take the form

$$\begin{cases} \text{Div } \left[\boldsymbol{B}(\omega)(\boldsymbol{\varepsilon}(\boldsymbol{u}) - (1-\omega)^{-1/3}\boldsymbol{\varepsilon}^p)\right] - \nabla\pi(\omega) + \rho_o \boldsymbol{b} = \boldsymbol{0} \quad \text{in } U, \\ \boldsymbol{u} = \boldsymbol{0} \quad \text{on } \Gamma_o, \\ \boldsymbol{B}(\omega)(\boldsymbol{\varepsilon}(\boldsymbol{u}) - (1-\omega)^{-1/3}\boldsymbol{\varepsilon}^p)\boldsymbol{\nu} = \pi(\omega)\boldsymbol{\nu} + \boldsymbol{t} \quad \text{on } \Gamma_1, \end{cases}$$

with evolution laws given by (5.11) and (5.12), namely (cf. (5.24) and (5.26))

$$\begin{aligned} \dot{\omega} &= F(\omega, \boldsymbol{\sigma}), \qquad \omega = 0 \text{ at t} = 0, \\ \dot{\boldsymbol{\varepsilon}}^p &= \boldsymbol{G}(\omega, \boldsymbol{\sigma}, \boldsymbol{\varepsilon}^p), \quad \boldsymbol{\varepsilon}^p = 0 \text{ at t} = 0. \end{aligned}$$

The initial conditions are taken for consistency with the assumption of an originally virgin material in a natural configuration, but they could be arbitrarily chosen for mathematical purposes. Recall also that the above evolution laws are valid within the limited framework of (nearly) proportional and monotone loading (see Section 5).

It will be somewhat more convenient to use the variable $\boldsymbol{S}^p$ introduced in (5.20) instead of $\boldsymbol{\varepsilon}^p$. Accordingly, we shall then consider the problem

$$\begin{cases} \text{Div } [\boldsymbol{B}(\omega)(\boldsymbol{\varepsilon}(\boldsymbol{u}) - \boldsymbol{S}^p)] - \nabla\pi(\omega) + \rho_o \boldsymbol{b} = \boldsymbol{0} \quad \text{in } U, \\ \boldsymbol{u} = \boldsymbol{0} \quad \text{on } \Gamma_o, \\ \boldsymbol{B}(\omega)(\boldsymbol{\varepsilon}(\boldsymbol{u}) - \boldsymbol{S}^p)\boldsymbol{\nu} = \pi(\omega)\boldsymbol{\nu} + \boldsymbol{t} \quad \text{on } \Gamma_1, \end{cases} \tag{6.1}$$

$$\begin{aligned} \dot{\omega} &= F(\omega, \boldsymbol{\sigma}), \\ \dot{\boldsymbol{S}}^p &= \boldsymbol{H}(\omega, \boldsymbol{\sigma}, \boldsymbol{S}^p), \end{aligned} \tag{6.2}$$

$$\begin{aligned} &\omega = 0 \text{ at } t = 0, \\ &\boldsymbol{S}^p = 0 \text{ at } t = 0, \end{aligned} \tag{6.3}$$

where, as before

$$\boldsymbol{\sigma} \equiv \boldsymbol{B}(\omega)(\boldsymbol{\varepsilon}(\boldsymbol{u}) - \boldsymbol{S}^p) \tag{6.4}$$

and

$$\boldsymbol{H}(\omega, \boldsymbol{\sigma}, \boldsymbol{S}^p) \equiv \frac{1}{3}(1-\omega)^{-1} F(\omega, \boldsymbol{\sigma})\boldsymbol{S}^p + (1-\omega)^{-1/3}\boldsymbol{G}(\omega, \boldsymbol{\sigma}, (1-\omega)^{1/3}\boldsymbol{S}^p). \tag{6.5}$$

In Sections 4 and 5, we confined our attention to the physically realistic values $0 \leq \omega \leq 1/2$. Here, it will be more appropriate to let ω run over the entire real line and extend the functions $\boldsymbol{B}$, π, F and $\boldsymbol{H}$ by setting

$$\begin{aligned} \boldsymbol{B}(\omega) &= \boldsymbol{B}(0)(= \boldsymbol{A}(0)), \\ \pi(\omega) &= \pi(0), \\ F(\omega, \boldsymbol{\sigma}) &= F(0, \boldsymbol{\sigma}), \\ \boldsymbol{H}(\omega, \boldsymbol{\sigma}, \boldsymbol{S}^p) &= \boldsymbol{H}(0, \boldsymbol{\sigma}, \boldsymbol{S}^p), \end{aligned} \tag{6.6}$$

if $\omega \leq 0$ and

$$\begin{aligned} \boldsymbol{B}(\omega) &= \boldsymbol{B}(1/2) = \boldsymbol{0}, \\ \pi(\omega) &= \pi(1/2) = 0, \\ F(\omega, \boldsymbol{\sigma}) &= F(1/2, \boldsymbol{\sigma}), \\ \boldsymbol{H}(\omega, \boldsymbol{\sigma}, \boldsymbol{S}^p) &= \boldsymbol{H}(1/2, \boldsymbol{\sigma}, \boldsymbol{S}^p), \end{aligned} \tag{6.7}$$

if $\omega \geq 1/2$.

With these extensions being performed, the structure of the problem (6.1)-(6.3) is reminiscent of others studied by Nečas and Hlavaček [23] (see also John [13]). Accordingly, existence and uniqueness results can be expected to follow from the variational characterization of $\boldsymbol{u}$, namely

$$\int_U \boldsymbol{B}(\omega_t)\boldsymbol{\varepsilon}(\boldsymbol{u}_t) : \boldsymbol{\varepsilon}(\boldsymbol{v}) - \int_U \boldsymbol{B}(\omega_t)\boldsymbol{S}_t^p : \boldsymbol{\varepsilon}(\boldsymbol{v}) =$$
$$\int_U \rho_o \boldsymbol{b}_t \cdot \boldsymbol{v} + \int_U \pi(\omega_t)\ \mathrm{div}\ \boldsymbol{v} + \int_{\Gamma_1} \boldsymbol{t}_t \cdot \boldsymbol{v}\mathrm{dA}, \quad \forall \boldsymbol{v} \in \mathrm{V}, \tag{6.8}$$

for every t of some time-interval $[0,T]$ (where, again, ω_t denotes the partial mapping $\omega(t,\cdot)$ and *not* a partial derivative and similarly with $\boldsymbol{u}_t$, $\boldsymbol{S}_t^p$, etc.), and where V is a suitable space of admissible displacements. Clearly, the formulation (6.8) suggests the choice[7]

$$V = \left\{ \boldsymbol{v} \in (H^1(U))^3;\ \ \boldsymbol{v} = \boldsymbol{0} \text{ on } \Gamma_o \right\}. \tag{6.9}$$

For consistency, it is then necessary that the coefficients of $\boldsymbol{B}(\omega_t)$ belong to $L^\infty(U)$ and one may anticipate that it will somewhere be necessary that these coefficients depend continuously on ω_t. This condition is met if one requires

$$\omega \in C^1([I,T],\ \mathcal{L}^\infty(\mathcal{U})). \tag{6.10}$$

But a difficulty then arises from the evolution equations (6.2), which, using (6.3), may be rewritten as

$$\begin{aligned} \omega_t &= \int_o^t F(\omega_s, \boldsymbol{\sigma}_s)ds, \\ \boldsymbol{S}_t^p &= \int_o^t \boldsymbol{H}(\omega_s, \boldsymbol{\sigma}_s, \boldsymbol{S}_s^p)ds. \end{aligned}$$

Indeed, no matter how smooth the functions F and $\boldsymbol{H}$, it follows from (6.4) that $F(\omega_s, \boldsymbol{\sigma}_s)$ and $\boldsymbol{H}(\omega_s, \boldsymbol{\sigma}_s, \boldsymbol{S}_s^p)$ will merely be square integrable since $\boldsymbol{\sigma}_s$ is no better than square integrable for $\boldsymbol{u}_s \in V$. Of course, one may think about looking for

[7]Standard notations are used regarding Sobolev spaces.

$\omega \in \mathcal{C}^1([I,T],\mathcal{L}^6(\mathcal{U}))$ instead of (6.10), as is done in [13,23]. But this is not compatible with the coefficients of $\boldsymbol{B}(\omega_t)$ being continuous function of ω_t in the $L^\infty(U)$-norm (although these coefficients *are* in $L^\infty(U)$ as soon as ω_t is measurable).

Remark 6.1: The above observations are not in contradiction with the results in [13,23]: a simple examination reveals that the existence and uniqueness results given there require much too stringent assumptions (in many respects) for our purposes.

To overcome these difficulties, it is reasonable to choose the following modification of the original problem: pick an arbitrary function $\theta \in L^\infty(\boldsymbol{R}^3)$ with compact support and set for $\boldsymbol{v} \in V$ ($\boldsymbol{\varepsilon}(\boldsymbol{v})$ being extended by $\mathbf{0}$ outside $\bar{U}$)

$$\boldsymbol{\varepsilon}^*(\boldsymbol{v}) \equiv \theta * \boldsymbol{\varepsilon}(\boldsymbol{v}) \in \mathcal{C}^1(\bar{\mathcal{U}}) \tag{6.11}$$

and (compare with (6.4))

$$\boldsymbol{\sigma}^* \equiv \boldsymbol{B}(\omega)(\boldsymbol{\varepsilon}^*(\boldsymbol{u}) - \boldsymbol{S}^p). \tag{6.12}$$

Now, instead of (6.2) and (6.3), prescribe the evolution of ω and $\boldsymbol{S}^p$ through

$$\begin{aligned} \dot{\omega} &= F(\omega, \boldsymbol{\sigma}^*), \qquad \omega = 0 \text{ at } t = 0, \\ \dot{\boldsymbol{S}}^p &= \boldsymbol{H}(\omega, \boldsymbol{\sigma}^*, \boldsymbol{S}^p), \quad \boldsymbol{S}^p = 0 \text{ at } t = 0. \end{aligned}$$

Then, the previous discrepancy has disappeared if F and $\boldsymbol{H}$ are continuous and

$$\boldsymbol{S}^p \in \mathcal{C}^1([I,T], \pm_t),$$

where

$$\Sigma_o = \{\boldsymbol{S} \in \Sigma, \quad Tr\boldsymbol{S} = 0\}$$

and

$$\Sigma = \left\{\boldsymbol{S} = (S_{ij}) \in (\mathcal{C}^1(\bar{\mathcal{U}}))^3; \quad \mathcal{S}_{|1} = \mathcal{S}_{|2}\right\}.$$

The above modification of the original problem is justified by the observation that $\boldsymbol{\varepsilon}^*(\boldsymbol{u}) = \boldsymbol{\varepsilon}(\boldsymbol{u})$ in the limiting case when θ is the Dirac delta (so that, in practice, θ should be taken as an approximation of the Dirac delta). Also, note the crucial property that

$$\boldsymbol{v} \in V \mapsto \boldsymbol{\varepsilon}^*(\boldsymbol{v}) \in \Sigma$$

is continuous, as it follows from standard results on convolution.

Summing up, we shall investigate existence and uniqueness of solution for the problem

$$\int_U \boldsymbol{B}(\omega_t)\boldsymbol{\varepsilon}(\boldsymbol{u}_t) : \boldsymbol{\varepsilon}(\boldsymbol{v}) - \int_U \boldsymbol{B}(\omega_t)\boldsymbol{S}_t^p : \boldsymbol{\varepsilon}(\boldsymbol{v}) =$$

$$= \int_U \rho_o \boldsymbol{b}_t \cdot \boldsymbol{v} + \int_U \pi(\omega_t)\ \text{div}\ \boldsymbol{v} + \int_{\Gamma_1} \boldsymbol{t}_t \cdot \boldsymbol{v}\text{dA},\ \forall \boldsymbol{v} \in \text{V}, \forall \text{t} \in [0, \text{T}], \quad (6.13)$$

$$\omega_t = \int_0^t F(\omega_s, \boldsymbol{\sigma}_s^*)ds, \quad (6.14)$$

$$\boldsymbol{S}_t^p = \int_0^t \boldsymbol{H}(\omega_s, \boldsymbol{\sigma}_s^*, \boldsymbol{S}_s^p)ds. \quad (6.15)$$

In what follows, it will be assumed that meas $\Gamma_o > 0$, F and $\boldsymbol{H}$ are locally Lipschitz continuous and

$$\rho_o \in L^\infty(U),$$

$$\boldsymbol{b} \in C^1([\prime, \infty), (\mathcal{L}^\epsilon(\mathcal{U}))^\ni),$$

$$\boldsymbol{t} \in C^1([\prime, \infty), (\mathcal{L}^\epsilon(-\infty))^\ni).$$

Call $\boldsymbol{u}_o \in V$ the solution of (6.13) for $t = 0$ (recall $\omega_o = 0$ and $\boldsymbol{S}_o^p = \boldsymbol{0}$). That $\boldsymbol{u}_o$ exists and is unique follows from $\boldsymbol{B}(0)$ being elliptic and Korn's inequality (see e.g. [15]). Identify $\boldsymbol{u}_o$ with the corresponding t-independent function in $C^1([\prime, \delta], \mathcal{V})$ where $\delta > 0$ is arbitrary and let $\mathcal{B}$ denote the (closed) ball with centre $\boldsymbol{u}_o$ and radius one in the space $C^1([\prime, \delta], \mathcal{V})$. Similarly, denote by $\mathcal{B}'$ the (closed) ball with centre $(0, \boldsymbol{0})$ and radius $1/4$ in the space $C_1^1([\prime, \delta], C^1(\mathcal{H}))$ x $C_1^1([\prime, \delta], \Sigma_o)$, where the subscript "$o$" in C_1^1 refers to those elements vanishing at $t = 0$.

Pick $\boldsymbol{u} \in \mathcal{B}$. Then, recalling (6.12) and our assumptions on F and $\boldsymbol{H}$, it follows from the classical theory of O.D.E.'s that the system (6.14) - (6.15) has a unique solution

$$(\omega, \boldsymbol{S}^p) \varepsilon C_1^1([\prime, \delta], C^1(\mathcal{H})) \times C_1^1([\prime, \delta], \pm_1).$$

It is straightforward to check when $\delta > 0$ is small enough that $(\omega, \boldsymbol{S}^p) \epsilon \mathcal{B}'$ and that the mapping

$$\boldsymbol{u} \in \mathcal{B} \mapsto (\omega, \boldsymbol{S}^{\checkmark}) \in \mathcal{B}', \tag{6.16}$$

is a contraction with constant $k(\delta)$ verifying

$$\lim_{\delta \to 0} k(\delta) = 0. \tag{6.17}$$

Conversely, pick $(\omega, \boldsymbol{S}^p) \in \mathcal{B}'$. Since $\mathcal{B}'$ has radius $1/4$, one has

$$\boldsymbol{B}(\omega_t)\boldsymbol{S} : \boldsymbol{S} \geq \boldsymbol{B}(1/4)\boldsymbol{S} : \boldsymbol{S} \geq \alpha |\boldsymbol{S}|^2, \tag{6.18}$$

for every symmetric 3 x 3 tensor $\boldsymbol{S}$, where α is a positive constant and where

$$|\boldsymbol{S}|^2 \equiv \boldsymbol{S} : \boldsymbol{S}.$$

It follows that the variational problem (6.13) has a unique solution $\boldsymbol{u}_t \in V$ for every $t \in [0, \delta]$. It is readily checked that this defines $\boldsymbol{u}$ as an element of $C^1([I, \delta], \mathcal{V})$ such that $\boldsymbol{u}_t = \boldsymbol{u}_o$ for $t = 0$. In particular, $\boldsymbol{u} \in \mathcal{B}$ if $\delta > 0$ is small enough. Moreover, the mapping

$$(\omega, \boldsymbol{S}^p) \in \mathcal{B}' \mapsto \boldsymbol{u} \in \mathcal{B}, \tag{6.19}$$

is Lipschitz continuous with constant $C > 0$ independent of δ. This is easily seen from (6.18) and the observation that the mappings $\boldsymbol{B}(\omega)$ and $\pi(\omega)$ are (uniformly) Lipschitz continuous functions of $\omega \in \boldsymbol{R}$. From (6.17), one thus finds that the composition of the mappings (6.19) and (6.16) has a unique fixed point ($\delta > 0$ small enough being fixed). Each such fixed point providing a solution to the system (6.13)-(6.15) verifying the desired continuous dependence in time, there follows the existence and uniqueness of such a solution on $[0, \delta]$.

Now, let $T > 0$ denote the upper bound of those δ's as above. Then, a unique solution to (6.13)-(6.15) exists on $[0, T)$. Suppose that $T < \infty$ and that

$$\sup_{t \in [0,T)} \| \omega_t \|_{C^1(\mathcal{B})} = a < 1/2. \tag{6.20}$$

and

$$\sup_{t\in[0,T)} \| \boldsymbol{S}_t^p \|_{\Sigma_o} < \infty. \tag{6.21}$$

Then,

$$\boldsymbol{B}(\omega_t)\boldsymbol{S} : \boldsymbol{S} \geq \boldsymbol{B}(a)\boldsymbol{S} : \boldsymbol{S} \geq \alpha|\boldsymbol{S}|^2, \quad \forall t \in [0,T), \tag{6.22}$$

for every symmetric 3 x 3 tensor $\boldsymbol{S}$ and some constant $\alpha > 0$. Taking $\boldsymbol{v} = \boldsymbol{u}_t$ in (6.13), it is immediate from (6.20)-(6.22) that

$$\sup_{t\in[0,T)} \| \boldsymbol{u}_t \|_V < \infty.$$

In turn, with (6.21) and (6.12), the above yields

$$\sup_{t\in[0,T)} \| \sigma_t^* \|_\Sigma < \infty. \tag{6.23}$$

Combining (6.20), (6.21) and (6.23), one finds that the functions $F(\omega_s, \boldsymbol{\sigma}_s^*)$ and $\boldsymbol{H}(\omega_s, \sigma_s^*, \boldsymbol{S}_s^p)$ are bounded for $s \in [0,T)$. Hence

$$|\omega_{t_1} - \omega_{t_2}| \leq M|t_1 - t_2|, \quad |\boldsymbol{S}_{t_1}^p - \boldsymbol{S}_{t_2}^p| \leq M|t_1 - t_2|, \tag{6.24}$$

for t_1, t_2 in $[0,T)$, where M is a constant independent of t_1 and t_2. Through Cauchy's criterion, (6.24) shows that

$$\begin{aligned} \omega_T &\equiv \lim_{t\to T^-} \omega_t \in C^1(\overline{\mathcal{A}}), \\ \boldsymbol{S}_T^p &\equiv \lim_{t\to T^-} S_t^p \in \Sigma_o, \end{aligned}$$

exist and define continuous extensions of ω and $\boldsymbol{S}^p$ on $[0,T]$. Inequality (6.22) remains valid for $t = T$, which suffices to guarantee the existence and uniqueness of a solution $\boldsymbol{u}_T \in V$ of (6.13) for $t = T$. There is no difficulty in checking that

$$\boldsymbol{u}_T = \lim_{t\to T^-} \boldsymbol{u}_t \in V,$$

which defines a continuous extension of $\boldsymbol{u}$ to $[0,T]$. But then, it is possible to extend the solution to the interval $[T, T+\delta]$ for $\delta > 0$ small enough (depending on T) and this

extension is unique. To see this, it suffices to repeat the arguments for existence and uniqueness on $[0,\delta]$ upon replacing $\mathcal{B}$ by the ball with centre $\boldsymbol{u}_T$ (constant function of t) and radius one and $\mathcal{B}'$ by the ball with centre $(\omega_T, \boldsymbol{S}^p_T)$ and radius $a/2$ (with a as in (6.20)) in the affine subspace of the space $\mathcal{C}^1([\mathcal{T},\mathcal{T}+\delta],\mathcal{C}^1(\bar{\mathcal{U}})) \times \mathcal{C}^1([\mathcal{T},\mathcal{T}+\delta],\ \pm_l)$ of those elements taking the value $(\omega_T,\ \boldsymbol{S}^p_T)$ for $t = T$. Since this contradicts the definition of T, we conclude that a solution

$$\begin{aligned}
&\boldsymbol{u} \in \mathcal{C}^1([\mathcal{I},\mathcal{T}),\mathcal{V}),\\
&\omega \in \mathcal{C}^1([\mathcal{I},\mathcal{T}),\mathcal{C}^1(\bar{\mathcal{U}})),\\
&\boldsymbol{S}^p \in \mathcal{C}^1([\mathcal{I},\mathcal{T}),\pm_l),
\end{aligned}$$

of the system (6.13)-(6.15) exists and is unique on the interval $[0,T)$ where T is the smallest value for which either

$$\sup_{t\in[0,T)} \| \omega_t \|_{\mathcal{C}^1(\bar{\mathcal{U}})} = 1/2, \tag{6.25}$$

or

$$\sup_{t\in[0,T)} \| \boldsymbol{S}^p_t \|_{\Sigma_o} = \infty. \tag{6.26}$$

In view of (5.20), it is clear that (6.26) occurs before (6.25) only if the plastic strain has become infinite before ω has reached the value $1/2$, a case with no significance in our model limited to small elastic and plastic strain. If $\| \boldsymbol{S}^p_t \|_{\Sigma_o}$ remains small, so that (6.25) happens first, then T can be taken as the failure time since the assumption $F \geq 0$ guarantees that $\omega_t \geq 0$ for every $t \in [0,T)$ and there must be points $\boldsymbol{x} \in \bar{U}$ such that $\sup_{t\in[0,T]} \omega_t(\boldsymbol{x}) = 1/2$. These points $\boldsymbol{x} \in \bar{U}$ are those at which failure occurs at time T and therefore are those at which crack initiation takes place.

The case of the pure traction problem (i.e. $\Gamma_o = \phi$) can be handled in a quite similar way. In this case, uniqueness is to be understood to within infinitesimal rigid motions and existence requires the compatibility conditions

$$\int_U \rho_o \boldsymbol{b}_t \cdot \boldsymbol{v} - \int_U \pi(\omega_t)\ \mathrm{div}\ \boldsymbol{v} + \int_{\partial U} \boldsymbol{t}_t \cdot \boldsymbol{v} \mathrm{d}A = 0,$$

to hold for every $t \geq 0$ and every infinitesimal rigid motion $\boldsymbol{v}$. As such a motion is always divergence-free, these conditions take the standard form

$$\int_U \rho_o \boldsymbol{b}_t + \int_{\partial U} \boldsymbol{t}_t dA = \boldsymbol{0},$$
$$\int_U \rho_o \boldsymbol{b}_t \times \boldsymbol{x} + \int_{\partial U} \boldsymbol{t}_t \times \boldsymbol{x} dA = \boldsymbol{0},$$

for every $t \geq 0$.

For completeness, let us mention that in the case of the *pure displacement* problem, an alternative proof of existence and uniqueness of solution to the problem (6.1)-(6.3) (and not of its variational and modified form (6.13)-(6.15)) can be given, at least if the functions F and $\boldsymbol{H}$ are *smooth enough* prior to be extended as in (6.6) and (6.7), such an extension being unnecessary. Again, the proof is based on a contraction argument, but solutions are sought in Hölder spaces. More precisely

$$\boldsymbol{u} \in C^1([I, T), \ C^{\epsilon,\alpha}(\bar{\Omega})),$$
$$\omega \in C^1([I, T), \ C^{\infty,\alpha}(\bar{\Omega})),$$
$$\boldsymbol{S}^p \in C^1([I, T), \ \pm_1^{\infty,\alpha})$$

where

$$\Sigma_o^{1,\alpha} = \{\boldsymbol{S} \in \Sigma^{1,\alpha}; \ \ Tr\boldsymbol{S} = 0\}$$

and

$$\Sigma^{1,\alpha} = \{\boldsymbol{S} = (S_{ij}) \in (C^{\infty\alpha}(\bar{\Omega}))^3; \ \ S_{|1} = S_{|2}\}.$$

Here, α denotes any real number such that $0 < \alpha < 1$. The data must be chosen accordingly, namely

$$\rho_o \in C^{1,\alpha}(\bar{\Omega})$$
$$\boldsymbol{b} \in C^1([I, \infty), \ (C^{1,\alpha}(\bar{\Omega}))^3)$$

with boundary values in $(C^{\epsilon,\alpha}(\partial\mathcal{U}))^3$. The proof no longer relies on the variational approach but makes essential use of regularity properties of the linearized system

of elasticity, in particular Theorem 6.3.7 of Morrey [22]. It follows that while this approach can be applied to the pure traction problem as well—assuming $\boldsymbol{t} \in \mathcal{C}^1([\prime, \infty), (\mathcal{C}^{1,\alpha}(\partial\mathcal{U}))^3)$ —it is not appropriate for the mixed displacement-traction problem. Recall indeed that good regularity results for the linearized system of elasticity are known to be lacking for mixed boundary conditions. Furthermore, smoothness of the functions F and $\boldsymbol{H}$ seems to be somewhat atypical and, in practice, they should then be replaced by smooth approximations. Since this approach does not eliminate a smoothing step of some kind, the details of the corresponding technical proof will be omitted.

Remark 6.2: A priori, the same fixed point method as above could also be applied to the non-quasistatic problem provided that suitable initial conditions are prescribed for $\boldsymbol{u}$ and $d\boldsymbol{u}/dt$. However, an unexpected difficulty arises from the fact that the mapping

$$\boldsymbol{v} \in V \mapsto \int_U \pi(\omega) \text{ div } \boldsymbol{v},$$

is obviously not continuous for the $(L^2(U))^3$ - topology. It follows that the classical results in Lions and Magenes [21] fail to provide existence and uniqueness of a solution $\boldsymbol{u} \in \mathcal{C}^1([\prime, T], \mathcal{V})$. More work thus needs to be done to determine an appropriate setting in which the non-quasistatic problem can be shown to have a unique solution up to failure.

Remark 6.3: If the evolution laws (6.2) for damage and plastic strains are replaced by suitable flow conditions as is required for the study of nonproportional or cyclic loading (see Section 5), the method described by Korneev and Langer [16] seems to be appropriate to establish existence and uniqueness of solutions (up to failure) in a reasonable approximate problem. Roughly speaking, the approximation consists in introducing some inertia in the yield condition to eliminate discontinuities. But this method uses regularity of the linearized operator of elasticity, hence is limited to the pure displacement or pure traction problems. In particular, the regularity statement

in [16, p. 53] about the mixed problem is incorrect.

References for Chapter 2

1. Argon, A.S., Im, J. and Safoglu, R., Cavity Formation from Inclusions in Ductile Fracture, *Metal. Trans.*, 6A, pp. 825-837 (1975).

2. Barbee, T. W., Seaman, L., Crewdson, R. and Curran, D., Dynamic Fracture Criteria for Ductile and Brittle Metals, *J. Materials*, 7, pp. 393-401 (1972).

3. Budiansky, B., Thermal and Thermoelastic Properties of Isotropic Composites, *J. Comp. Materials*, 4, pp. 286-295 (1970).

4. Ciarlet, P.G., *Elasticité Tridimensionnelle*, RMA1, Masson (1985).

5. Ciarlet, P.G., *Mathematical Elasticity*, Vol 1, North-Holland (to appear).

6. Cocks, A.C.F. and Ashby, M.F., On Creep Fracture by Void Growth, *Prog. Mat. Sc.*, 27, pp. 189-244 (1982).

7. Davison, L. and Stevens, A.L., Thermomechanical Constitution of Spalling Elastic Bodies, *J. Appl. Phys.*, 44, pp. 667-674 (1973).

8. Davison, L., Stevens, A.L. and Kipp, M.E., Theory of Spall Damage Accumulation in Ductile Metals, *J. Mech. Phys. Solids*, 25, pp. 11-28 (1977).

9. Fardshisheh, F. and Onat, E.T., Representation of Creep Rate Sensitivity and Plasticity, *Siam J. Appl. Math.*, 25, pp. 522-538 (1973).

10. Gel'Fand, I.M. and Shapiro, Z. Ya, Representations of the Group of Rotations in Three-Dimensional Space and Their Applications, *AMS Translations*, (2), 2, pp. 207-316 (1956).

11. Goods, S.M. and Brown, L.M., The Nucleation of Cavities by Plastic Deformation, *Act. Metal.* 27, pp. 1-15 (1979).

12. Hutchinson, J.W., Constitutive Behavior and Crack Tip Fields for Materials Undergoing Creep-Constrained Grain Boundary Cavitation, *Act. Metal.*, 31, pp. 1079-1088 (1983).

13. John, O., On the Solution of the Displacement Boundary Value Problem for Elastic - Inelastic Materials, *Apl. Mat.*, 19, pp. 61-71 (1974).

14. Kachanov, L.M., Time of the Fracture Process Under Creep Conditions, *Izv. Akad. Nauk SSSR*, 8, pp. 26-31 (1958).

15. Kikuchi, N. and Oden, J.T., *Contact Problems in Elasticity*, SIAM Publications (1988).

16. Korneev, V.G. and Langer, U., *Approximate Solution of Plastic Flow Theory Problems*, Teubner-Texte zur Mathematik, 69, (1984).

17. Krajcinovic, D., Constitutive Equation for Damaging Materials, *J. Appl. Mech.*, 50, pp. 355-360 (1983).

18. Krajcinovic, D. and Fonseka, G.U., The Continuous Damage Theory of Brittle Materials, Part I: General Theory, *ASME J. Appl. Mech.*, 48, pp. 809-815 (1981).

19. Lee, E.H., Elastic Plastic Deformations at Finite Strains, *J. Appl. Mech. Tran. ASCE*, pp 1-6 (1969).

20. Lemaitre, J., Coupled Elasto - Plasticity and Damage Constitutive Equations, in *FENOMECH '84*, J. St. Doltsinis ed., pp 31-49, North-Holland (1985).

21. Lions, J. L. and Magenes, E. *Nonhomogeneous Boundary Value Problems and Applications, Vol. I*, Grund.Math.Wiss., 181, Springer (1972).

22. Morrey, C.B., *Multiple Integrals in the Calculus of Variations*, Grund.Math.Wiss., 130, Springer (1966).

23. Nečas, J. and Hlavaček, I., *Mathematical Theory of Elastic and Elasto-Plastic Bodies: An Introduction*, Studies Appl. Mech., 3, Elsevier (1981).

24. Nicholson, D.W., Constitutive Model for Rapidly Damaged Structural Materials, *Act.Mech.*, 39, pp. 195-205 (1981).

25. Onat, E.T. and Leckie, F.A., A Continuum Description of Creep Damage, *T & A.M. Report#469*, Dept. Theor. Appl. Mech., Univ. Illinois at Urbana-Champaign (1984).

26. Rodin, G.J., Constitutive Equations for Damaged Creeping Materials, *PhD Dissertation*, Dept. Mech. Eng., MIT, Cambridge, MA (1986).

27. Trampczynski, W.A., Hayhurst, D.R. and Leckie, F.A., Creep Rupture of Copper and Aluminum under Non-Proportional Loading, *J. Mech. Phys. Solids*, 29, pp. 353-374 (1981).

28. Tvergaard, V., Influence of Void Nucleation on Ductile Shear Fracture at a Free Surface, *J. Mech. Phys. Solids*, 30, pp. 399-425 (1982).

3.

NUMERICAL SOLUTION OF THE EVOLUTION EQUATIONS OF DAMAGE AND RATE-DEPENDENT PLASTICITY

Prologue

This final chapter is a reproduction of the material in publication #3 listed in Section 1.2 of this report. It focuses on the design of stable schemes for integrating the evolution equations of damage theory and of viscoplasticity which are robust enough to model jumps in the stress due to cyclic loading. Extensive numerical experiments are described and conditions for the construction of effective schemes for these classes of problems are established.

1 Introduction

In recent years, the success of modeling progressive damage and rate-dependent plasticity have led to the application of such theories to an increasing list of engineering problems. Typically, such theories are characterized by constitutive equations which include evolution equations for some type of internal variable which could represent such features such as a loss of stiffness due to an increase in microcrack density, hardness, plastic strain, dislocation density, etc. While such phenomenological theories can be very effective in modeling history effects, damage, viscoplastic deformation, and other phenomena, the numerical integration of the equations often presents serious difficulties, particularly when cyclic loading cases are considered. These difficulties are related to the mathematical stiffness inherent in damage theories and in internal-state-variable formulations, with the result that many of the standard numerical schemes, particularly the explicit schemes, encounter serious stability or convergence problems.

Several computational schemes have been proposed in the literature for solving initial-boundary-value problems in viscoplasticity. These schemes include explicit and implicit methods of time integration which are used in conjunction with both constant stiffness [1-7], and tangent stiffness [8-11] formulations of the equilibrium equations. Due to the stiffness of the

evolution constitutive equations, many of these schemes are only conditionally stable and may produce results which diverge rapidly from the true solution when applied to an arbitrary history of loading.

For this reason, an investigation of several such schemes is taken up in the present paper and two schemes are identified which appear to yield acceptable results when applied to problems with arbitrary loading histories. These techniques include an Euler forward predictor with trapezoidal corrector and time step control, given in [12], and Gear's stiffy stable methods with time steps selected by numerically approximating the truncation error; see Ref. [13-14]. These integration techniques have been implemented in a new algorithm which appears to be more computationally efficient than those previously proposed in the literature. Our primary mission here is to review schemes which can be used successfully for these classes of problems and to present results of applications to representative problems.

This paper is divided into seven sections. Following this introduction, a brief discussion of typical models is presented. This overview includes a discussion of the general mathematical structure of these models, and a synopsis of several recently proposed theories of this type. Section 3 discusses the problem of mathematical stiffness of the governing equations and presents a weak formulation of the problem. Section 4 and 5 are devoted to the efficiency and reliability of several computational schemes for solving initial-boundary-value problems in internal-state-variable viscoplasticity. Here we are able to show that some methods are unsuitable for use in general purpose finite element codes while others appear to be robust, stable and efficient for certain problems. The final two sections present the results of some numerical test cases for two representative constitutive theories.

2 Models of Viscoplasticity and Damage

This section contains a brief discussion of internal-state-variable models for metals exhibiting time-dependent nonelastic deformation.

Mathematical Structure. Many of the internal-state-variable theories and damage theories for infinitesimal nonelastic deformation have the same general structure, typified by the following properties:

1. A strain-rate decomposition of the form

$$\varepsilon = \varepsilon^e + \varepsilon^n$$

where ε is the total strain rate tensor, ε^e is the elastic strain rate tensor, and ε^n is the nonelastic strain rate tensor which includes both a time independent inelastic component and a time dependent

anelastic component.

2. The nonelastic strain rate is a function of the stress, the damage, and a set of internal state variables

$$\varepsilon^n = f(\sigma, d, z_k)$$

where σ is the stress tensor, d is the damage, and z_k is a set of state variables, and both d and z_k may be tensors and/or scalars.

3. The state variables vary along a loading path according to certain laws, and the history dependence of the rate of nonelastic strain, up to the current time, is completely characterized by the current values of the damage and the state variables. The constitutive relations for the evolution of the damage and the state variables are of the general form

$$d = D(\sigma, d, z_k)$$

$$z_i = g_i(\sigma, z_k) .$$

4. Often the nonelastic deformation rate is deviatoric,

$$\text{tr } \varepsilon^n = 0 .$$

5. There need not exist yield criteria nor loading or unloading conditions. Hence, nonelastic deformation is assumed to occur at all stages of loading.

These five properties characterize the general structure of most of the damage and/or internal-state-variable models, although some models may deviate slightly from the above descriptions. A list of some representative examples follows:

The Bodner and Partom / Bodner and Stouffer's Theories [15-22]. In the period 1979-1983, an anisotropic hardening law was proposed by Bodner and Stouffer [18,21] in which a tensor relationship for the nonelastic strain rate and a single scalar state variable equation appear. This model also uses a hardness tensor which is related to the single internal state variable and is responsible for the anisotropic material characterization. The nonelastic deformation rate in an anisotropic formulation is given by

$$\varepsilon^n_{ij} = \frac{D_0 S_{ij}}{\sqrt{J_2}} \exp\left(-0.5 \left(\frac{z^2_{ij}}{3J_2}\right)^n \left(\frac{n+1}{n}\right)\right) .$$

Here D_0 is a scale factor, z_{ij} a hardness tensor, S_{ij} are the deviatoric stress components, J_2 the second invariant of the stress deviator, and n is a material constant related to the rate sensitivity.

In this model, the single internal state variable is the plastic work, which has the constitutive form

$$z = S_{ij} \stackrel{n}{\varepsilon}_{ij} .$$

Hart's Theory. [23-27]. The equations for the nonelastic deformation rate are given by

$$\varepsilon^n = \frac{(a^*[\,\| S - \mu a \| / \mu]^M}{\| S - \mu a \|} (S - \mu a)$$

where a*, M and μ are material constants, S is the stress deviator, **a** is a tensor internal state variable, and $\| \sigma \| \ldots \sqrt{\sigma_{ij}\, \sigma_{ij}}$. The evolution equations for the internal state variables, σ^* and **a**, are

$$\sigma^* = \sigma^* \Gamma\varepsilon^* / (l_n (\sigma^* / \| \mu a \|))^{1/\lambda}$$

and

$$\mathbf{a} = \varepsilon^n - \frac{[\,\varepsilon^*/ (\ln (\sigma^* / \| \mu a \|))^{1/\lambda}]}{\| \mu\, a \|} \mu\, a .$$

Here Γ is a material function of σ^* and $\| \mu a \|$, λ is a material constant, and ε^* is a function dependent on the temperature and σ^*.

The Gillis & Jones Theory [28]. This theory, proposed for polycrystalline metals, is limited to materials having a linear dependence of dislocation velocity on the stress and contains only one internal state variable, the nonelastic strain.

The nonelastic strain rate is

$$\varepsilon^n = \phi b f \rho^* \upsilon_0 (\beta + \alpha\varepsilon^n) \; < \sigma/\sigma_0 - (1 + h\varepsilon^n) >$$

Here ϕ is an orientation factor, b is the magnitude of the Burgers vector, f is the fraction of mobile

dislocations, $\rho^*\beta$ is the initial dislocation density, $\rho^*\alpha$ is a dislocation multiplication coefficient, v_0 is the dislocation speed produced by a stress of magnitude σ_0, and h is a strain hardening coefficient. In this expression, $< \cdot >$ denotes use of the step function $<\psi> = 0$ if $\psi < 0$ and $<\psi> = \psi$ if $\psi > 0$.

Robinson's Theory [29-30]. In this model, the multiaxial representation for the nonelastic deformation rate is given by

$$\varepsilon^n_{ij} = \frac{1}{2}\left[\frac{(S_{kl}-\alpha_{kl})\,(S_{kl}-\alpha_{kl})}{2K^2}\right]^{\frac{M-1}{2}}(S_{ij}-\alpha_{ij}) ,$$

where S_{ij} is the deviatoric stress tensor, α_{ij} is the tensor-valued internal state variable ($\alpha_{ij}=z_{ij}$), and M and K are material constants. The evolutionary equations for the internal state variable, given in a work hardening-recovery format, are

$$\alpha_{ij} = \frac{2\mu H\,\varepsilon^n_{ij}}{\left(\frac{\alpha_{kl}\,\alpha_{kl}}{2K^2}\right)^{\beta/2}} - R\left(\frac{\alpha_{kl}\,\alpha_{kl}}{2K^2}\right)^{\frac{n-\beta-1}{2}}\alpha_{ij} .$$

Here μ, H, n, β and R are also material constants.

Miller's Theory [31-32]. The development of this model stems from a desire to accurately model steady-state creep deformation. Using this as a basis, the following one-dimensional generalized form for the nonelastic deformation rate is obtained:

$$\varepsilon^n = B\theta'\left[\sinh\left(\frac{|\sigma - R|^{1.5}}{D}\right)\right]^n \operatorname{sgn}(\sigma-R) ,$$

where

$$\theta' = \exp\left[\left(\frac{-Q}{0.6KT_m} \right) - \left(\ln\left(\frac{0.6T_m}{T} \right) + 1 \right) \right] \quad ; \; T \leq 0.6T_m$$

$$= \exp\left[\frac{-Q}{KT} \right] \quad ; \; T > 0.6T_m$$

In these expressions B, and n are material constants, R and D are internal state variables representing the back stress and drag stress, respectively, σ is the applied stress, Q is an activation energy, K is Boltzman's constant, T is the temperature, T_m is the melting temperature, and sgn represents the signum function. The evolution equations for the internal state variables are

$$R = H_1 \varepsilon^n - H_1 B\theta' (\sinh (A_1 |R|))^n \operatorname{sgn}(R)$$
$$D = H_2 |\varepsilon^n| (C_2 + |R| - A_2 / A_1) D^3 - H_2 C_2 B\theta' (\sinh (A_2 D^3))^n .$$

Here H_1, H_2, C_2, A_1, and A_2 are also material constants.

The Krieg, Swearengen and Rhodes Theory [33]. In 1978, Krieg et al. proposed a unified model for creep and plasticity in metals, using two internal state variables to reflect the current microstructural state. The model is applicable to metals under isothermal conditions in the temperature range of 0.3 T_m to 0.7 T_m, where T_m is the homologuous temperature.

The constitutive equations for the non-elastic deformation rate are based on a general function form for dislocation glide given by

$$\varepsilon^n = \varepsilon_0 \left[\frac{\|S - \alpha\|}{R} \right]^m \frac{S - \alpha}{\|S - \alpha\|} .$$

In this expression, S is the deviatoric applied stress, α is the back stress tensor, R is the drag stress, ε_0 and m are temperature-dependent material constants, and $\|\sigma\| = \sqrt{\sigma_{ij}\,\sigma_{ij}}$. The evolution equations for the two internal state variables are postulated as

$$\alpha = A_\alpha \varepsilon^n - \frac{r_\alpha \alpha}{\|\alpha\|} \quad \text{and} \quad R = A_R \|\varepsilon^n\| - r_\alpha$$

where A_α, A_R, r_α and r_R are hardening and recovery functions, respectively;. Specific forms for these hardening and recovery functions are given in [33].

Cernecky and Krempl's Theory [34-38]. In 1980, Krempl and associates proposed a coupled infinitesimal theory of thermo-visco-plasticity. This constitutive model is based on a nonlinear, multiaxial generalization of the standard linear solid, which consists of a spring in parallel with a Maxwell element. This generalization leads to a proposed constitutive form of

$$\sigma_{pq} + K_{pqmn}(\sigma, \varepsilon, T)\,\sigma_{mn} = G_{pq}(\varepsilon, T) + M_{pqmn}(\sigma, \varepsilon, T)\,\varepsilon_{mn} \tag{2.1}$$

where K_{pqmn}, G_{pq}, and M_{pqmn} are material functions determined from experimental data, and

$$K^{-1}_{ijmn}\, M_{mnkl} = D_{ijkl} \tag{2.2}$$

D_{ijkl} being the tensor of linear elastic moduli. Solving equation (2.1) for σ_{mn} and using equation (2.2) gives the following relation for the nonelastic strain rate

$$\dot{\varepsilon}^{n}_{ij} = M^{-1}_{ijmn}\,(\sigma, \varepsilon, T)\,[\dot{\sigma}_{mn} - G_{mn}(\varepsilon, T)] \tag{2.3}$$

Also by using the relation

$$\dot{\varepsilon}_{mn} = D^{-1}_{ijmn}\,\dot{\sigma}_{kl} + \dot{\varepsilon}^{n}_{mn}$$

for the total strain rate in (2.3), a final form for the nonelastic strain rate is obtained which is a function only of the stress and internal variable.

The Cescotto and Leckie Theory [39]. The constitutive forms for the nonelastic strain rate and internal variables are

$$\dot{\varepsilon}^{n} = f\left(\left|\frac{\sigma-\alpha_2}{\alpha_3}\right|\right)\,\mathrm{sgn}\,(\sigma-\alpha_2)$$

$$\alpha_2 = \frac{3}{2} h_\alpha \ \varepsilon^n - r_\alpha \alpha_2$$

and

$$\alpha_3 = h_k - r_k$$

where f is the nonelastic strain rate function, h_α and h_k are hardening functions, and h_α and r_k are recovery functions. Here sgn represents the signum function which takes on the values of 1, 0, and -1, depending on whether the argument is positive, zero or negative. No particular form of the functions f, h_α, h_k, r_α and r_k is assumed a priori, and a set of experiments is required to define those functions.

3 Stiffness and Approximation

A wide range of techniques has been proposed in the literature to numerically integrate the evolution equations described above. These methods include constant stiffness and tangent stiffness formulations of the equilibrium equations used in conjunction with either explicit or implicit time integration techniques. Testing of these techniques is often done in the context of a monotonic loading situation and for restricted forms of the constitutive equations, even though arbitrary loading histories, especially cyclic loading situations often present very severe numerical difficulties.

In this section, we examine several computational methods and integration techniques. We focus on computational issues, stability and overall performance of representative algorithms. For definiteness, we confine our attention to internal state variable theories appropriate for quasi-static, infinitesimal, isothermal deformations.

The general form of the constitutive relationships given above is:

$$\varepsilon^n = f(\sigma, Z_k)$$

$$Z_i = g_i(\sigma, Z_k)$$

$$\sigma = E(\varepsilon - \varepsilon^n) = E(\varepsilon - f(\sigma, Z_k)).$$

where here Z_k can also represent a damage measure. These differential equations are to be integrated over a time interval (0,T) subject to the constraint imposed by the equilibrium equations on the total strain rate. Assuming that the total strain rates are prescribed over time, it is obvious that $\Delta\varepsilon^n$ is available upon inverting

$$\Delta\sigma = \mathbf{E} (\Delta\varepsilon - \Delta\varepsilon^n) .$$

Thus it is desirable to integrate σ and Z_i subject to the equilibrium constraint.

If ε is prescribed, then the above problem reduces to a system of the form

$$\sigma = \mathbf{k} \ (\sigma, Z_k)$$

$$Z_i = g_i (\sigma, Z_k)$$

which can be rewritten simply as the dynamical system,

$$\mathbf{y} = \mathbf{F} (\mathbf{y}) .$$

Such a system of differential equations given by $\mathbf{y} = \mathbf{F} (\mathbf{y})$ is said to be stiff (see Lambert [40] if

(1) $\lambda_i < 0$ for $i = 1,2, \ldots m$

(2) $\max_i | \mathrm{Re}\ \lambda_i | \ >> \ \min_i | \mathrm{Re}\ \lambda_i |$

where λ_i are the eigenvalues of the Jacobian matrix $\partial \mathbf{F} / \partial \mathbf{y}$ and m is the number of equations in the system.

Thus, a system of stiff differential equations is one in which the components of the solution may be changing or decaying at greatly different rates over a time interval. Then the evolution of the rapidly decaying component of the solution may require very small time steps to be used in a numerical scheme while the component associated with the largest eigenvalue may need to be integrated over a relatively large period of time.

In the classical numerical solutions to ordinary differential equations, the problem of

numerical stability concerns the growth of truncation and round-off errors from one time step to another in a given numerical integration scheme. A numerical integration scheme is said to be *absolutely stable* for a given time step Δt and differential equation, if the change in the solution due to a perturbation δ in one mesh value y_n is no larger than δ in all subsequent values y_m for $n < m$ (cf. Gear [41]).

For the standard test problem, $\dot{x} = \lambda x$, λ being constant, one can define the region of absolute stability of a given algorithm as that set of values Δt and λ for which a perturbation in a single value x_n will produce subsequent values which do not increase from time step to time step. Thus, for the forward Euler integration of the test equation $\dot{x} = \lambda x$ given by

$$x_{n+1} = x_n + \Delta t\ \dot{x}_n = (1 + \lambda \Delta t)\ x_n \ .$$

there is no region of absolute stability for $\lambda \geq 0$. For $\lambda < 0$ it is necessary that $|1+\lambda\Delta t| < 1$ so that $\lambda\Delta t$ lies in the unit circle centered at -1 in the $\lambda\Delta t$ complex plane. For these values of $\lambda\Delta t$ inside the unit circle, the integration may be performed without errors growing from one time step to another. Similarly, regions of absolute stability may be determined for any numerical method.

Sample Time Step Calculations. For the one-dimensional form of the constitutive equations of Bodner et al., eigenvalue calculations have been performed for various materials and total strain rates. These eigenvalues were then used to estimate stable time steps for the forward Euler type integration. The results are presented in Figs. 1 and 2 with the stable time steps set to 0.65 seconds in the initital "elastic region" where, otherwise, very large values would have been obtained. From this data large variations in eigenvalues can be seen for different regions of strain, for various materials and strain rates. It is notable that for the strain rate of 2.0 E-4 / sec. to a strain of 2 percent, say, may require between 12,000 and 20,000 time steps for the copper or aluminum specimens.

The shapes of these time step curves may also be used to explain the oscillations in some numerically obtained stress-strain curves such as that in Fig. 3. In this figure, time steps were initially selected slightly larger than the acceptable stable time step. Therefore, on exiting the elastic region, errors were introduced which were oscillatory in nature but not catastrophic. As the integration continued, the stable time step increased and the oscillations decayed as the time step entered the stable region.

Weak Formulation. Subsequent calculations are performed on systems resulting from a finite element approximation of weak forms of the momentum equations,

$$(E_{ijkl}\ \overset{e}{\varepsilon}_{kl})_{,j} = -\ b_i \qquad \text{in } \Omega \tag{3.1}$$

where

$$\overset{e}{\varepsilon}_{kl} = u_{(k,l)} - \overset{n}{\varepsilon}_{kl}$$

$$\overset{n}{\varepsilon}_{kl} = f_{kl}\,(\sigma, Z_k) \tag{3.2}$$

$$Z_i = g_i\,(\sigma, Z_k)\,.$$

Here

$$\sigma = \int_0^t \dot{\sigma}\, dt + \sigma\ , \quad \dot{\sigma} = \mathbf{E}\ \dot{\varepsilon}^e \tag{3.3}$$

$$Z_i = \int_0^t \dot{Z}_i\, dt + Z_i\ . \tag{3.4}$$

A weak form of (3.1) is obtained in the usual way: multiply (3.1) by a suitably smooth test function $\upsilon_i = \upsilon_i(x)$, integrate over Ω, and use the Green-Gauss divergence theorem to integrate by parts the stress-power terms. Let V denote the space of test functions

$$V = \{\ \upsilon_i \in W^{m,p}\ (\Omega)\ |\ \upsilon_i = 0 \quad \text{a.e. on } \partial\Omega_l,\ 1 \le i \le N\ \}$$

where $W^{m,p}\,(\Omega)$ is the Sobolev space of order (m,p), with $m \ge 0$, $m \in \mathbf{IR}$, $1 \le p \le \infty$, and where specific values of m and p depend upon the particular forms of the constitutive equations governing the material under consideration, (for the cases considered here $m = 1$, $p = 2$). The weak form of the boundary-initial-value problem (3.1) - (3.4) is then:

Find a displacement rate field $t \mapsto \mathbf{u}\,(\mathbf{x},t) \in V + \{\hat{\mathbf{u}}\}$ such that for every $t \in [0,T]$,

$$\int_\Omega E_{ijkl}\, u_{k,l}\, \upsilon_{i,j}\, \partial\Omega = \int_\Omega E_{ijkl}\ \overset{n}{\varepsilon}_{kl}\,(\mathbf{u})\ \upsilon_{i,j}\, d\Omega$$

$$+ \int b_i\, \upsilon_i\, d\Omega + \int T_i\, \upsilon_i\, ds \quad \forall\ \upsilon_i \in V \tag{3.5}$$

Ω $\partial\Omega_2$

with

$$\overset{n}{\varepsilon}_{kl} = f_{kl}(\sigma, Z_k)$$

and σ and Z_i are given by (3.3) and (3.4). Here $\partial\Omega$ and ds are volume and surface measures, $\hat{u}$ is any function defined on Ω such that its trace on the boundary segment $\partial\Omega_1$ is $\hat{u}$ (where $u_i \mid_{\partial\Omega_1} = \hat{u}_i$), and σ and Z_i are understood to depend upon $u_{i,j}$ through (3.3) and (3.4), and to satisfy initial conditions $\sigma_{ij}(x, 0) = \sigma_{ij}(x)$, $Z_i(x, 0) = Z_i(x)$. It is easily verified that any sufficiently smooth solution of (3.5) will also satisfy the governing equations. Conversely, any solution of the governing equations and boundary conditions will also satisfy (3.5).

Using standard notations, a finite element approximation of (3.5) leads to the discrete system of evolution equations. If the discrete velocity components are of the form

$$\overset{i}{u}_h(x, t) = \sum_{j=1}^{N} \overset{i}{u}_j(t)\, \phi_j(x) \tag{3.6}$$

where N is the number of nodes, i indicates the vector component, ϕ_j is a basis function, $\overset{i}{\upsilon}_j$ is the value of the test function $\overset{i}{\upsilon}_h$ at node x_j, and $\overset{i}{u}_j(t)$ is the value of $\overset{i}{u}_h$ at node x_j at time t, then we wish to find the vector of nodel displacements $\mathbf{u}$ such that

$$\int_\Omega \mathbf{B}^T \mathbf{E}\, \mathbf{B}\, \mathbf{u}\, d\Omega = \int_\Omega \mathbf{B}^T \mathbf{E}\, \varepsilon^n\, d\Omega + \int_\Omega \phi^T \mathbf{b}\, d\Omega + \int_{\partial\Omega_2} \phi^T \mathbf{T}\, ds$$

$$(\varepsilon^n = \mathbf{f}(\sigma(\mathbf{u}), Z_k)\ ,\ \ Z_k = g(\sigma, Z_k)\ . \tag{3.7}$$

4 Algorithms for Integrating Stiff Evolution Equations of Viscoplasticity

We now outline three popular algorithms for rate-dependent plasticity found in the literature and propose an alternative scheme that performs very well for cyclic loading cases.

The general strategy in these algorithms is as follows: with the initial distribution of the stress and internal variables specified, use the equilibrium equations to supply the spatial variation of the constraint (the momentum equations). Then integrate the constitutive equations forward in time,

evaluating principal variables at the integration points. With the updated values of the stress and internal variables at the new time, the constraint condition is again imposed. This sequence of determining the constraint, then advancing the constitutive equations in time is continued until the desired history of the initial-boundary-value problem has been traced.

The Initial Strain Rate Method. This method was originally proposed in 1972 in [7]. Starting with governing differential equations in the rate form, a finite element approximation of the equilibrium equations is constructed (as in (3.7)), giving

$$\int_{\Omega} \mathbf{B}^T \mathbf{E}\, \mathbf{B}\, \mathbf{u}\, d\Omega = \int_{\Omega} \mathbf{B}^T \mathbf{E}\, \varepsilon^n\, d\Omega + \mathbf{F} \tag{4.1}$$

where $\mathbf{F}$ is the vector of force rates derived from surface traction rates and body force rates. The algorithm is then:

1. Initialize σ ; Z_i , set $t_n = 0$.
2. Calculate $\varepsilon^n = \mathbf{f}(\sigma, Z_k)$ at $t = t_n$ (thus determining the right-hand-side of (4.1)).
3. Solve the equilibrium condition for $\mathbf{u}_h(t_n)$.
4. Calculate $\varepsilon(t_n) = \mathbf{B}\, \mathbf{u}_h(t_n)$.
5. Calculate $\sigma(t_n) = \mathbf{E}\,(\varepsilon(t_n) - \varepsilon^n(t_n))$.
6. Calculate $Z_i(t_n) = g_i(\sigma(t_n), Z_k(t_n))$.
7. Integrate σ, Z_i forward over some appropriate Δt to $\sigma(t_{n+1})$, $Z_i(t_{n+1})$.
8. If $t_n = \Delta t < T$ to (2) .
9. Stop.

Step (7) characterizes an explicit scheme, and this step can be displaced by a subroutine for implicit method, if needed. If predictor-corrector type integration schemes are used, a slight modification is necessary beginning with (7).

7. Estimate $\overset{0}{\sigma}(t_{n+1})$, $\overset{0}{Z_i}(t_{n+1})$ using a predictor.
8. Solve (4.1) for $\mathbf{u}_h(t_{n+1})$ using latest entries for $\sigma(t_{n+1})$, $Z_i(t_{n+1})$.
9. Calculate $\varepsilon^l(t_{n+1})$ and $\sigma^l(t_{n+1})$.
10. Use a corrector to update $\sigma^c(t_{n+1})$, $\overset{c}{Z_i}(t_{n+1})$.
11. Check an appropriate tolerance index for convergence. If not achieved, go to (8) with a new estimate of $\sigma(t_{n+1})$ and $Z_i(t_{n+1})$.

12. Set $\sigma(t_{n+1}) = \sigma^{\#}(t_{n+1})$ and $Z_i(t_{n+1}) = Z_i^{\#}(t_{n+1})$.

13. If $t + \Delta t < T$ to 2.

14. Stop.

The Initial Strain Method. This method differs from that above in that the equilibrium equations are written in incremental form rather than rate form. This results in a finite element approximation of the equilibrium equations of the form

$$\int_{\Omega} \mathbf{B}^T \mathbf{E}\, \mathbf{B}\, \Delta \mathbf{u}\, d\Omega = \int_{\Omega} \mathbf{B}^T \mathbf{E}\, \Delta \varepsilon^n\, d\Omega + \Delta \mathbf{F} \tag{4.2}$$

where Δ represents an increment of the proposed quantity.

Thus the computational scheme becomes (for the case of explicit integration in steps (2) and (7)):

1. Initialize σ, Z_i, set $t_n = 0$.
2. Calculate $\Delta \varepsilon^n$ over Δt.
3. Solve (4.2) for $\Delta \mathbf{u}_h$.
4. Calculate $\Delta \varepsilon$ over Δt from $\Delta \varepsilon = \mathbf{B} \Delta \mathbf{u}_h$.
5. Calculate $\Delta \sigma = \mathbf{E}(\Delta \varepsilon - \Delta \varepsilon^n)$.
6. Calculate $Z_i = g_i(\sigma(t_n), Z_k(t_n))$.
7. Integrate Z_i forward over Δt to $Z_i(t_{n+1})$.
8. Set $\sigma(t_{n+1}) = \sigma(t_n) + \Delta \sigma$.
9. If $t_n + \Delta t < T$ to (2).
10. Stop.

A similar revision to that discussed earlier for implementation of predictor-corrector methods can be made.

A Forward Gradient Scheme. This method is considerably different from the methods introduced above. It involves a tangent stiffness matrix calculation updated from step to step, and a particular type of numerical integration specified for the time integration.

Beginning with the incremental form of the equilibrium equations, we have

$$\int_{\Omega} \mathbf{B}^T \mathbf{E}\, \mathbf{B}\, \Delta \mathbf{u}\, d\Omega = \int_{\Omega} \mathbf{B}^T \mathbf{E}\, \Delta \varepsilon^n\, d\Omega + \Delta \mathbf{F}$$

or

$$\int_{\Omega} \mathbf{B}^T \Delta\sigma \, d\Omega = \Delta\mathbf{F} .$$

It is assumed that $\Delta\varepsilon^n$ and ΔZ_i are given by

$$\Delta\varepsilon^n = \Delta t \{ (1 - \theta) \varepsilon^n (t_n) + \theta\varepsilon^n (t_{n+1}) \}$$
$$\Delta Z_i = \Delta t \{ (1 - \theta) Z_i (t_n) + \theta Z_i (t_{n+1}) \} .$$

Expanding $\varepsilon^n (t_{n+1})$ and $Z_i (t_{n+1})$ in a Taylor series about t_n results in

$$\Delta\varepsilon^n = \Delta t \{ \varepsilon^n (t_n) + \theta A_n \Delta\sigma + \theta B_n \Delta Z_i \} \quad (4.3)$$
$$\Delta Z_i = \Delta t \{ Z_i (t_n) + \theta C_n \Delta\sigma + \theta D_n \Delta Z_i \} \quad (4.4)$$

where

$$A_n = \frac{\partial \varepsilon^n}{\partial \sigma} \Big|_{t_n} ; \quad B_n = \frac{\partial \varepsilon^n}{\partial Z_i} \Big|_{t_n} ; \quad C_n = \frac{\partial Z_i}{\partial \sigma} \Big|_{t_n} ; \quad D_n = \frac{\partial Z_i}{\partial Z_k} \Big|_{t_n} .$$

Solving for ΔZ_i gives

$$\Delta Z_i = [\mathbf{I} - \theta\Delta t \, D_n]^{-1} \Delta t [Z_i (t_n) + \theta C_n \Delta\sigma] . \quad (4.5)$$

Substituting this into (4.3) for ΔZ_i and neglecting terms of order Δt^2 gives

$$\Delta\varepsilon^n = \varepsilon^n (t_n)\Delta t + \theta\Delta t A_n \Delta\sigma .$$

Thus,

$$\Delta\sigma = \mathbf{E} \left[\Delta\varepsilon - \Delta\varepsilon^n\right] = \left[\mathbf{I} + \theta\Delta t \, \mathbf{E} A_n\right]^{-1} \mathbf{E}\left[\mathbf{B}\Delta\mathbf{u} - \Delta t\varepsilon^n(t_n)\right]$$

$$= \mathbf{D} \left[\mathbf{B}\Delta\mathbf{u} - \Delta t \, \varepsilon^n(t_n)\right] . \quad (4.6)$$

Finally, substituting this into the equilibrium equation gives

$$\int_{\Omega\,\Omega} \mathbf{B}^T \mathbf{D}\, \mathbf{B}\, \Delta \mathbf{u}\, d\Omega = \int \mathbf{B}^T \mathbf{D}\, \Delta t\, \varepsilon^n (t_n)\, d\Omega + \Delta \mathbf{F}\,. \tag{4.7}$$

The computational algorithm then becomes

1. Initialize σ; Z_i, set $t_n = 0$.
2. Calculate $\varepsilon^n (t_n) = \mathbf{f}(\sigma (t_n),\ Z_i (t_n))$.
3. Solve (4.7) for $\Delta \mathbf{u}_h$.
4. Calculate $\Delta\varepsilon = \mathbf{B}\Delta \mathbf{u}_h$.
5. Calculate $\Delta\sigma$ from (4.6).
6. Calculate ΔZ_i from (4.5).
7. Update $\sigma (t_{n+1}) = \sigma (t_n) + \Delta\sigma$
   $Z_i (t_{n+1}) = Z_i (t_n) + \Delta Z_i$.
8. If $t + \Delta t < T$ set $t_n = t + \Delta t$ go to (2).
10. Stop.

New Algorithm. A new computational method suggests itself, which is similar to the initial strain algorithm in that an incremental form of the equilibrium constraint condition is imposed as

$$\int_{\Omega\,\Omega} \mathbf{B}^T \mathbf{E}\, \mathbf{B}\, \Delta \mathbf{u}\, d\Omega = \int \mathbf{B}^T \mathbf{E}\, \Delta\varepsilon^n\, d\Omega + \Delta \mathbf{F}\,. \tag{4.8}$$

We then proceed as follows:

1. Initialize σ, Z_i, set $t_n = 0$, and select ΔT.
2. Estimate $\Delta\varepsilon_n$ over ΔT (using predictor method).
3. Solve the equilibrium constraint for $\Delta \mathbf{u}_h$.
4. Calculate $\Delta\varepsilon = \mathbf{B}\, \Delta \mathbf{u}_h$.
5. Assume $\varepsilon = \Delta\varepsilon/\Delta T$ is constant over ΔT.
6. Subincrement and integrate σ, Z_i accurately over ΔT, neglecting the previous estimate of $\Delta\varepsilon^n$.
7. Calculate a new guess of $\Delta\varepsilon^n = \Delta\varepsilon - \mathbf{E}^{-1}\Delta\sigma$.
8. Check for convergence of $\Delta\varepsilon^n$ with $\Delta\varepsilon^n$; if no convergence occurs set $\Delta\varepsilon^n = \Delta\varepsilon^n$ and go to (3), otherwise set $\Delta\sigma = \mathbf{E}(\Delta\varepsilon - \Delta\varepsilon^n)$.
9. If $t_n + \Delta T = T$, Stop
10. Select a new ΔT and go to (2).

This method possesses the following desirable characteristics:

1. A constant elastic stiffness matrix is used throughout the solution process.
2. Different time steps at different integration points allowed and the overall ΔT is not restricted to be the smallest time step.
3. Integration using subincrement requires the coordinates and geometry of each elment to be loaded much less frequently in the finite element simulation.
4. By selecting a larger overall time step ΔT, fewer total time steps may be taken and thus fewer right hand sides need be considered.

5 Numerical Integration

This section presents techniques for integration of the constitutive equations which constitutes a critical step in the algorithms discussed in Section 4. To test the applicability of various integration techniques, a group of one-dimensional test problems has been selected which covers a variety of loading histories. These problems have been taken from examples in the literature to ensure that the constitutive models are used in the correct context. The constitutive models being integrated are those of Bodner and associates and Hart which are representative of the general exponential or power law form often assumed for the nonelastic strain rates.

The first technique to be considered is the simple forward Euler method. This method is the simplest and easiest to use but suffers from being a first-order method and only conditionally stable. To use this method, it is necessary to select time steps so that the CFL conditions on stability are not violated and an acceptably small truncation error is introduced. This selection of a suitable time step for arbitrary loading histories, constitutive equations, and material types prohibits the method from being useful without some kind of automatic time step selection.

A first possibility of time step selection is that of calculating the maximum eigenvalue at each point in time. This calculation is, however, too time consuming and is also generally unacceptable since the maximum eignevalue may be changing over the time step.

A second possibility, proposed in [2,3], consists of selecting a time step so that the increment of nonelastic strain over the step is some fraction of the total strain. Thus, a proposed step is given by $\Delta t = \tau\bar{\varepsilon} / \bar{\varepsilon}^{n}$, where τ is a constant, generally around 0.1, and the bars represent equivalent values of the indicated quantities. Unfortunately, this method of time step selection is also generally unacceptable because, for stress states in the "elastic region", $\bar{\varepsilon}^{n} = 0$ and a very large time step is them indicated. Results obtained using this type of step selection, with a maximum allowable step size imposed, are similar to those shown in Fig. 4.

A third method of time step selection is presented in [12] for a single differential equation $y = F(y)$. This time step control is based on a comparison of a suitably defined error

$$e = \frac{| \Delta t_k \, (y(t_k) - y(t_{k-1})) |}{| y(t_k) |}$$

with prescribed error limits e_{max} and e_{min}. The time step at the k-th step, Δt_k, is then defined on the basis of its estimate Δt_k, according to

$e_{max} < e$: replace Δt_k by $\Delta t_{k/2}$ and recompute e

$e \leq e_{max}$: set $\Delta t_k = \Delta t_k$ and compute $y(t_{k+1})$

where the initial time step Δt_1 is prescribed. The next step size is then estimated by

$e_{min} < e \leq e_{max}$: set $\Delta t_{k+1} = \Delta t_k$

$e < e_{min}$: set $\Delta t_{k+1} = 2\Delta t_k$.

An extension of this technique to the vector case $y = F(y)$ is accomplished by introducing the infinity error norm and thus selecting the maximum value of e from all vector components to determine an acceptable step size.

This a-priori method of time step selection suffers from deficiencies similar to those of the second time step method, as can be seen from Fig. 5. Satisfactory results were obtained, however, for the constraint strain rate simulations (see Figs. 7 - 11) the strain rate change tests (Figs. 12 - 13) and the stress relaxation tests (see Fig. 15). Results obtained by using this method on the loading, unloading and reloading test, and also in cyclic testing situations, as is demonstrated in Fig. 5, were less than satisfactory. Note that the success of using this method depends strongly on the size of the initial step size prescribed.

For initial steps that are "too large", stability difficulties or spurious loading paths may be encountered in any of the test problems. Thus it appears that *the forward Euler method with or without time step control is probably not a good choice.*

Another group of integration techniques suggested in the literature are the higher-order explicit schemes. These techniques which include second- and fourth-order Runge-Kutta, and Adams-Bashford methods, and are suggested by some authors with the hope that higher order methods will allow larger time steps because of thier inherently smaller truncation errors. Unfortuantely, for such methods the issue of conditional stability is of central importance and

dominates the issue of time-step selection. These methods have regions of absolute stability which are approximately equivalent to the stability region of the forward Euler method, with the result that often no appreciable difference can be seen between the results of these higher order methods and the forward Eule method.

A third group of integration techniques are the implicit schemes which employ direct or Jacobi iteration in the solution of the resulting nonlinear equations. These methods may be expressed, for a single equation $y = F(y)$, in a general form as

$$y_{n+1} = \beta \Delta t \, F(y_{n+1}) + q \tag{5.1}$$

where $n + 1$ indicates evaluation at time t_{n+1}, Δt is the time step, β is a constant dependent on the numerical scheme, and q is a known function of previously calculated values of y and F. Using direct or Jacobi iteration implies that

$$y_{n+1}^{(s+1)} = \beta \Delta t \, F(y_{n+1}^{(s)}) + q \equiv \phi(y_{n+1}^{(s)}) \tag{5.2}$$

and (s) indicating the iteration number and y_{n+1} is provided by some predictor calculation. This sequence of approximations given by (5.2) will converge to the solution of (5.1) whenever $\phi(y_{n+1})$ satisfies a Lipschitz condition

$$| \phi(y_{n+1}) - \phi(y_{n+1}^{*}) | < M | y_{n+1} - y_{n+1}^{*} |$$

for all y_{n+1} and y_{n+1}^{*}, where the Lipschitz constant M satisfies $0 \leq M \leq 1$. Then there exists a unique solution γ of (5.1), and the sequence of approximations defined by (5.2) is such that $\lim y^{(s)} = \gamma$ (see [40]). A similar result also applies for systems of equations with the absolute values replaced by norms of corresponding vectors.

Integration techniques suggested in the literature which fall into this category include forward Euler predictor with trapezoidal corrector, forward Euler predictor with backward Euler corrector, and mid-step integration where rates at the midpoint of the time step are used in the integration. These methods are superior to those discussed in the proceeding paragraphs, in that they have large regions of absolute stability, which include the negative complex half plane and essentially eliminate the stiffness difficulty. They are, however, limited by the radius of convergence of the direct iteration technique. For example, if the partial derivatives of the Jacobian matrix $J = \partial F / \partial y$ are

continuous and bounded in an appropriate region, then the Lipschitz constant of $\mathbf{F}$ may be taken to $L = \| J \|$. Now for any matrix A, we have $\| A \| \geq \rho(A)$ where $\rho(A) = \max_i |\lambda_i|$ and λ_i are the eigenvalues of J. This implies that the Lipschitz constant L, is greater than or equal to the magnitude of the maximum eigenvalue. Considering the general form given in (5.1), we can choose the Lipschitz constant M to be $L\Delta t|\beta|$ which implies that (5.2) converges to the solution of (5.1) if $\Delta t < 1/(L|\beta|)$ or approximately $\Delta t < 1/(|\beta|\lambda_{max})$. This result suggests a time step restriction, again related to the maximum eigenvalue, which may be as restrictive as the stability requirements of the previous methods.

If these predictor corrector methods with direct iteration are to be used, some type of time step control is again necessary. One possible time step selection technique for use with the forward Euler predictor, trapezoidal corrector is given in [12] for a single differential equation $y = F(y)$. This automaic control is implicit in nature in that an initial time step size is estimated from the previous time step and then adjusted after the corrector calculations have been performed. This time step control is basically the same as the third technique described above for use with the forward Euler method, except that for this case the error is defined by

$$e = \frac{|\Delta t_k (F^p_{k+1} - F_k)|}{2|y^c_{k+1}|}$$

where y^c_{k+1} is the corrector value of y_{k+1} and $F^p_{k+1} = F(y^p_{k+1})$.

This combination of predictor-corrector with time step control performed satisfactorily on all the test problems, but was not efficient in test situations when the constitutive equations were fairly stiff. Results for the constant strain rate simulations, the strain rate change test, the stress relaxation tests, creep test, and the stress change test are the same as those obtained by the forward Euler method with time step control, with plotting accuracy. Use of this combination on the loading, unloading, reloading test is shown in Fig. 14, on the cyclic tension compression tests is shown in Figs. 19 - 22, on the cyclic relaxation test in Fig. 23, and on the cyclic creep test in Fig. 24.

We also mention a very popular group of integration techniques: predictor-corrector methods which use Newton iteration in the correction process. For a system of m-equations in m-unknowns such as $\mathbf{H(y)} = \mathbf{0}$, the Newton method can be written as

$$y^{(s+1)} = y^{(s)} - J^{-1}(y^{(s)})\, H(y^{(s)}), \quad s = 0, 1, 2 \ldots$$

where (s) is the iteration number and J^{-1} is the inverse of the Jacobian matrix $\partial H/\partial y$. If this

method is applied to equation (5.1), we obtain the sequence of approximations

$$y_{n+1}^{(s+1)} = y_{n+1}^{(s)} - \left[I - \Delta t\beta \frac{\partial F(y_{n+1}^{(s)})}{\partial y} \right]^{-1} (y_{n+1}^{(s)} - \Delta t\beta F(y_{n+1}^{(s)}) - q \quad s = 0, 1, 2 \ldots$$

where I is the identity matrix.

Proposed integration techniques to be used in conjunction with Newton iteration include the implicit methods mentioned above and stiffy stable methods discussed by Gear [41]. These methods are presented in the predictor-corrector format with a p-th order predictor formula of the form

$$\overset{\circ}{y}_{n+1} = \alpha_1 y_n + \ldots + \alpha_p y_{n+1-p} + \eta \Delta t F(y_n)$$

and a corrector

$$y_{n+1}^{(s+1)} = \overset{*}{\alpha}_1 y_n + \ldots + \overset{*}{\alpha}_p y_{n+1-p} + \overset{*}{\eta} \Delta t F(y_{n+1}^{(s)})$$

with α_1, η, $\overset{*}{\alpha}_i$, and $\overset{*}{\eta}$ constants depending on the order p. This format differs significantly from the more conventional methods in that only one rate term is used with several previous solution values rather than several rate terms with one previous solution value.

All of these predictor-corrector methods also have infinite regions of absolute stability (for linear dynamical systems) and the use of Newton iteration provides for better convergence limits than standard direct iteration techniques. A drawback to these methods, however, is that they generally require the calculation and "inversion" of the Jacobian matrix, for each time step or, at least, periodically during the solution process. For only mildly stiff problems, such calculations may be more time consuming than simply using a smaller time step size and direct iteration. For the test problems considered here, Gear stiffy stable methods performed better than the other predictor-corrector methods, with numerical results being the same, to within plotting accuracy, as those obtained using the forward Euler predictor-trapezoidal corrector with time step control.

6. Test Cases

The computational methods and integration techniques discussed earlier were tested on a series of one-dimensional problems to determine which techniques performed best and some of these results are given in Figs. 4 - 24. These problems were selected from results reported in the

literature, so that comparisons of the numerical results could be made with published data. Also, along these test cases are problems which involve many of the complex loading histories which internal-state-variable constitution equations are capable of modeling. While only two sets of constitutive equations were considered, the Bodner and Partoms equations in both the original and deviatoric form were used in these calculations. The following shorthand notation is used:

BPO - Bodner-Partom equations in the original form
BPN - Bodern-Partom equations in the deviatoric form
H - Harts equations
TI - titanium
A1 - 1100 aluminum
CU - OFHC copper
SS - 304 stainless steel

In all problems using Bodners equations the reference temperature is room temperature, while the problems dealing with Harts equations were at temperatures 250°C and 400°C for the 1100 aluminum and 304 stainless steel, respectively. The other material data may be found in Refs. [15 - 27].

Test Problem #1. Constant Strain Rate Tests

Several constant strain rate simulations were performed under the following conditions:

Equ Type	Mat Type	Strain Rate	Total Strain %
BPO/BPN	TI	3.2E-3/sec	2%
		1.6E-3/sec	2%
		1.6E-4/sec	2%
		1.6E-5/sec	2%
BPN	CU	2.0E-3/sec	1%
		2.0E-4/sec	1%
		2.0E-5/sec	1%
H	AL/SS	3.33E-3/sec	1% - 2%
		3.33E-4/sec	1% - 2%
		3.33E-5/sec	1% - 2%

This large number of constant strain rate tests were performed due to the large changes in stiffness of the constitutive equations for different material types and strain rates. Note the large differences

in the results for the TI material using the original and deviatoric form of Bodners equations, see Figs. 7 - 8. Also note the strain rate insensitivity of the copper and stainless steel specimen, Figs. 9 - 11, and non-hardening nature of the aluminum specimen under these conditions, Fig. 10.

Test Problem #2. Strain Rate Change Tests

Several strain rate change tests were simulated under the following conditions:

Equ Type	Mat Type	History of Loading
BPO	TI	Strain at 1.6E-5/sec to 1% strain then change to 3.2E-3/sec and strain to 2%
BPO	TI	Strain at 3.2E-3/sec to 1% strain then change to 1.6E-5/sec and strain to 2%
H	SS	Strain to 3.33E-3/sec for 0-30 sec then change to 3.33E-4/sec for 30-60 sec.

Results for this type of testing may be seen in Figs. 12 - 13. Generally, this type of loading did not lead to numerical difficulties when changing from a high strain rate to lower rate, but caused some problems when changing from a low to high. This was due to the larger time steps allowd in the initial lower strain rate simulations. Also note the asymptotic approach of the results to the constant loading situation for Bodners equations, while Harts equations predict an almost immediate jump in the response to the constant loading case.

Test Problem #3. Loading, Unloading, and Reloading Test

A single example of loading at one strain rate, unloading into the "elastic region", and reloading at a different strain rate was performed under the following conditions:

Equ Type	Mat Type	History of Loading
BPO	TI	Strain at 1.65E-5/sec up to 1% strain, unload into the "elastic region" and then reload at 3.2E-3/sec up to 2% total strain.

Results for this test problem using the forward Euler predictor-trapezoidal corrector are shown in Fig. 14. The forward Eule predictor with time step control from [12] experienced difficulties in the reloading part of this problem. For this problem using the old form of the

equations and the TI specimen, the predictor-corrector with direct iteration performed the best.

Test Problem #4. Stress Relaxation Tests

Stress relaxation simulations were conducted under the following conditions:

Equ Type	Mat Type	History of Loading
BPO	TI	Strain to 2% at 1.65E-5/sec and hold for 70 min.
H	AL	Strain to .03% total strain at 3.33E-4/sec and hold for 10 hours.

Results of this testing are shown in Figs. 15 - 16. For this problem there were no rapid load changes or serious stiffness problems and thus the forward Euler method with time step control performed as well as the other methods.

Test Problem #5. Creep Test.

Two creep simulations were performed under the following conditions:

Equ Type	Mat Type	History of Loading
H	AL	Rapidly stress to 1500 psi and then hold constant over 0-100 hours.
H	AL	Rapidly stress to 1000 psi and then hold constant over 0-100 hours.

Results are reported in Fig. 17 for a 1-inch material specimen. This problem also posed no stiffness difficulties due to the low level of initial stressing, and thus the simpler methods are more efficient for this case.

Test Problem #6. Stress Change Test

A single stress change test was simulated under the following conditions:

Equ Type	Mat Type	History of Loading
H	SS	Rapidly stress to 20000 psi and hold constant over 0 - 10 hours, then rapidly increase the load to 30000 psi and hold constant over 10 - 100 hours.

Results of the numerical integration for this problem are shown in Fig. 18. This problem having an imposed stress history and relatively large hold times poses no large stiffness problem and therefore the simpler methods are more efficient here also.

Test Problem #7. Cyclic Tension-Compression Tests

Several cyclic tension-compression simulations were performed for:

Equ Type	Mat Type	Strain Rate (=)	# Cycles	± % Strain
BPN	TI	3.2E-3/sec	10	1%
BPN	AL	2.0E-3/sec	5	1%
BPN	CU	2.0E-4/sec	1	1%
H	SS	1.0E-3/sec	5	0.5%

(See Figs. 19 - 22 for results of this simulation.) In this group of problems, the constitutive equations were significantly stiffer for AL, CU and SS specimens. Also, the region of time over which the equations were stiff was large in relation to the total time and therefore the stiffy stable methods Gear perfor ıed best in these cases. Note that the number of cycles and/or percent strain was in some cases limited by the stiffness of the equations, so that the predictor-corrector methods using direct iteration were competitive in total computing time.

Test Problem #8. Cyclic Relaxation

A single cyclic relaxation simulation was performed under the following conditions:

Equ Type	Mat Type	History of Loading
BPO	TI	Strain at 2.5E-3/sec between 1.25% total strain and 0.225% total strain over 5 cycles

Results of the numerical integration for this problem are shown in Fig. 23. Five cycles were selected here because at this point an almost steady state was reached. For this problem the

constitutive equations were only moderately stiff and the predictor corrector with direct iteration and Gears method performed approximately the same.

Test Problem #9. Cyclic Creep Test

A single cyclic creep test was simulated under the following conditions:

Equ Type	Mat Type	History of Loading
BPO	TI	Stress to 325 MPa at 32.5 MPa/sec and then to -225 MPa at -32.5 MPa/sec and continue for 9 cycles.

Results for this history of loading shown in Fig. 24. This problem also has only a prescribed stress history and the predictor methods with direct iteration performed well here.

In summary, we list for the test problems considered:

1. The computational methods in Section 4 produced identical results with all the time integration techniques discussed in Section 5, with no particular advantage of one algorithm over the other.
2. Gears integration package of [14] showed some inadequacies in strain control situations. These difficulties were overcome by a slight modification of his methods of time step selection.
3. The forward gradient scheme presented in Section 4 showed much the same type of deficiencies as the other forward type of integration methods. The results for a cyclic loading situation may be seen in Fig. 6 where the time steps have been selected as a fraction of the total strain.
4. For reasons mentioned in Section 5 and from results of the test problems, no method suggested in all of the literature examined is completely satisfactory. Of those actually tested, the two that performed best were forward Euler predictor-trapezoidal corrector with direction iteration and step control of [12] in conjunction with either the initial strain of the initial strain method, and Gears stiffy stable methods wit' Newton iteration corrections in conjunction with the new algorithm of Section 4.

7. Other Applications

In this final section, we apply two of the better techniques described earlier to some specific engineering problems found in the literature. The methods used are:

1) the forward Euler predictor-trapezoidal corrector with direct iteration and time step control of [23] in conjunction with the initial strain method or the initial strain rate method, and

2) Gears stiffy stable method in conjunction with the new algorithm of Section 4.

Example Problem #1 (Composite Sheet using Bodners Equations). This problem, taken from [2], is essentially one-dimensional in nature. It consists of a composite material strip half titanium and half copper, supported by two walls (see Fig. 25). The specimen is rapidly loaded at the material interface with a uniform pressure of 150 MPa, which is approximately six times the "yield stress" of the copper, and held constant over a period of 100 hours. The finite element model and 100 times the deformed configuration at time = 100 hours is shown in Fig. 26. The one-dimensional elastic bar elements which have been included are essentially rigid and are used here to allow a homogenous mode of deformation to be modeled. The stress in the copper and titanium components is plotted versus time in Fig. 27. This plot shows the rapid change in stress from the initial elastic solution to almost steady state values. Figure 28 shows the relative displacement-time curve for a point on the material interface. In this figure, U_{el} is the elastic displacement of the interface. These results compare well with those in [2], even though a different constitutive model, Bodners model, was used.

For this problem, the first method of solution required approximately 3 min 20 sec of CPU time, while the second method required 5 min 20 sec (on a Harris 800 II).

Example Problem #2 (Pressure Cylinder usi· ·s Equations). A hollow circular aluminum cylinder, with an internal radius of 5 inches and external radius of 10 inches, is loaded under plane strain conditions with an internal pressure of 750 psi. The pressure is rapidly applied, so that an initial elastic stress distribution is present, and held constant over 100 hours. The finite element discretization for this problem consists of five, eight-node quadratic elements along the cylinder thickness.

Plots of the radial stress, a·ial stress, and circumferential stress distributions at various times are shown in Figs. 29 - 31. These results are essentially the same as those given in [5].

For this problem, method 1 required 11 min 30 sec of CPU time, while method 2 required 22 min 10 sec.

Example Problem #3 (Perforated Torsion Strip using Bodners Equations). A rectangular perforated tension strip is loaded with a uniform tensile stress as is shown in Fig. 32. The stress is applied rapidly, so that an initial elastic stress distribution is present, and held constant for a period of 30 seconds.

For a stress of 100 MPa, plots of the axial stress versus time along section A-A are shown in Fig. 33. The advancement of the "plastic zone" from 0.5 sec to 30 sec is also shown in Fig. 34, with regions of equivalent nonelastic strain at time = 30 seconds shown in Fig. 35.

This tension strip was also subjected to a stress of 125 MPa and held constant for 30 seconds as above. The corresponding growth of the "plastic zone" is shown in Fig. 36. Comparing this figure with Fig. 34, we observe a large increase in size of the nonelastic region for an increased loading.

For loading up to 100 MPa, the first integration method required 100 minutes 20 seconds of CPU time, while the second algorithm used 49 minutes 20 seconds. For the 125 MPa loading, the first solution method completed in 226 minutes 10 seconds and the second method required 131 minutes 40 seconds (on a Harris 800 II).

REFERENCES

1. HAYHURST, D.R. and KRZECZKOWSKI, A.J., "Numerical Solution of Creep Problems," *Computer Methods in Appl. Mech. and Engng.*, Vol. 20, pp. 151-171, 1979.

2. ZIENKIEWICZ, O.C. and CORMEAU, I.C., "Visco-Plasticity Solution by Finite Element Process," *Archives of Mechanics*, Vol. 24, pp. 873-889, 1972.

3. ZIENKIEWICZ, O.C. and CORMEAU, I.C., "Visco-Plasticity - Plasticity and Creep in Elastic Solids - A Unified Numerical Solution Approach," *Intl. J. for Num. Meth. in Engng.*, Vol. 8, pp. 821-845, 1974.

4. SHIH, C.F., DeLORENZI, H.G., and MILLER, A.K., "A Stable Computational Scheme for Stiff Time-Dependent Constitutive Equations," **4th International Conference on Structural Mechanics in Reactor Technology**, L212, 1977.

5. KUMAR, V. and MUKHERJEE, S., "Time-Dependent Inelastic Analysis of Metallic Media Using Constitutive Relations with State Variables," *Nuclear Engng. and Design*, Vol. 41, pp. 27 - 43, 1977.

6. MUKHERJEE, S., KUMAR, V. and CHANG, K. J., "Elevated Temperature Inelastic Analysis of Metallic Medical Under Time Varying Loads Using State Variable Theories," *Intl. J. Solids Structures*, Vol. 14, p. 663-679, 1978.

7. BAZANT, Z.P., "Matrix Differential Equation and Higher-Order Numerical Methods for

Problems of Non-Linear Creep, Viscoelasticity and Elastoplasticity," *Intl. J. for Num. Meth. in Engng.*, Vol. 4, pp. 11 - 15, 1972.

8. ARGYRIS, J. H., VAZ, L.E., and WILLIAM, K.E., "Improved Solution Methods for Inelastic Rate Problems," *Computer Meth. in Appl. Mech. and Engng.*, Vol. 16, pp. 231 - 277, 1978.

9. HUGHES, T.J.R. and TAYLOR, R.L., "Unconditionally Stable Algorithms for Quasi-Static Elasto/Visco-Plastic Finite Element Analysis," *Computers and Structures,* Vol. 8, pp. 169 - 173, 1978.

10. KANCHI, M.B., ZIENKIEWICZ, O.C., and OWEN, D.R.J., "The Visco-Plastic Approach to Problems of Plasticity and Creep Involving Geometric Nonlinear Effects," *Intl. J. for Num. Meth. in Engng.*, Vol. 12, pp. 169 - 191, 1978.

11. MARQUES, J.M.M.C. and OWEN, D.R.J., "Strain Hardening Representation for Implicit Quasistatic Elasto-Viscoplastic Algorithms," *Computers and Structures,* Vol. 17, pp. 301 - 304, 1983.

12. KUMAR, V., MARJARIA, M., and MUKHERJEE, S., "Numerical Integration of Some Stiff Constitutive Models of Inelastic Deformation," *J. Engng. Mat. Tech.*, Vol. 102, pp. 92 - 96, 1980.

13. GEAR, C.W., "The Automatic Integration of Ordinary Differential Equations," *Communications of the ACM*, Vol. 14, pp. 176 - 179, 1971.

14. GEAR, C.W., " DIFSUB for Solution of Ordinary Differential Equations," *Communications of the ACM*, Vol. 14, pp. 185 - 190, 1971.

15. BODNER, S.R. and PARTOM, Y., "A Large Deformation Elastic-Viscoplastic Analysis of a Thick-Walled Spherical Shell," *J. Applied Mech.*, Vol. 94, pp. 751 - 757, 1972.

16. BODNER, S.R. and PARTOM, Y., "Constitutive Equations for Elastic Viscoplastic Strain-Hardening Materials," *J. Applied Mech.*, Vol. 42, pp. 385 - 389, 1975.

17. BODNER, S.R., "A Hardness Rule for Inelastic Deformation," *Intl. J. of Engng. Sci.*, Vol. 16, pp. 221 - 230, 1977.

18. STOUFFER, D.C., and BODNER, S.R., "A Constitutive Model for the Deformation Induced Anisotropic Plastic Flow of Metals," *Intl. J. of Engng. Sci.*, Vol. 17, pp. 757 - 764, 1979.

19. BODNER, S.R. and PARTOM, I. and PARTOM, Y., "Uniaxial Cyclic Loading of Elastic-Viscoplastic Materials," J. of Applied Mech., Vol. 46, pp. 805 - 810, 1979.

20. ABONDI, J. and BODNER, S.R., "Dynamic Response of a Slab of Elastic-Viscoplastic Material That Exhibits Induced Plastic Anisotrophy," *Intl. J. Engng. Sci.*, Vol. 18, pp. 801 - 813, 1980.

21. BODNER, S.R. and STOUFFER, D.C., "Comments on Anisotropic Plastic Flow and Incompressibility," *Intl. J. Engng. Sci.*, Vol. 21, pp. 211 - 215, 1983.

22. BODNER, S.R., "Review of a Unified Elastic-Viscoplasticity Theory (The Bodner Equations)," Interim Scientific Report, Oct. 1984.

23. HART, E.W., "A Theory for Flow of Polycrystals," *Acta Metallurgica*, Vol. 15, pp. 1545 - 1549, 1967.

24. HART, E.W., "A Phenomenological Theory for Plastic Deformation of Polycrystalline Metals," Acta Metallurgica, Vol. 18, pp. 599 - 610, 1970.

25. HART, E.W., YAMEDA, H., LI, C.Y., and WIRE, G.L., "Phenomenological Theory: A Guide to Constitutive Equations and Fundamental Deformation Properties," **Constitutive Equations in Plasticity**, Argon, A.S., ed., M.I.T. Press, Cambridge, Mass., 1975.

26. HART, E.W., "Constitutive Relations for the Nonelastic Deformation of Metals," *J. Engng. Mat. Tech.*, Vol. 98, pp. 193 - 202, 1976.

27. HART, E.W., "Constitutive Relations for Nonelastic Deformation," *Nuclear Engng. and Design*, Vol. 46, pp. 179 - 185, 1978.

28. GILLIS, P. and JONES, S., "Linearly Viscoplastic Materials," *J. of Applied Physics*, Vol. 43, pp. 2845 - 2849, 1977.

29. ROBINSON, D.N., "A Unified Creep-Plasticity Model for Structural Metals at High Temperatures," ORNL-TM-5969, 1978.

30. ROBINSON, D.N., PUGH, C.E., and CORUM, J.M., "Constitutive Equations for Describing High-Temperature Inelastic Behavior of Structural Alloys," **IAEA International Working Group on Fast Reactors, Specialists - Meeting on High Temperature Structural Design Technology**, April, 1976.

31. MILLER, A., "An Inelastic Constitutive Model for Monotonic, Cyclic and Creep Deformation: I - Equations, Development and Analytical Procedures, " *J. Engng. Mat. Tech.*, Vol. 98, pp. 97 - 105, 1976.

32. MILLER, A., "An Inelastic Constitutive Model for Monotonic, Cyclic and Creep Deformation: II - Application to Type 304 Stainless Steel," *J. Engng. Mat. Tech.*, Vol. 98, pp. 106 - 113, 1976.

33. KRIEG, R.D., SWEARENGEN, J.C., and ROHDE, R.W., "A Physically-Based Internal State Variable Model for Rate Dependent Plasticity," **Proceedings at ASME/CSME PVP Conference**, pp. 15 - 27, 1978.

34. CERNOCKY, E.P. and KREMPL, E., "A Nonlinear Uniaxial Integral Constitutive Equation Incorporating Rate Effects, Creep and Relaxation," *Intl. J. Nonlinear Mech.*, Vol. 14, pp. 183 - 203, 1978.

35. CERNOCKY, E.P. and KREMPL, E., "A Theory of Viscoplasticity Based on Infinitesimal Total Strain," *Acta Mechanica*, Vol. 36, pp. 263 - 269, 1980.

36. LIU, M.C.M. and KREMPL, E., "A Uniaxial Viscoplastic Model Based on Total Strain and Overstress," *J. Mech. Phys. Solids*, Vol. 27, pp. 377 - 391, 1979.

37. CERNOCKY, E.P. and KREMPL, E., "A Theory of Thermoviscoplasticity Based on Infinitesimal Total Strain," *Intl. J. Solids Structures*, Vol. 16, pp. 723 - 741, 1980.

38. CERNOCKY, E.P. and KREMPL, E., "A Coupled, Isotropic Theory of Thermoviscoplasticity Based on Total Strain and Overstress and its Predictions in Monotonic Torsional Loading," *J. of Thermal Stresses*, Vol. 4, pp. 69 - 82, 1981.

39. CESCOTTO, S. and LECKIE, F., "Determinatio of Unified Constitutve Equations for Metals at High Temperature," **Proc. Intl. Conference on Constitutive Laws for Eng. Mater.**, pp. 105 - 111, 1983.

40. LAMBERT, J.D., **Computational Methods in Ordinary Differential Equations**, Wiley, London, New York, 1973.

41. GEAR, C.W., **Numerical Initial Value Problems in Ordinary Differential Equations**, Prentice-Hall, Englewood Cliffs, N.J., 1971.

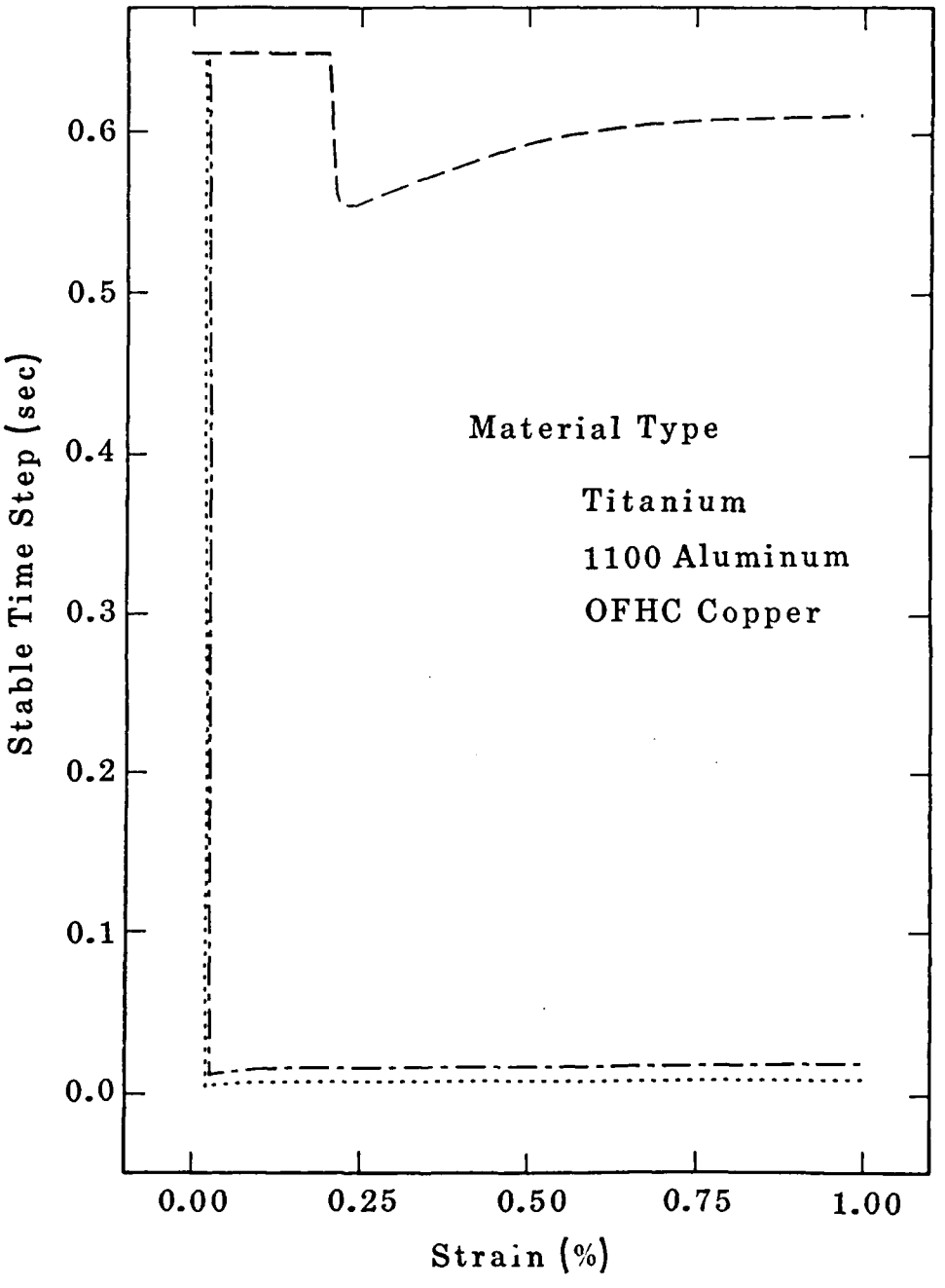

Figure 1 Stable Time Steps for Forward Euler Integration of Bodner's Constitutive Equations for Various Materials.

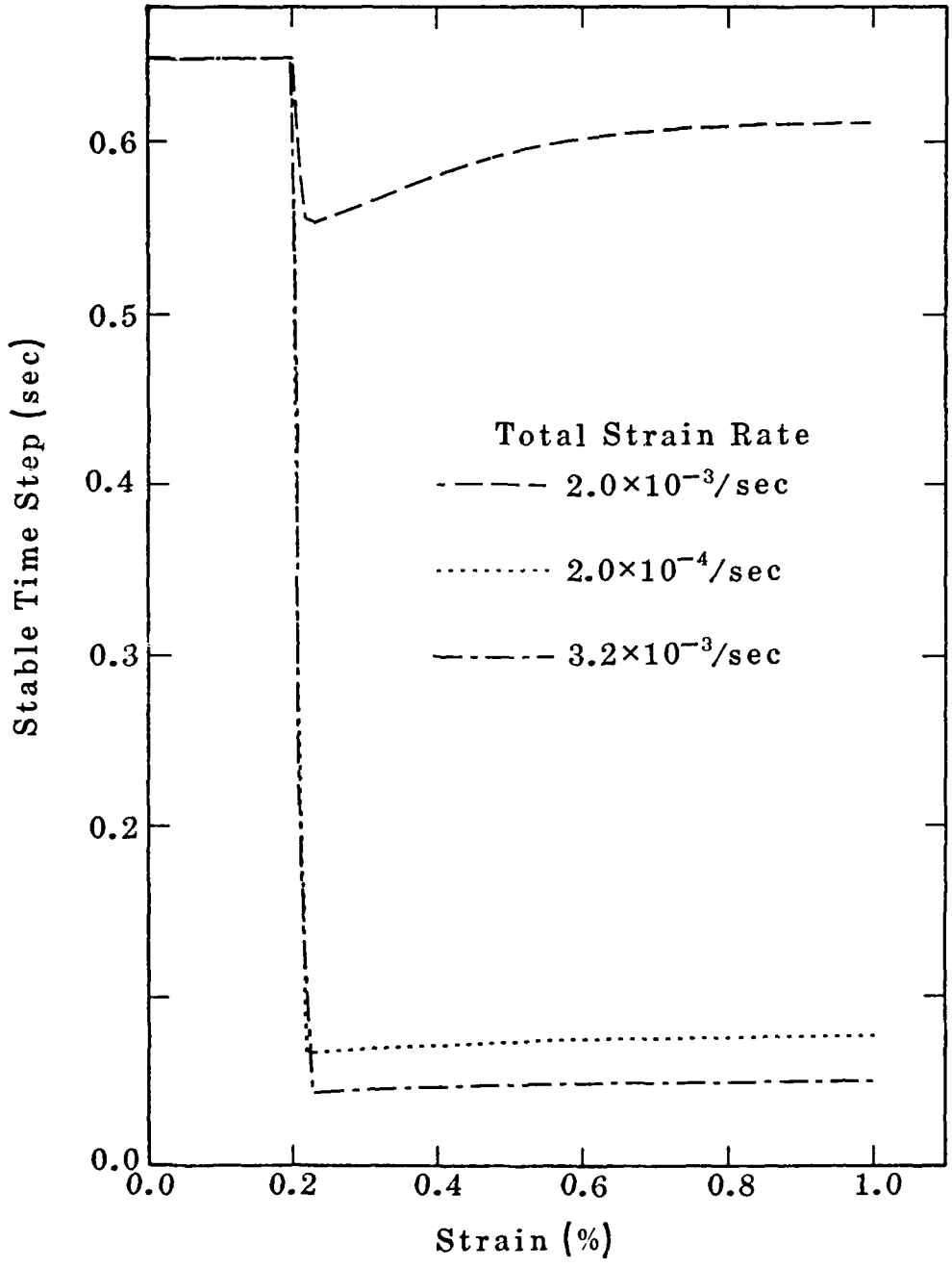

Figure 2 Stable Time Steps for Forward Euler Integration of Bodner's Constitutive Equations for Titanium.

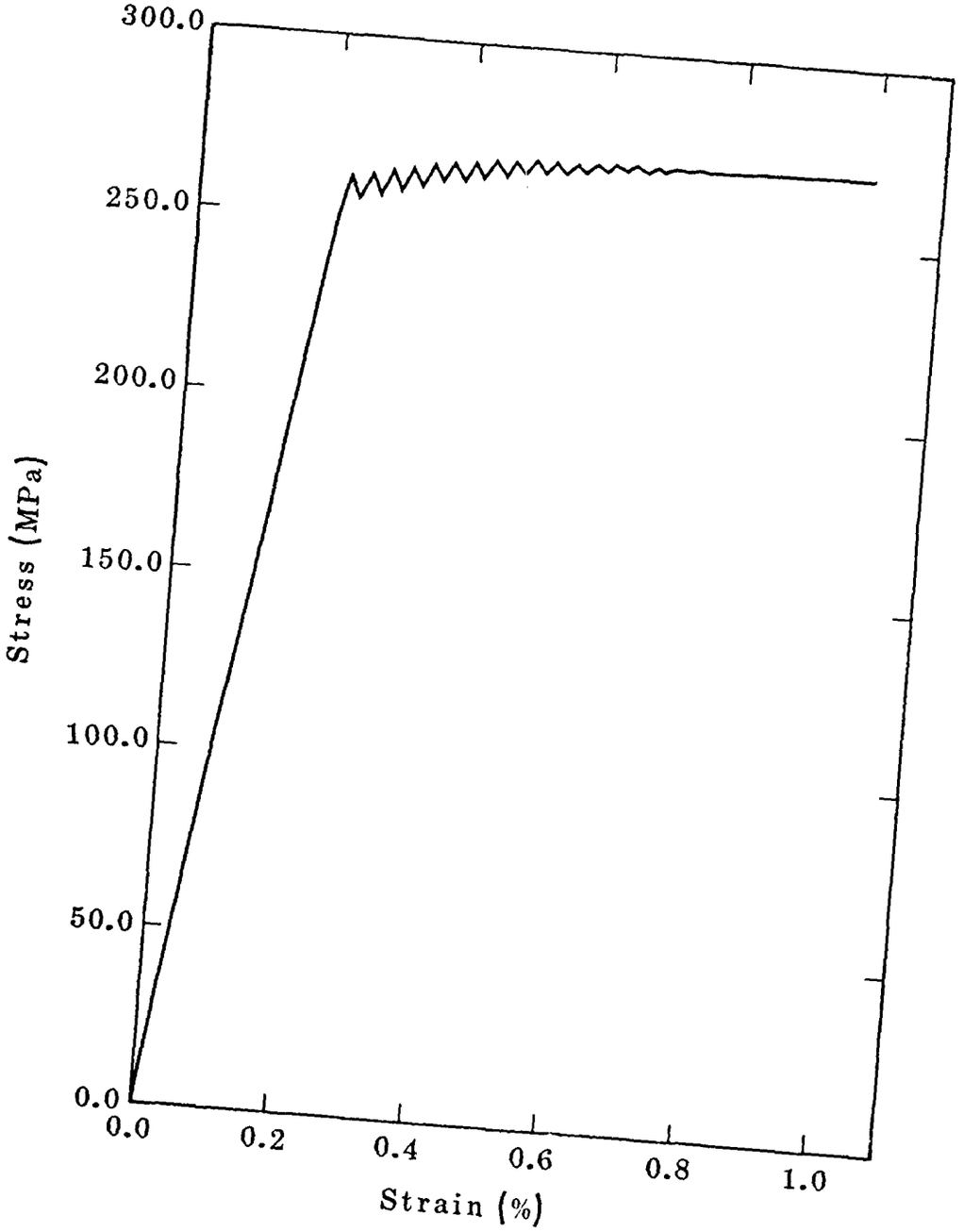

Figure 3 Decay of Oscillatory Behavior for a Conditionally Stable Time Integration Method.

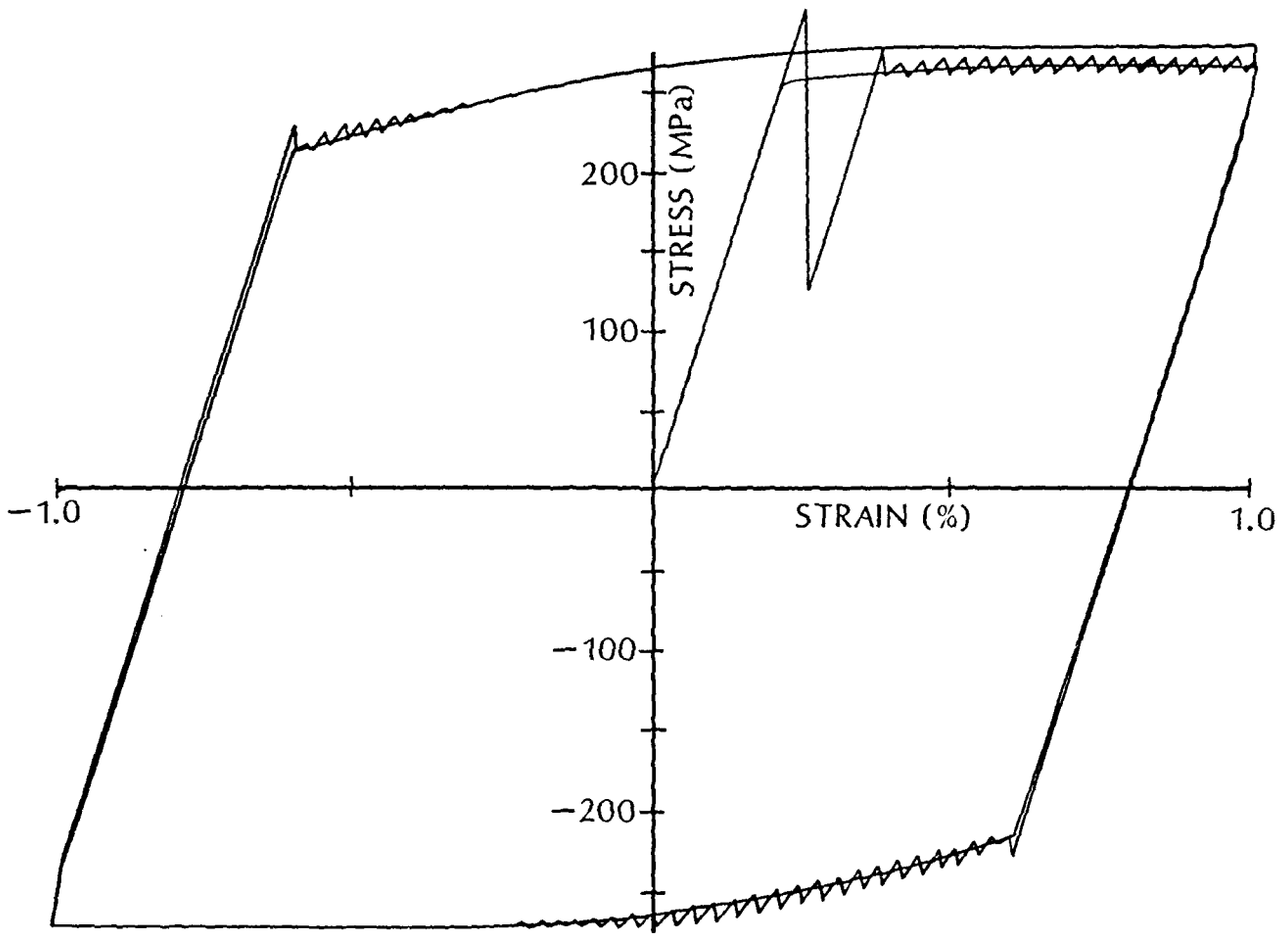

Figure 4 Calculated Stress-Strain Curve for Titanium with Time Steps Selected from $\tau\bar{\Delta}\varepsilon / \bar{\varepsilon}^{n}$.

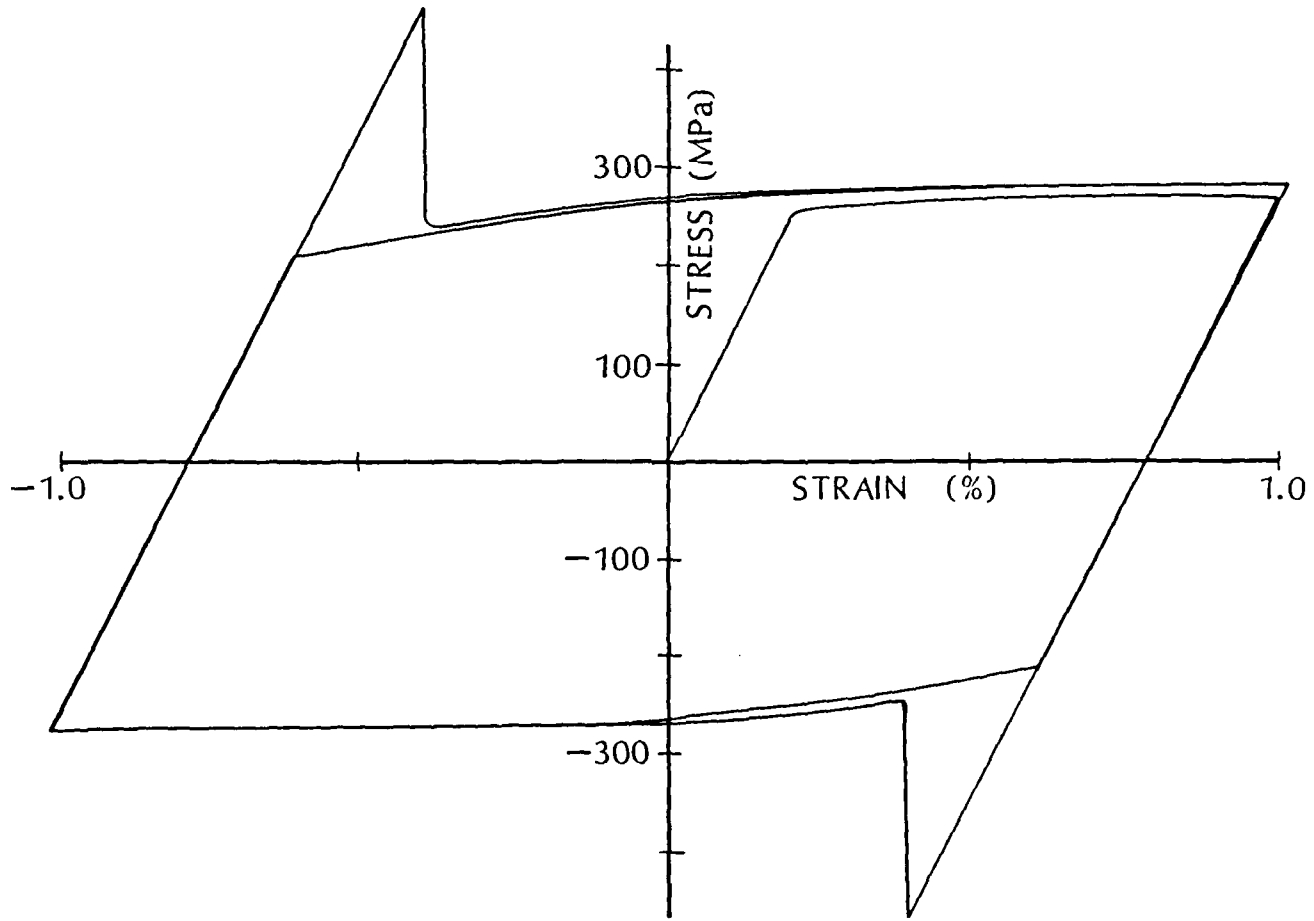

Figure 5 Calculated Stress-Strain Curve for Titanium with Time Steps Selected from a Doubling/Halfing Technique.

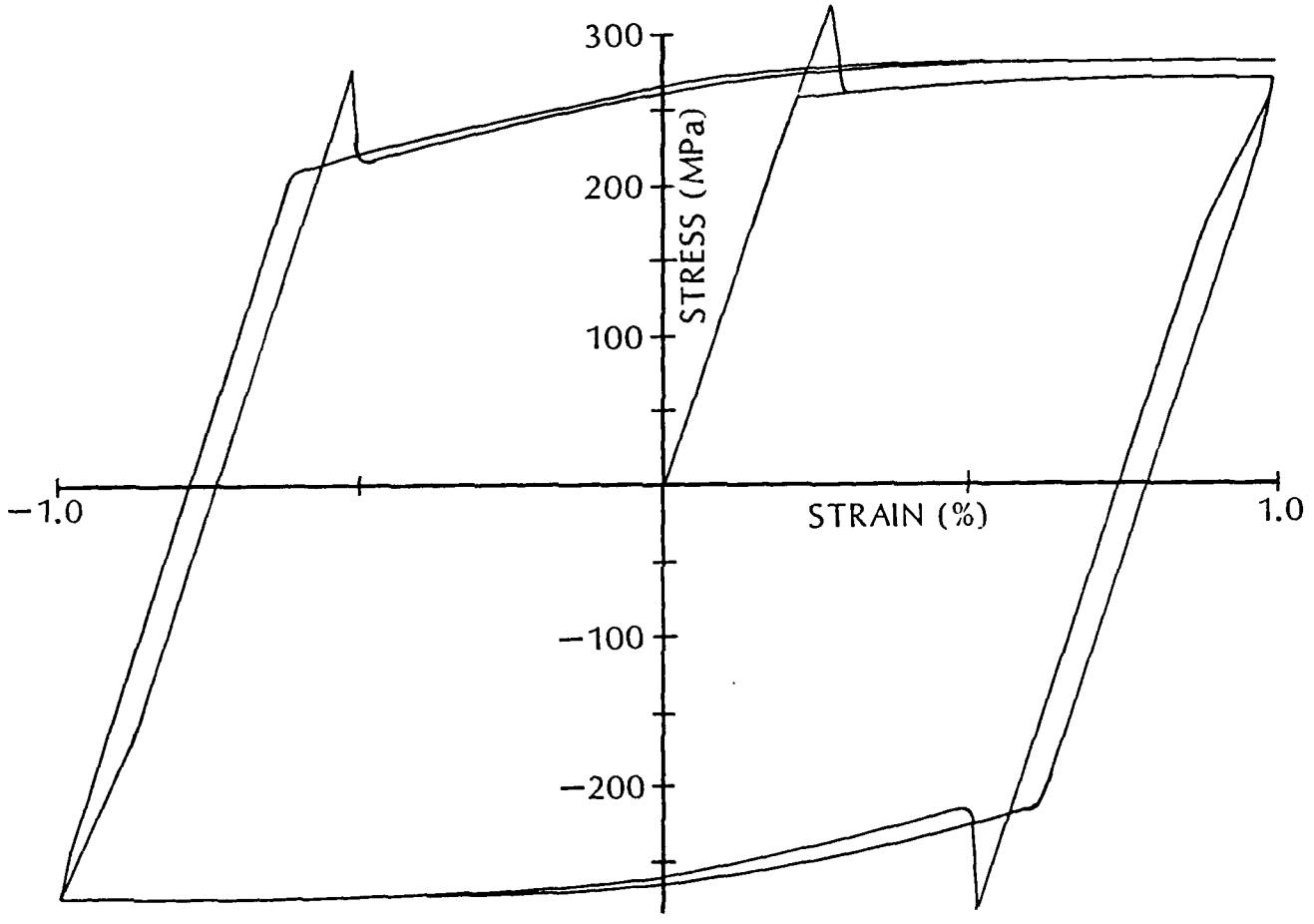

Figure 6 Calculated Stress-Strain Curve for Titanium Obtained using the Forward Gradient Scheme.

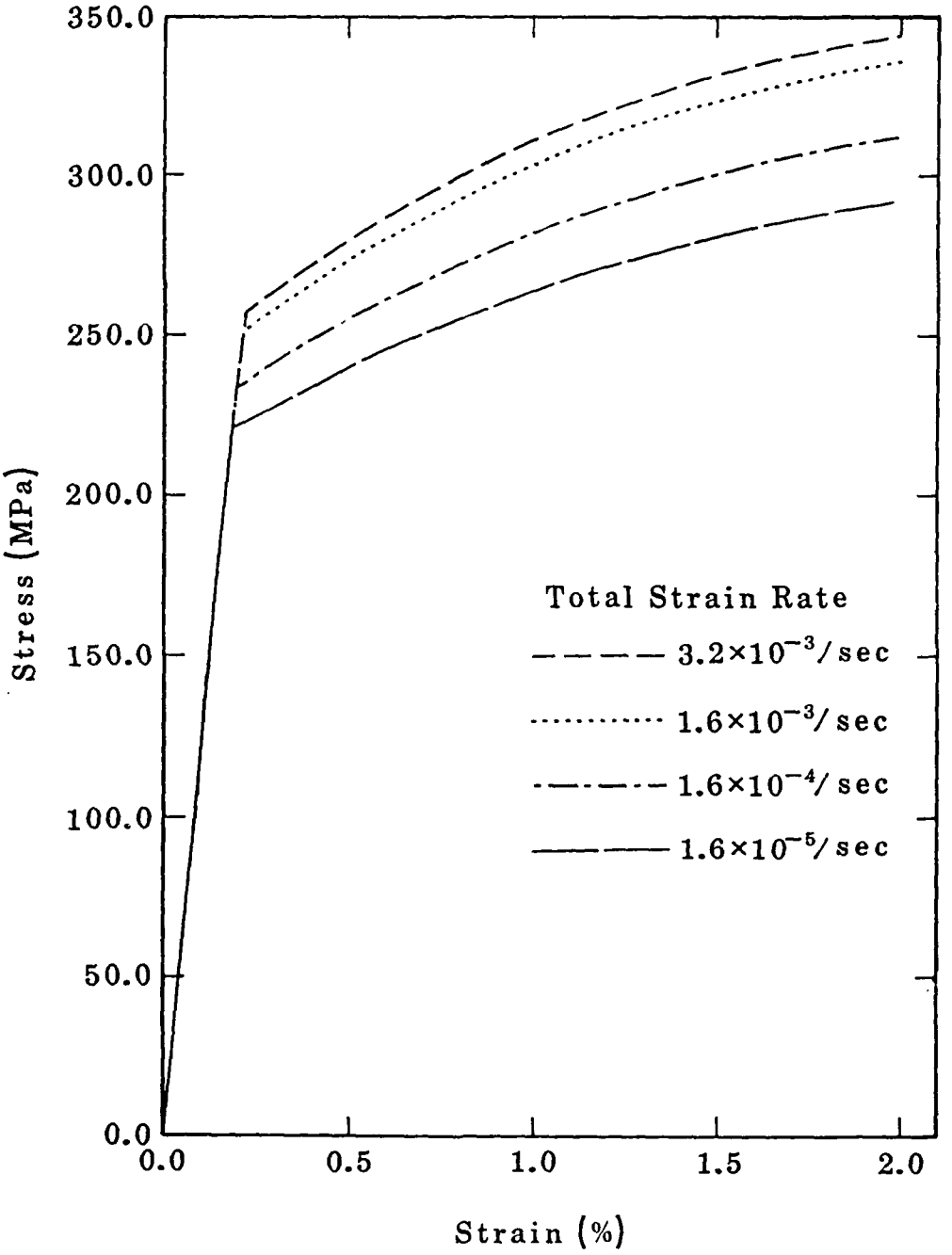

Figure 7 Monotonic Stress-Strain Curves for Titanium at Constant Strain Rates (Bodner's Equations in the Original Form.)

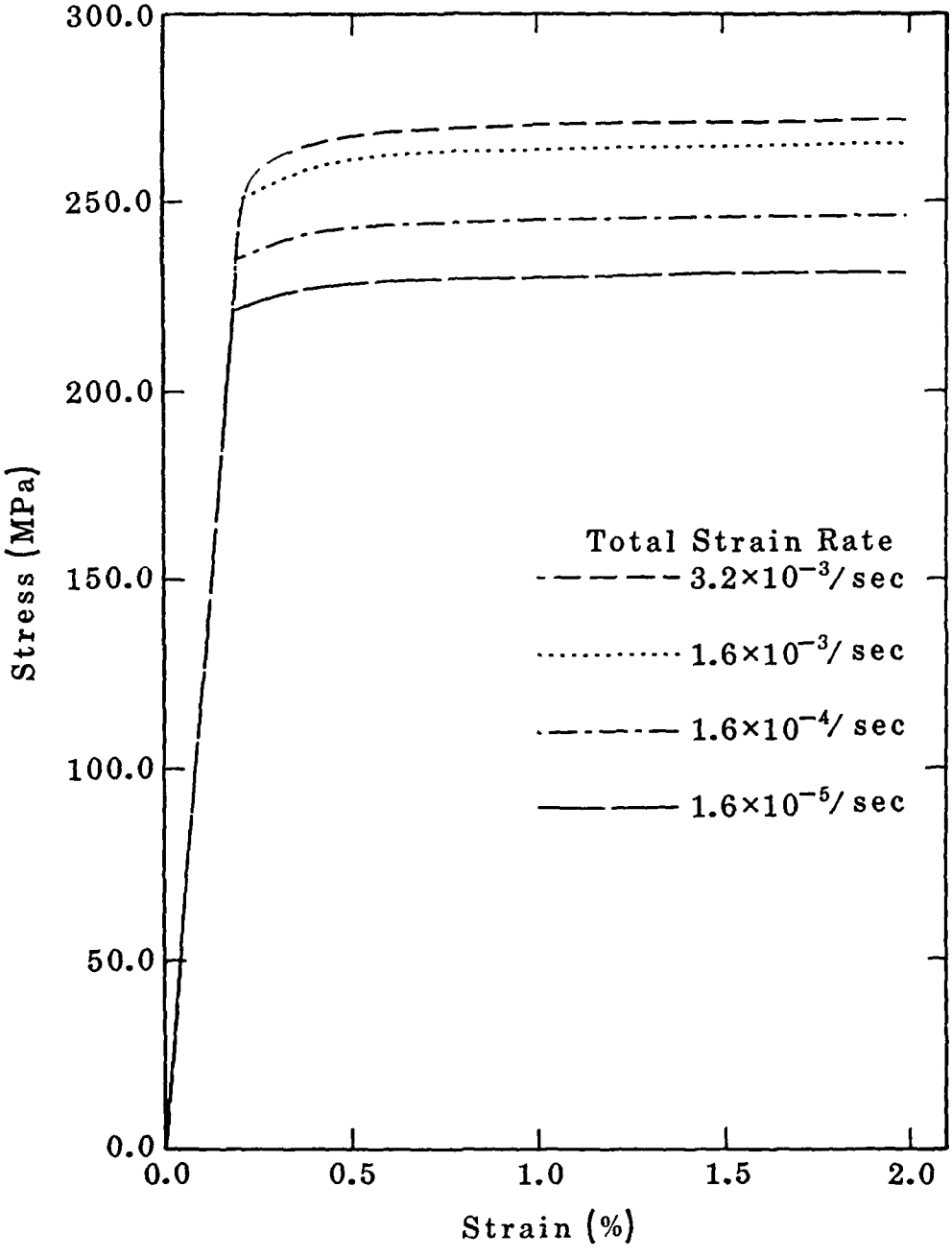
300.0
250.0
200.0
150.0
100.0
50.0
0.0
Stress (MPa)
0.0
0.5
1.0
1.5
2.0
Strain (%)
Total Strain Rate
3.2×10⁻³/sec
1.6×10⁻³/sec
1.6×10⁻⁴/sec
1.6×10⁻⁵/sec

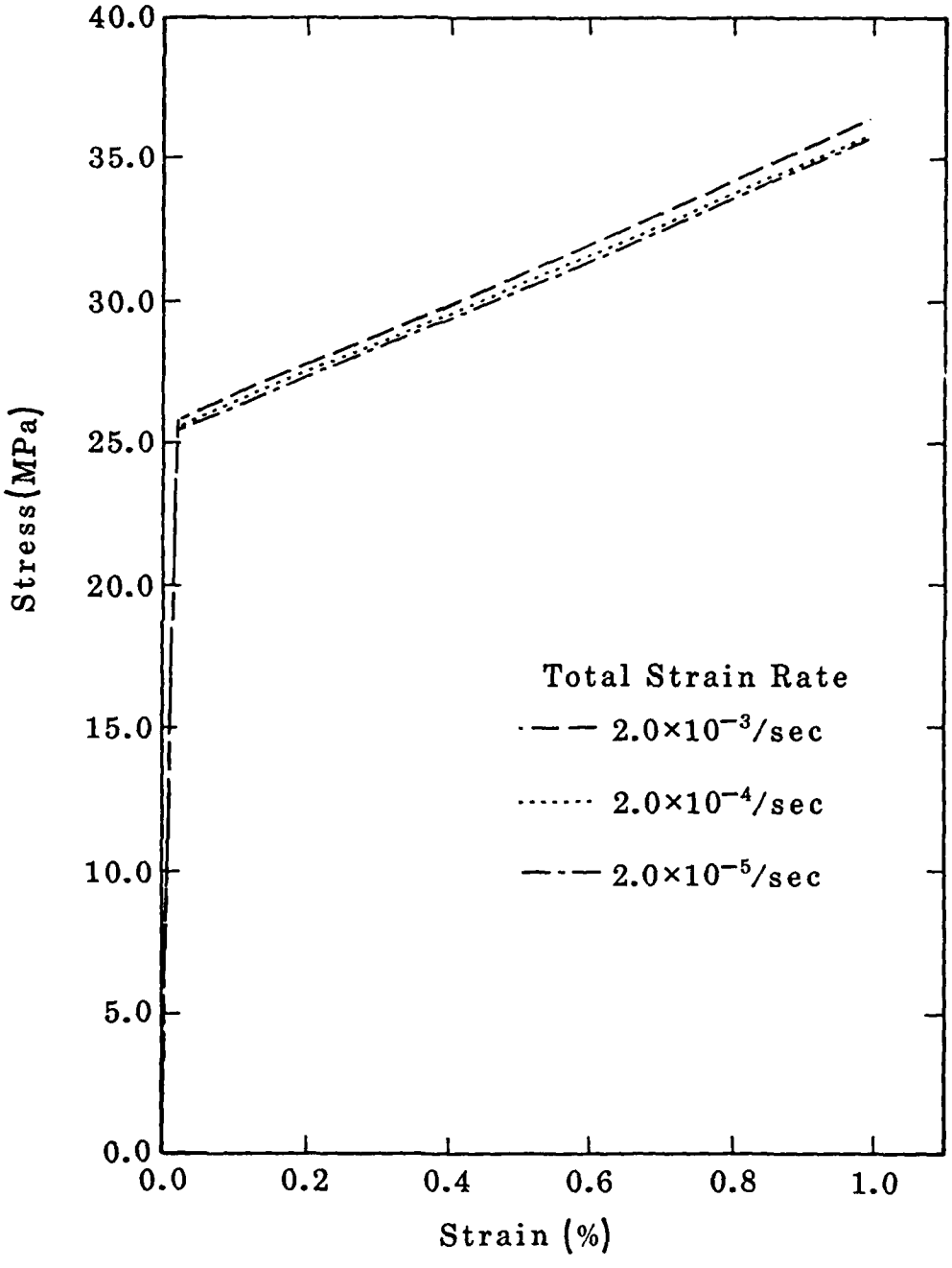

Figure 9 Monotonic Stress-Strain Curves for OFHC Copper at Constant Strain Rates (Bodner's Equations.)

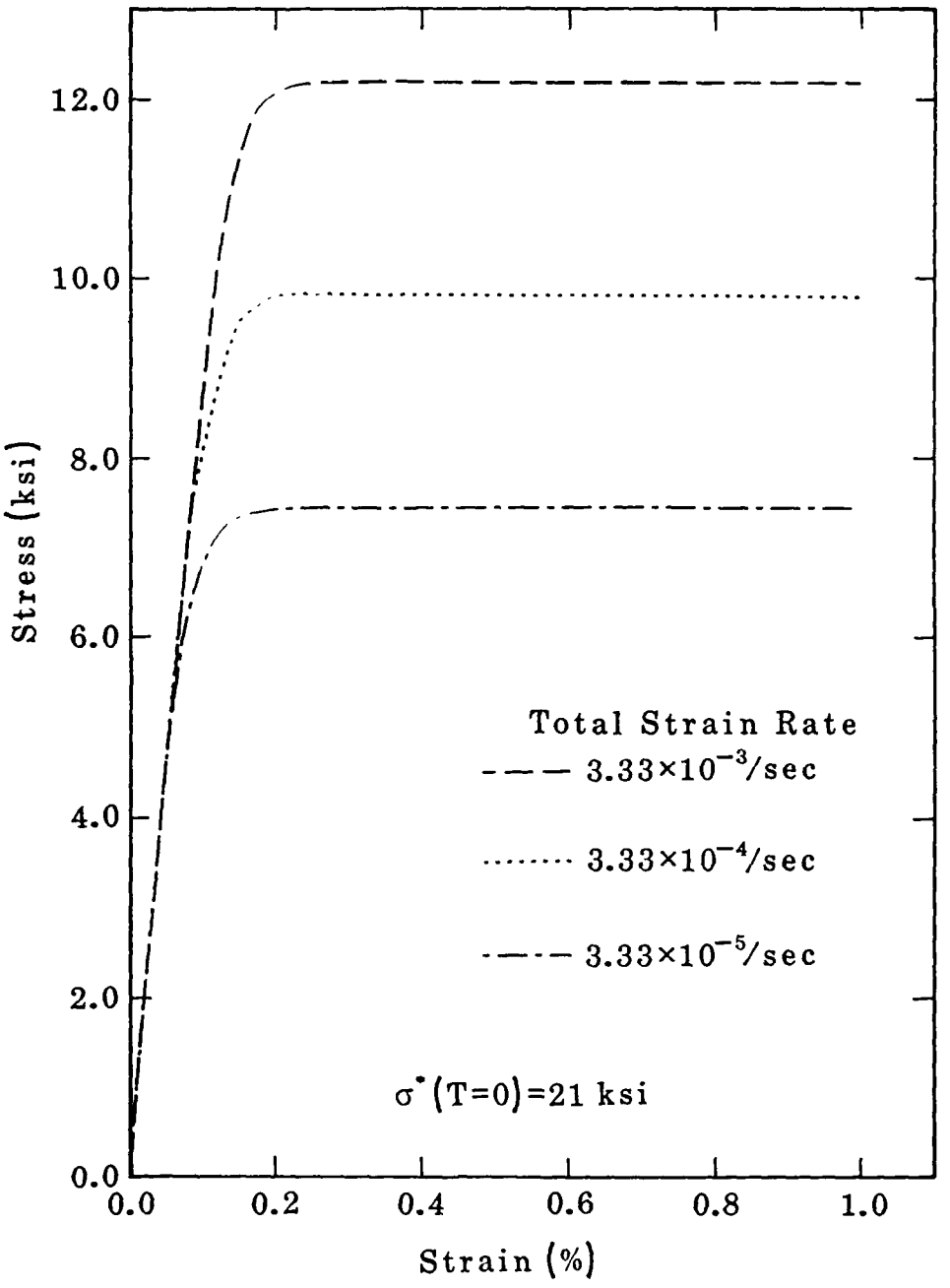

Figure 10 Monotonic Stress-Strain Curves for 1100 Aluminum at Constant Strain Rates (Hart's Equations.)

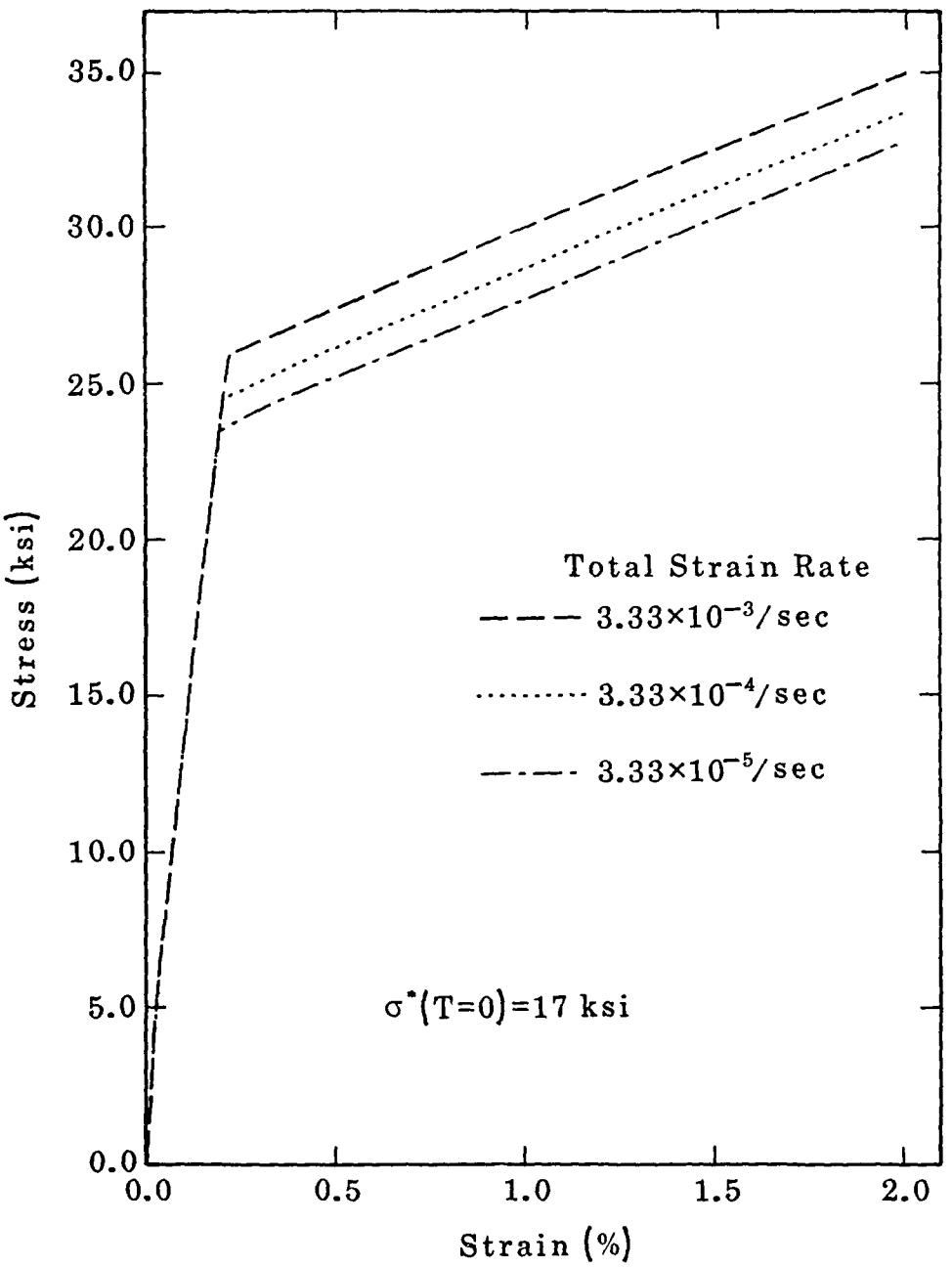

Figure 11 Monotonic Stress-Strain Curves for 304 Stainless Steel at Constant Strain Rates (Hart's Equations.)

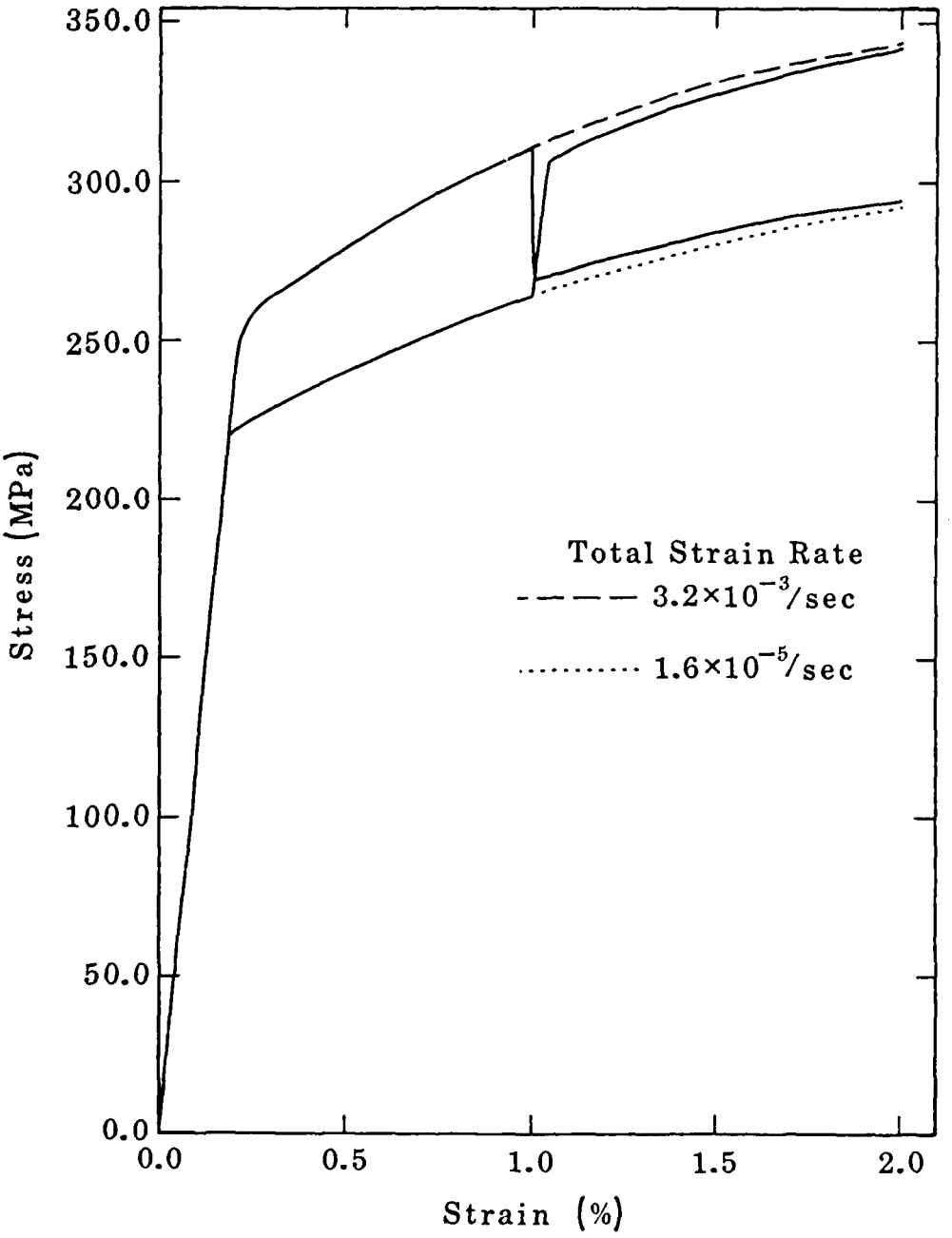

Figure 12 Stress-Strain Curves for Titanium Subjected to Rapid Changes in Strain Rate (Bodner's Equations.)

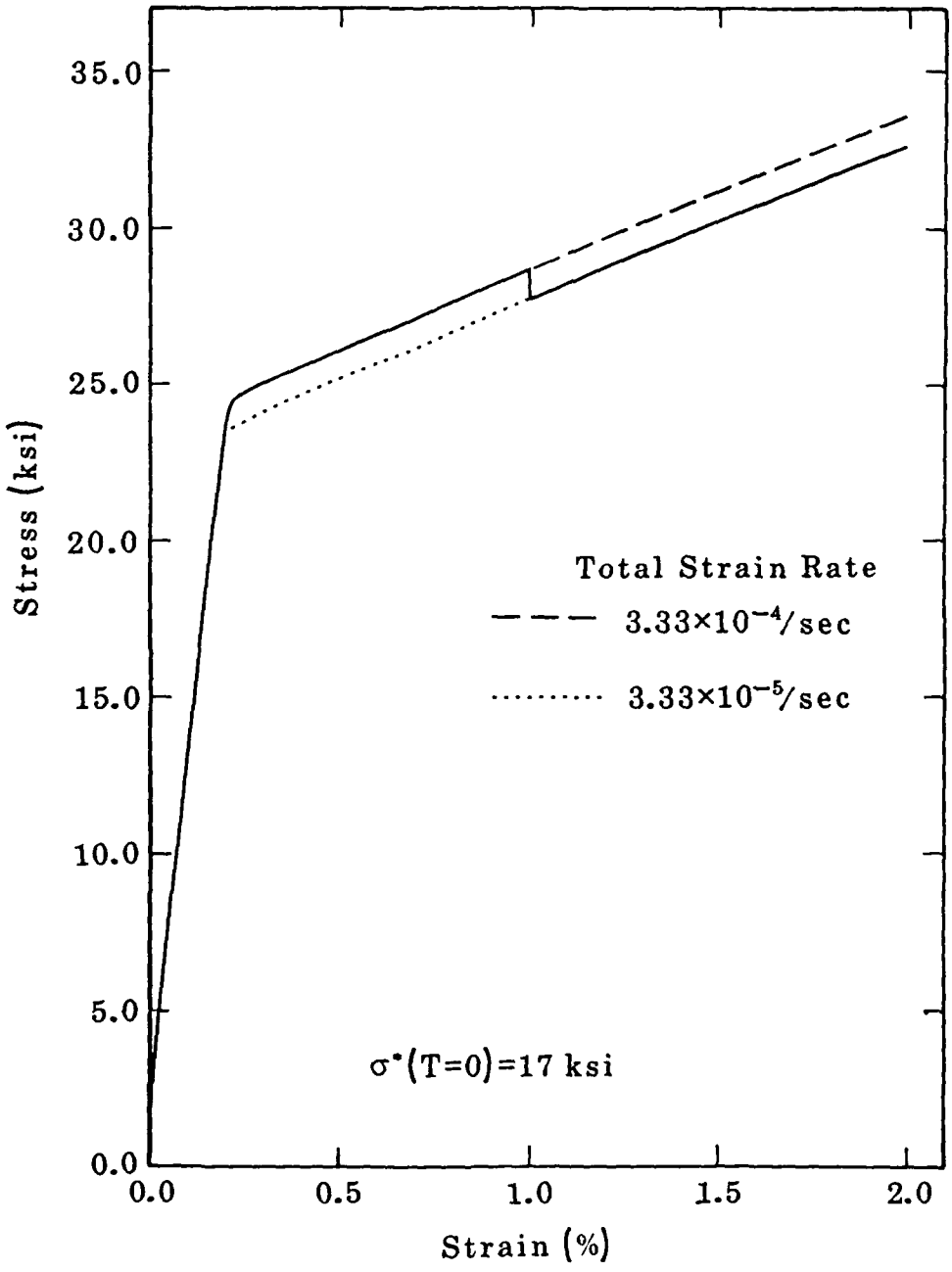

Figure 13 Stress-Strain Curves for 304 Stainless Steel Subjected to Rapid Changes in Strain Rate (Hart's Equations.)

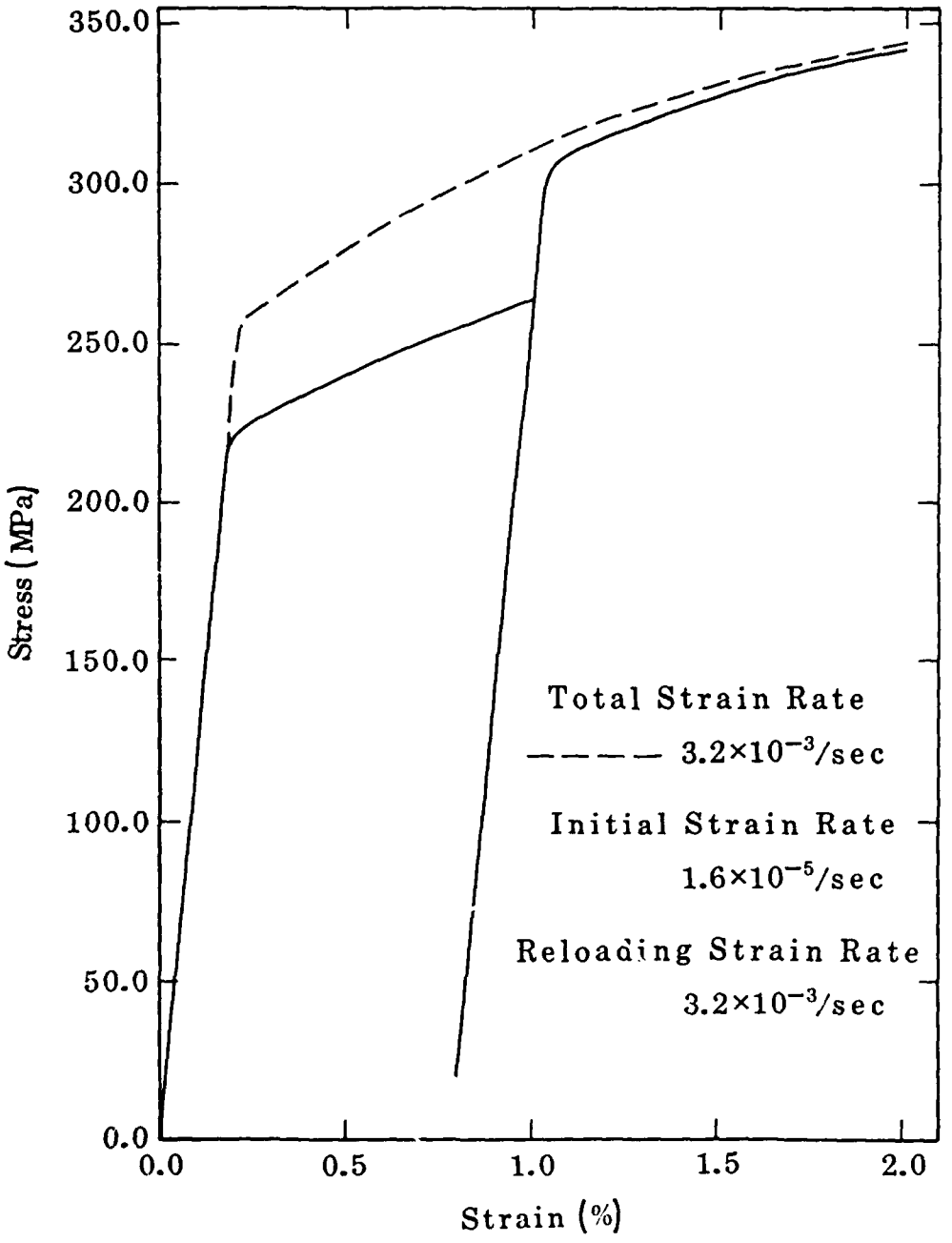

Figure 14 Stress-Strain Curves of Titanium Subjected to Unloading and Subsequent Reloading at a Faster Rate (Bodner's Equations.)

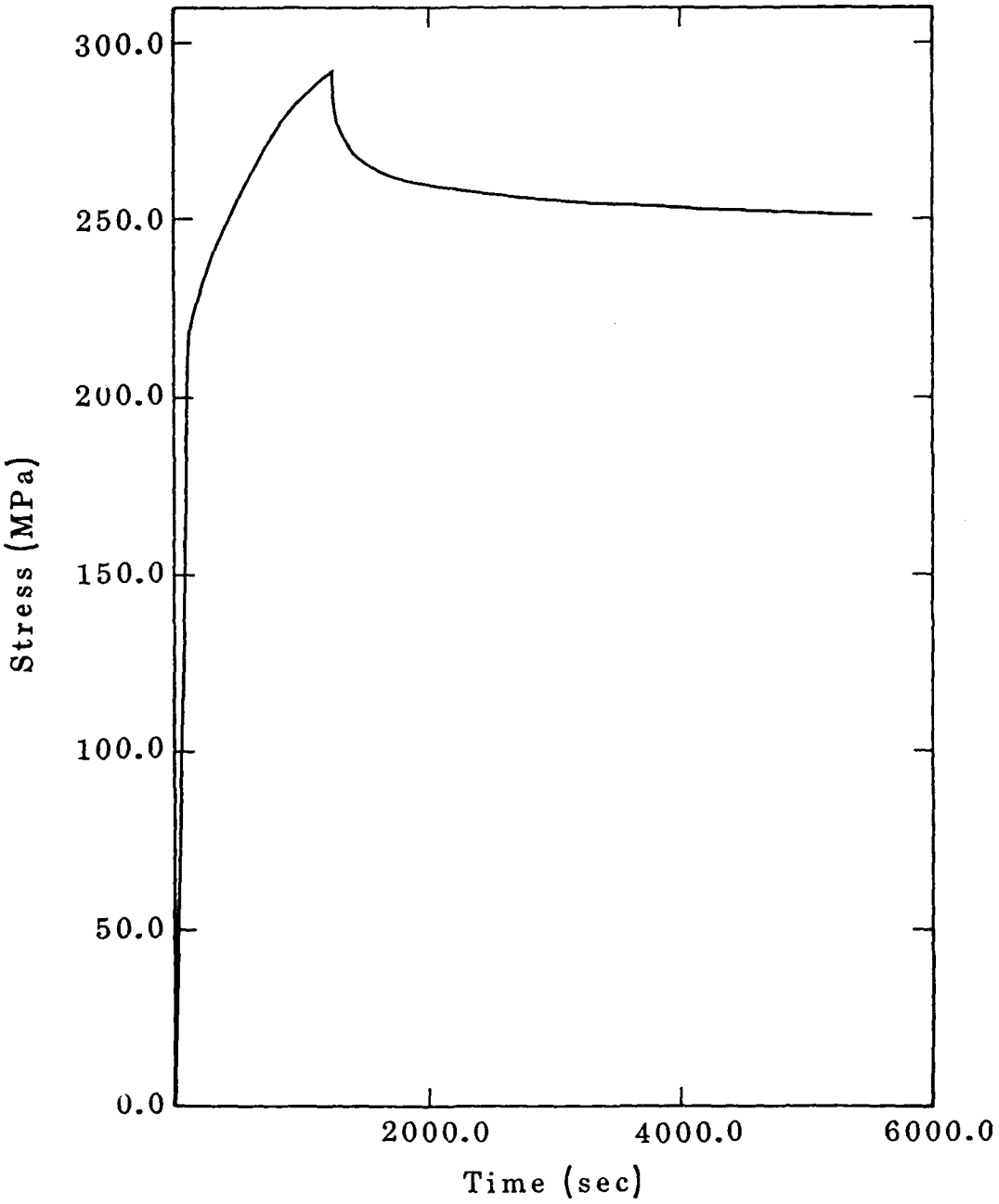

Figure 15 Stress Relaxation Curve for Titanium After Preloading to 2% Strain at 1.6E-5/sec (Bodner's Equations.)

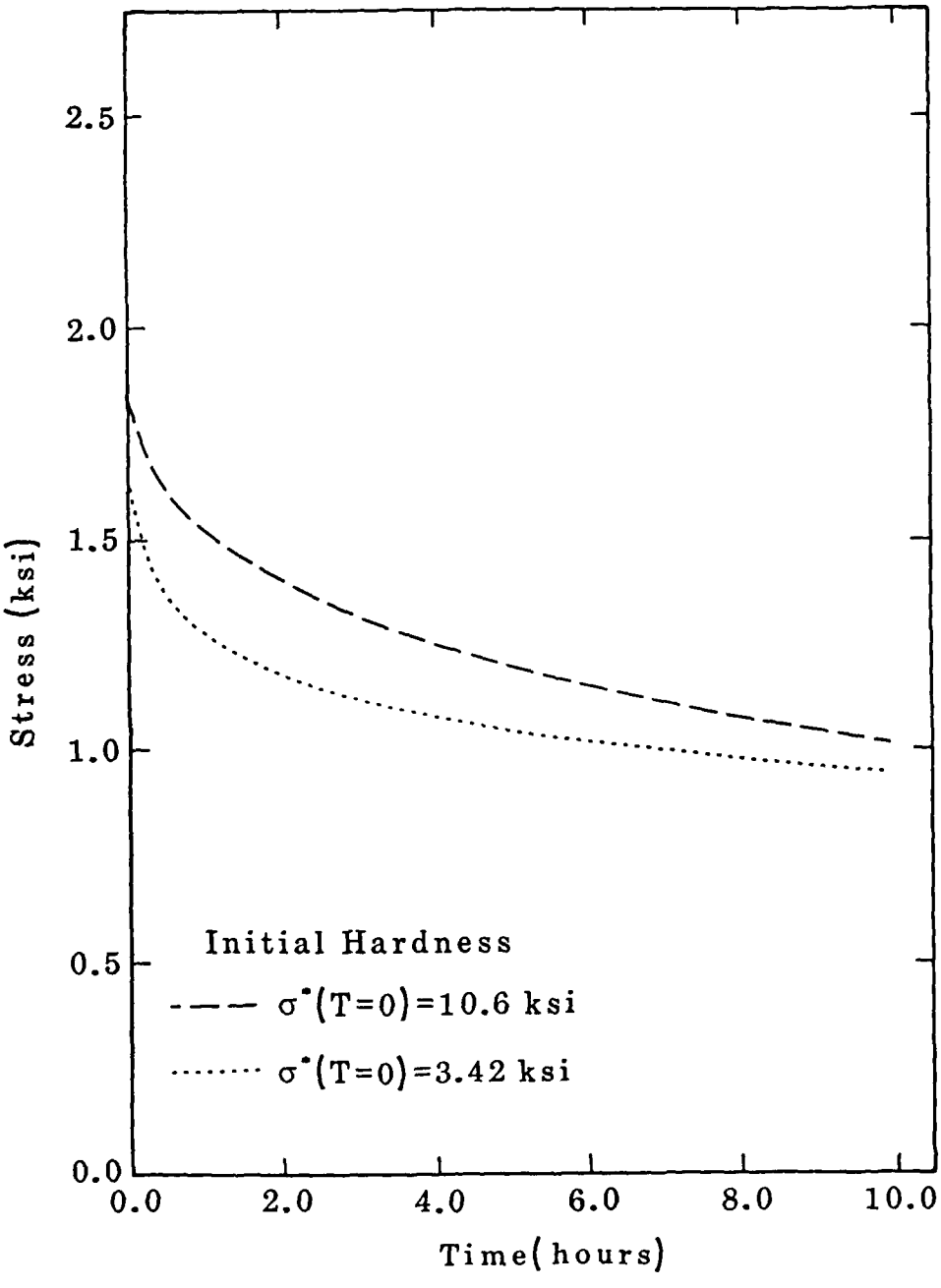

Figure 16 Stress Relaxation Curves for 1100 Aluminum with Different Initial Hardness Values (Hart's Equations.)

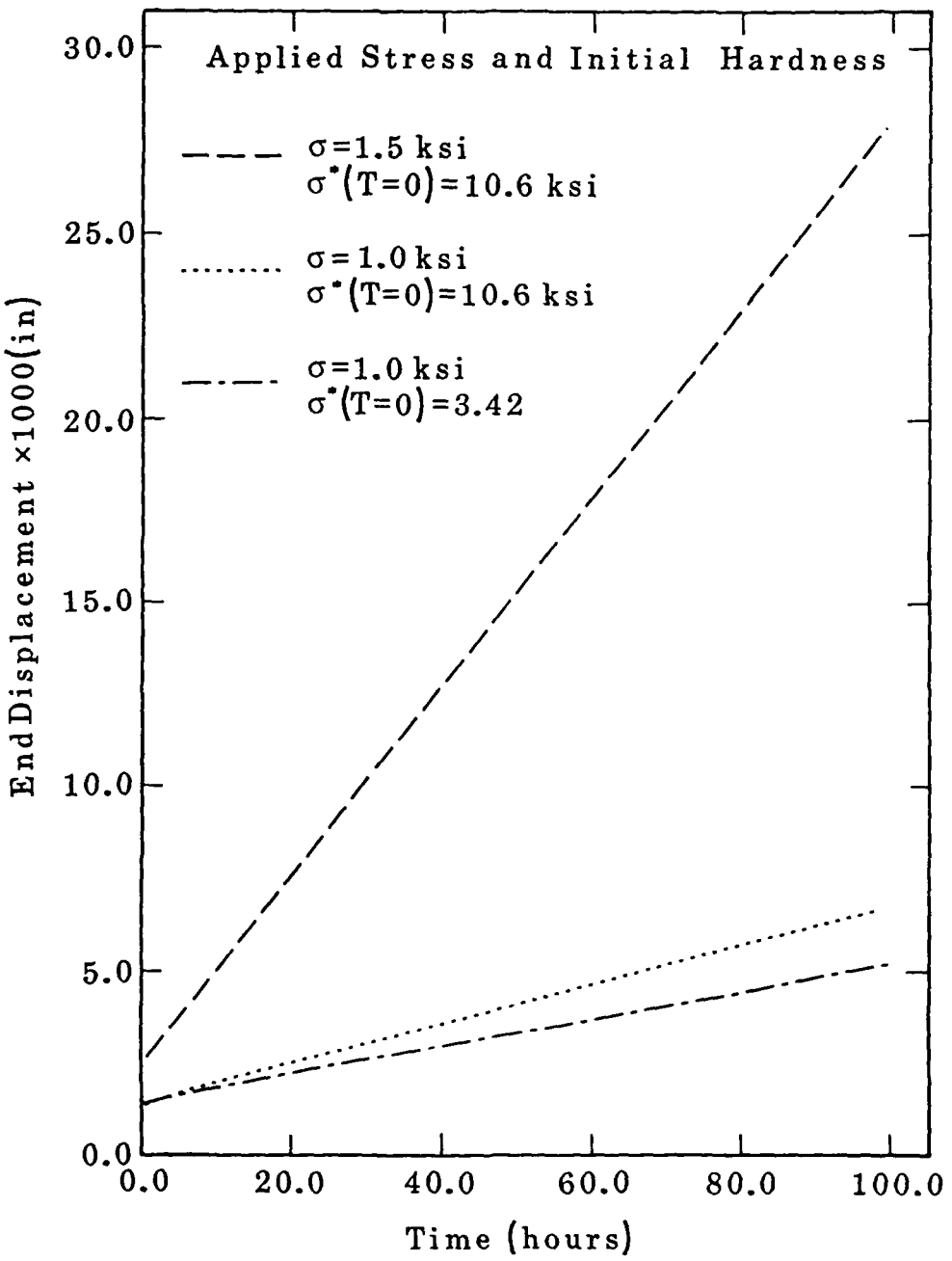

Figure 17 Creep Curves of 1100 Aluminum with Variable Initial Hardness and Applied Stress (Hart's Equations.)

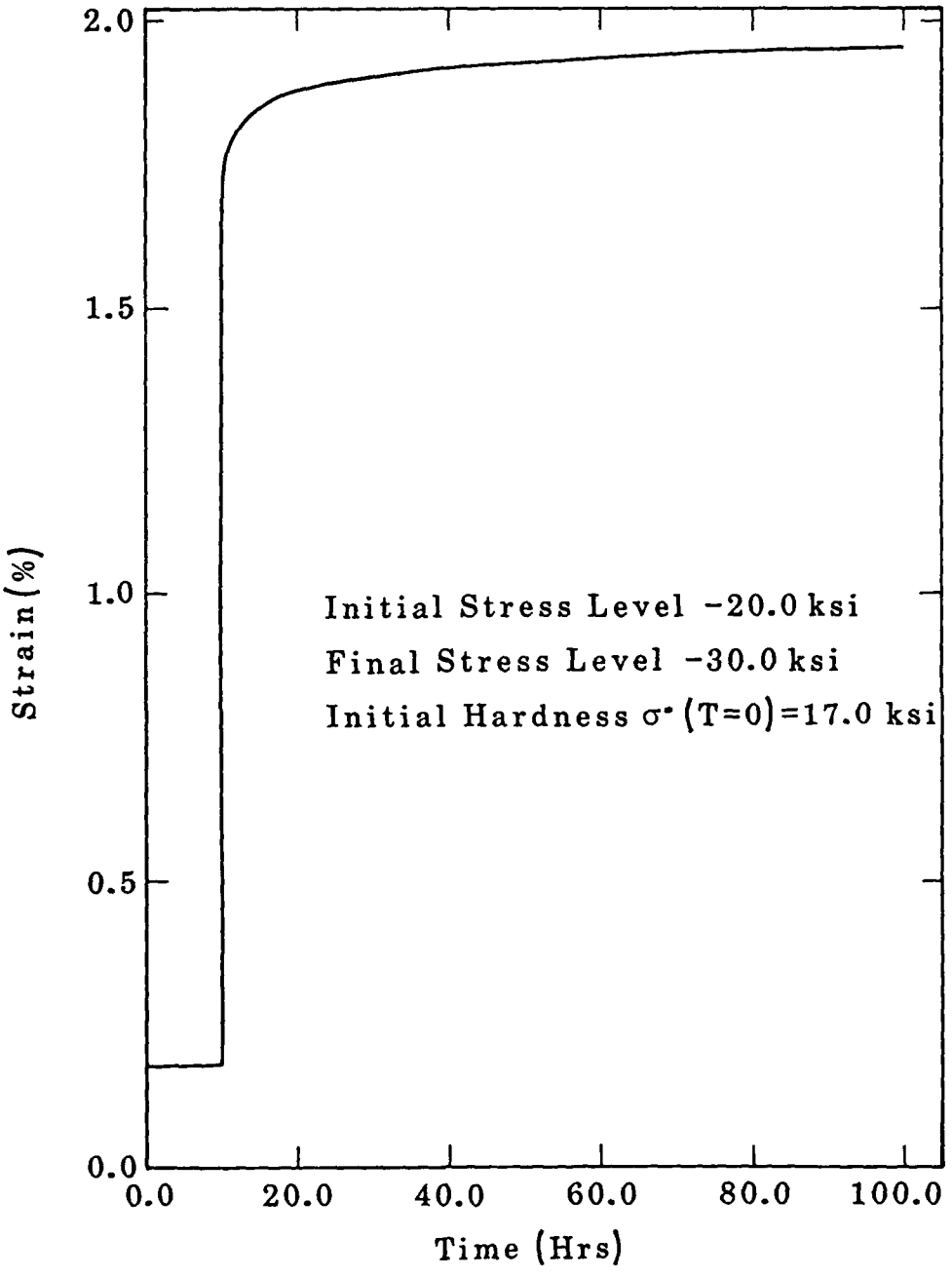

Figure 18 Calculated Strain-Time Curve for 304 Stainless Steel Subjected to a Stress Change Test (Hart's Equations.)

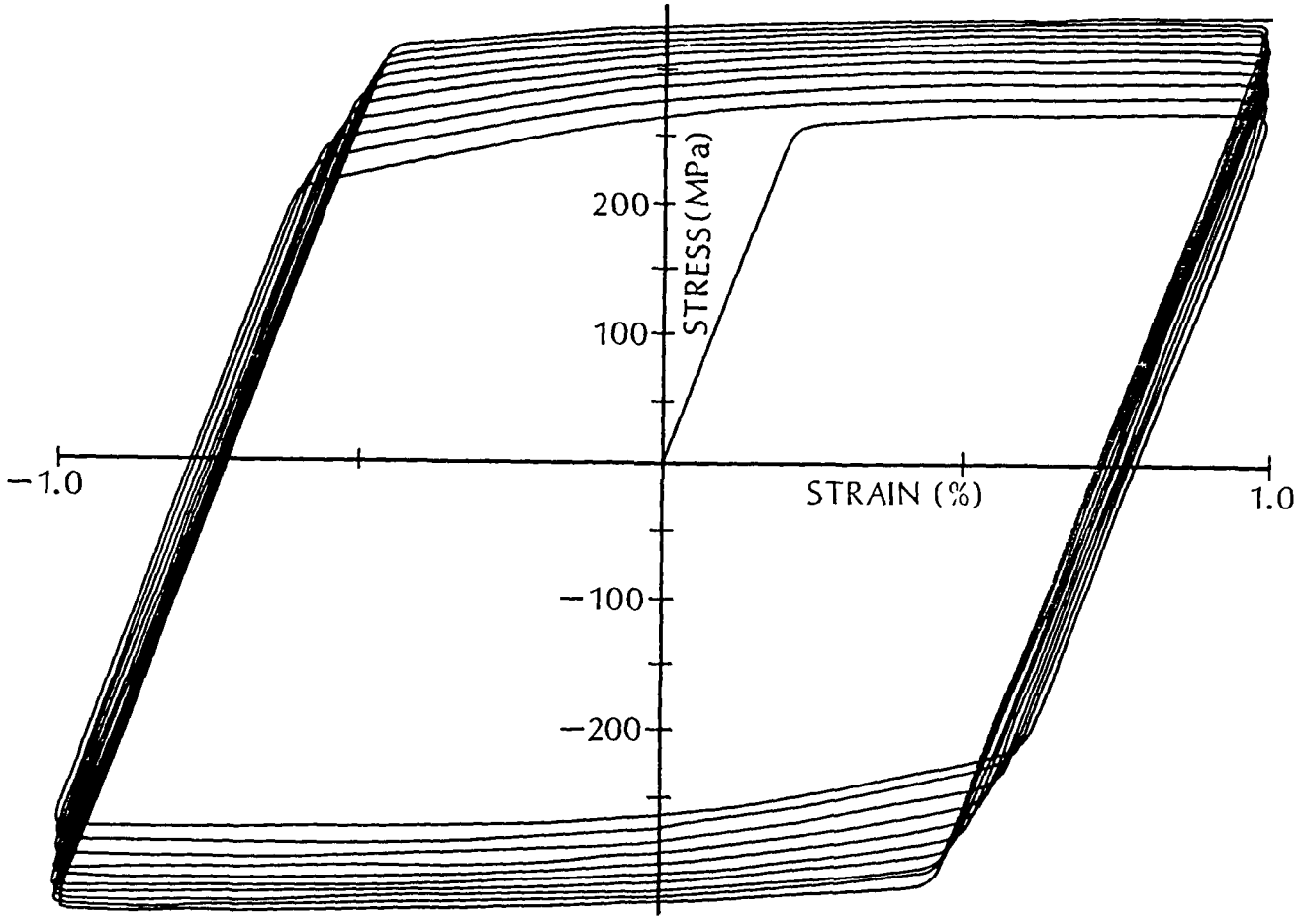

Figure 19 Cyclic Stress-Strain Curves for Titanium for ± 1-Percent Strain (Bodner's Equations.)

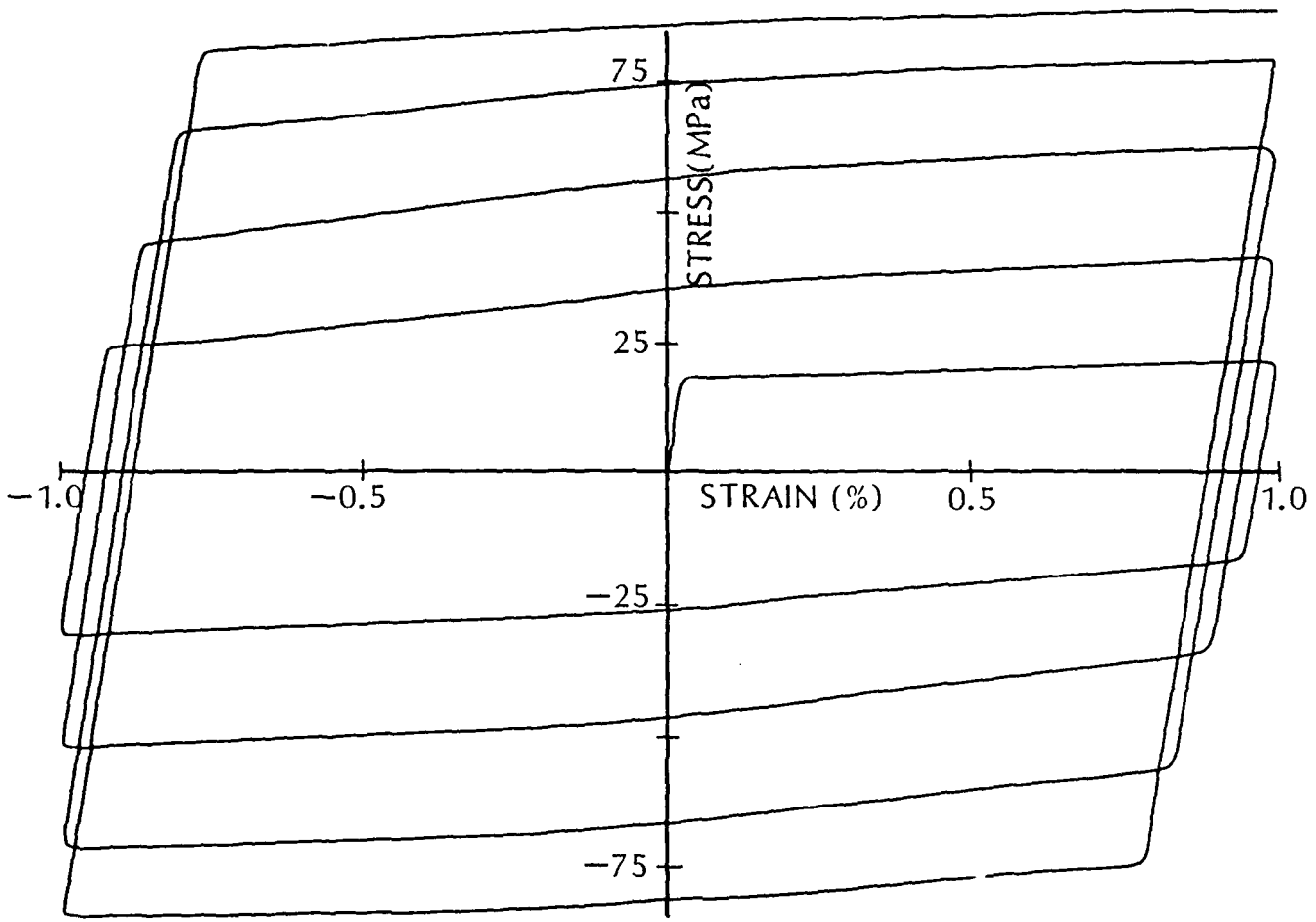

Figure 20 Cyclic Stress-Strain Curves for 1100 Aluminum for ± 1-Percent Strain (Bodner's Equations.)

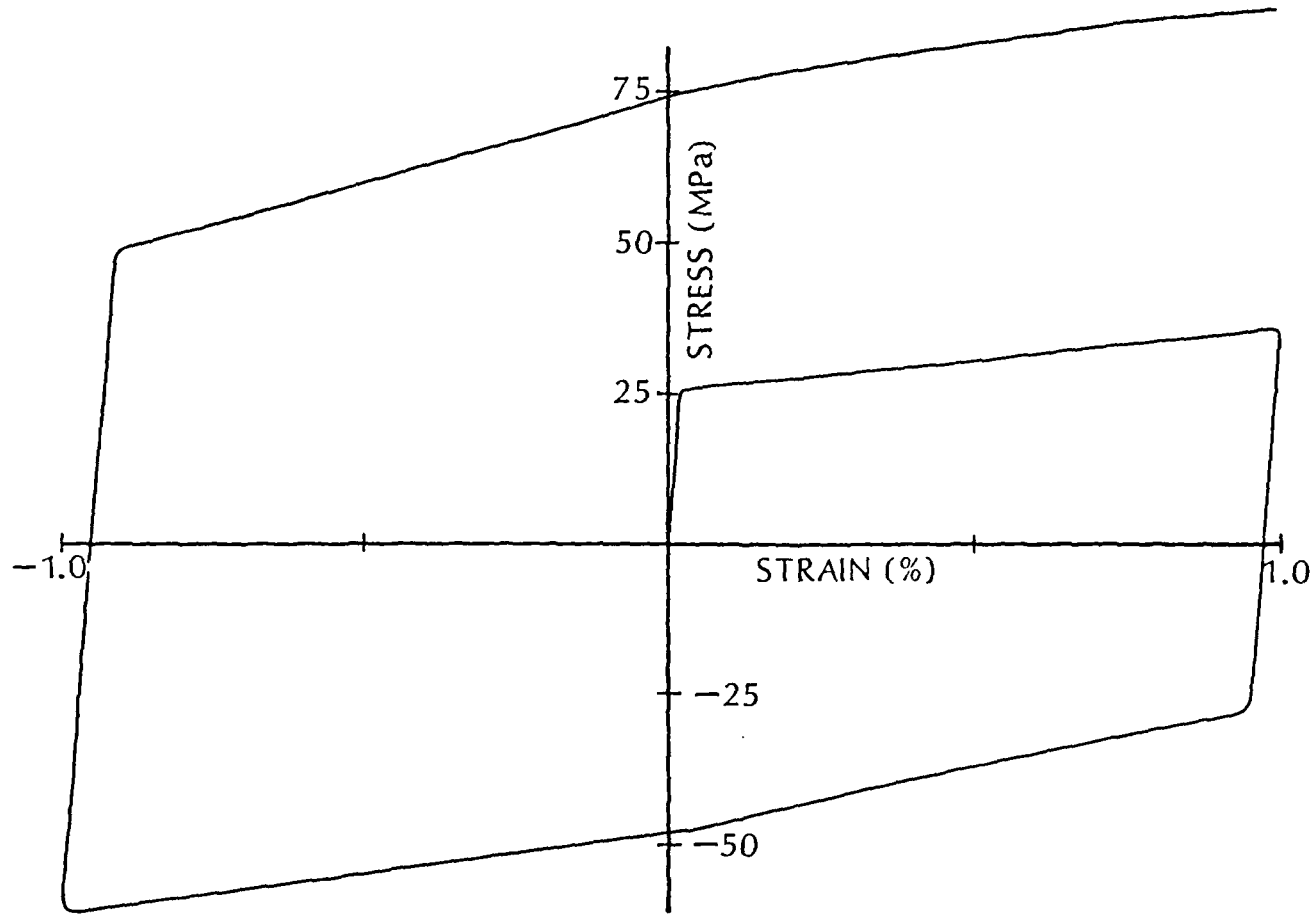

Figure 21 Cyclic Stress-Strain Curves for OFHC Copper for ± 1-Percent Strain (Bodner's Equations.)

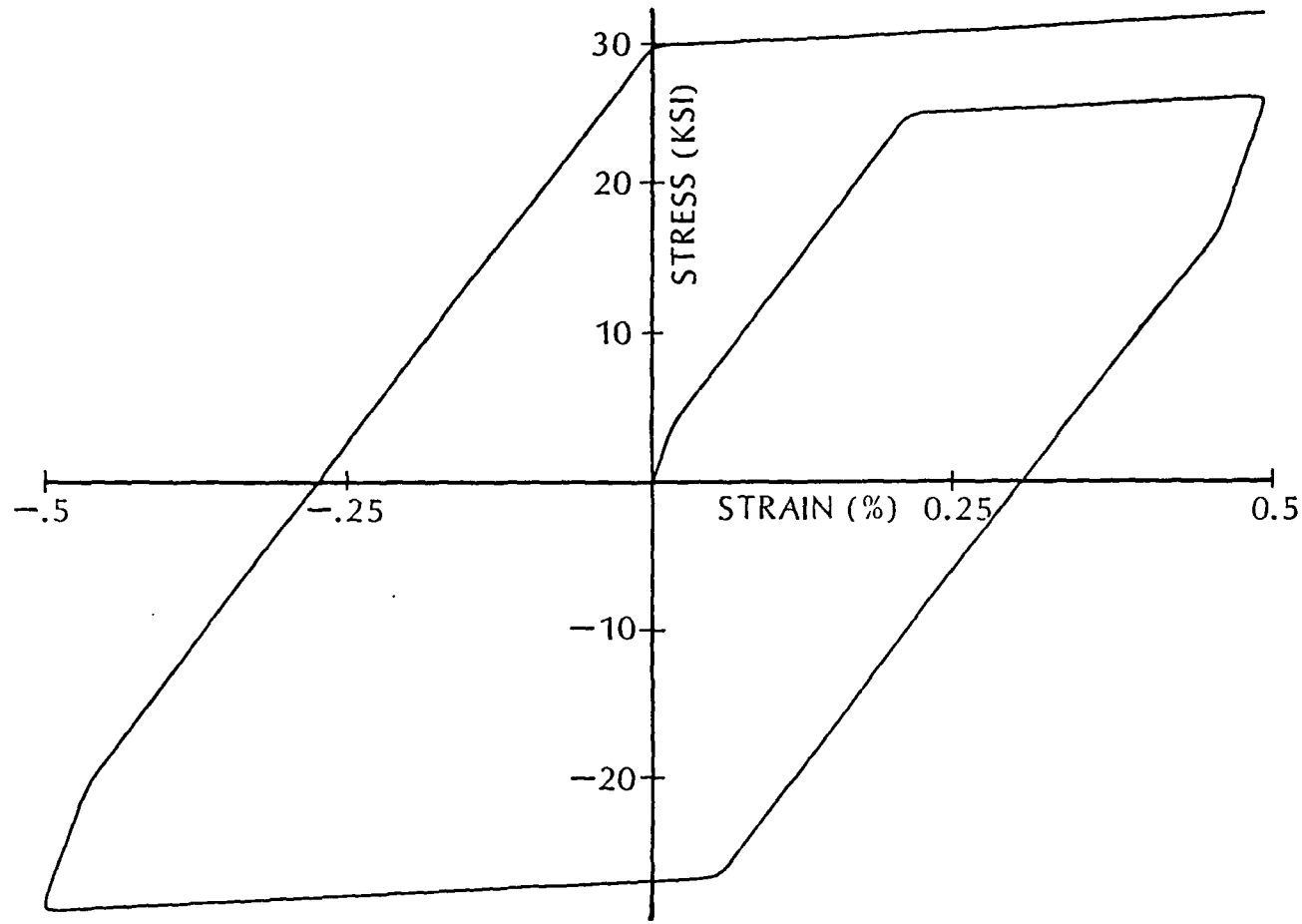

Figure 22 Cyclic Stress-Strain Curves for 304 Stainless Steel for ± 0.5-Percent Strain (Hart's Equations.)

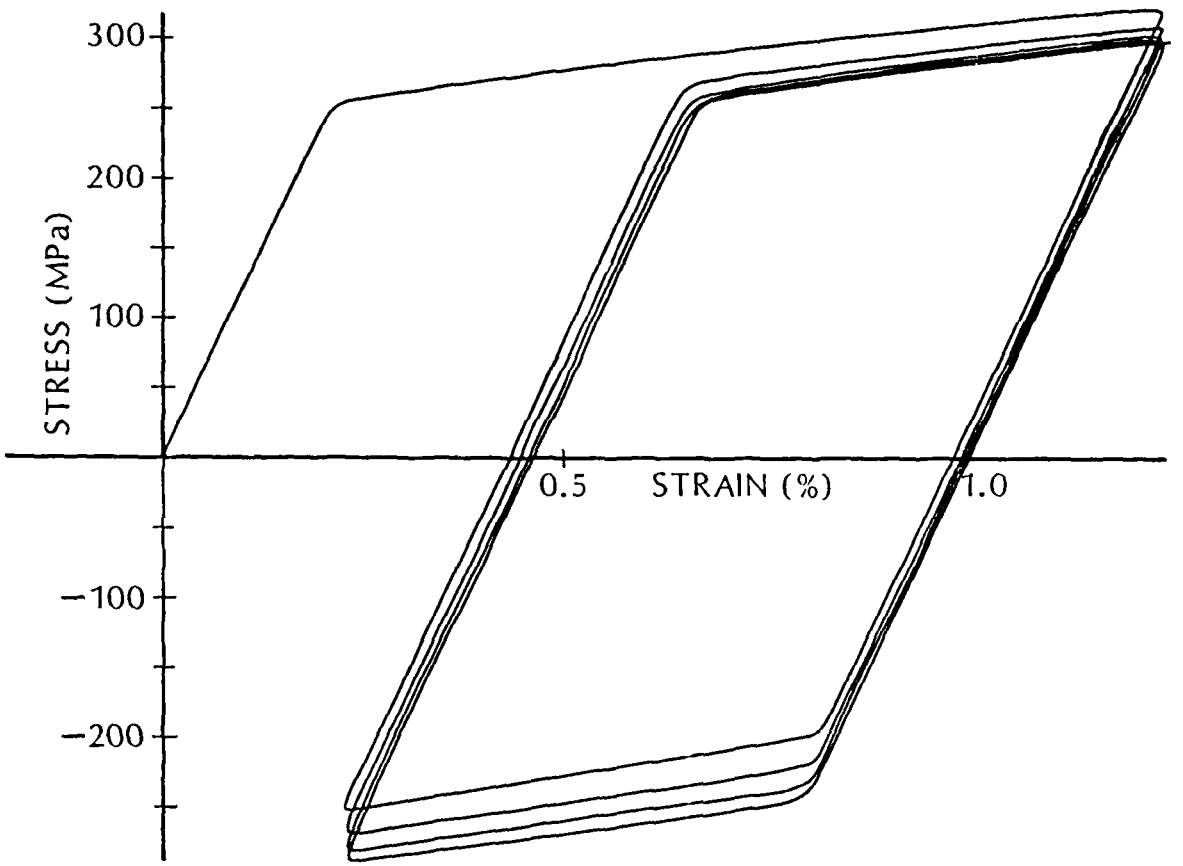

Figure 23 Computed Stress-Strain Curves for Titanium for Strain Controlled Cycling with Positive Strain Limits Showing Creep Relaxation (Bodner's Equations.)

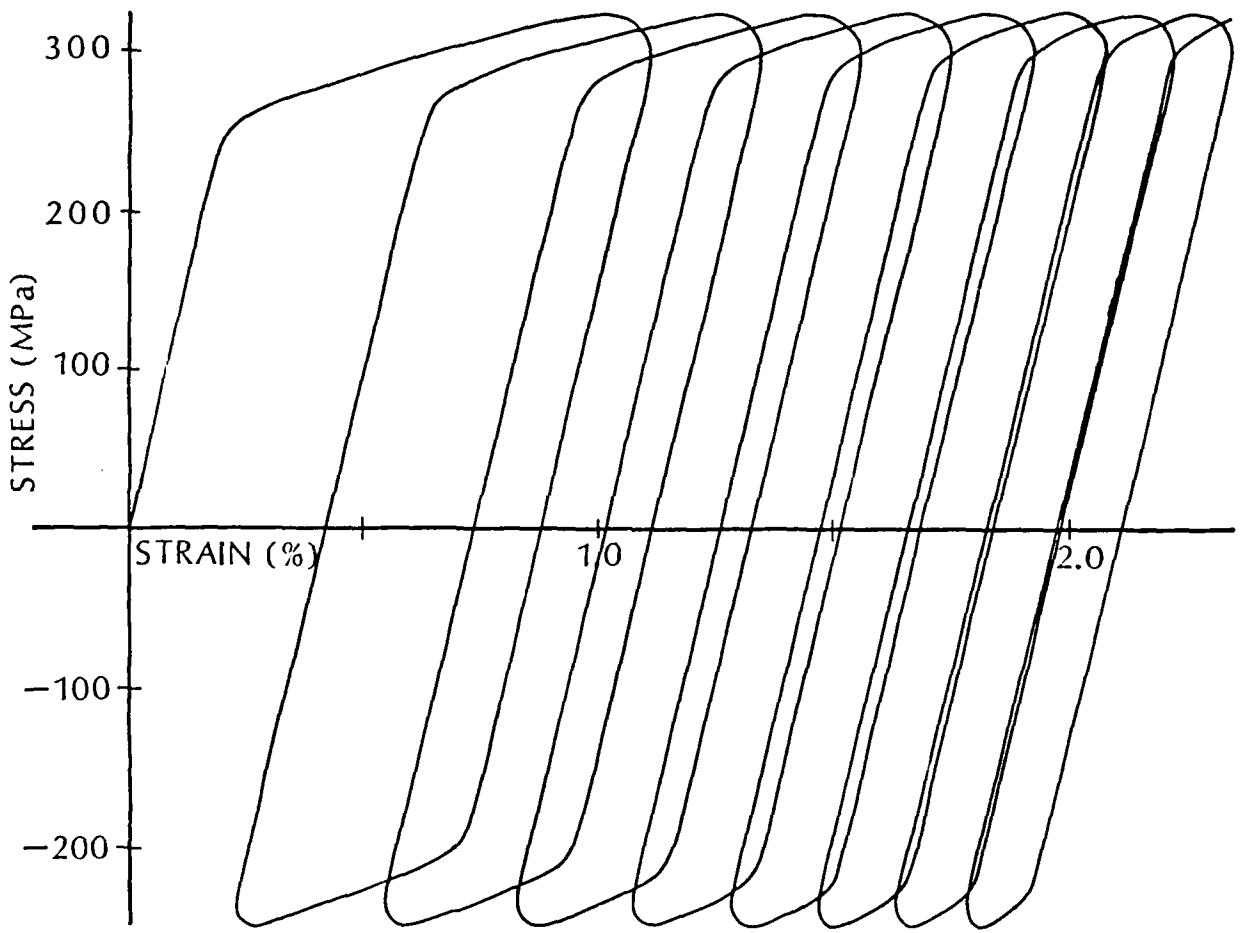

Figure 24 Computed Stress-Strain Curves for Titanium for Stress Controlled Cycling with a Positive Mean Stress Cyclic Creep (Bodner's Equations.)

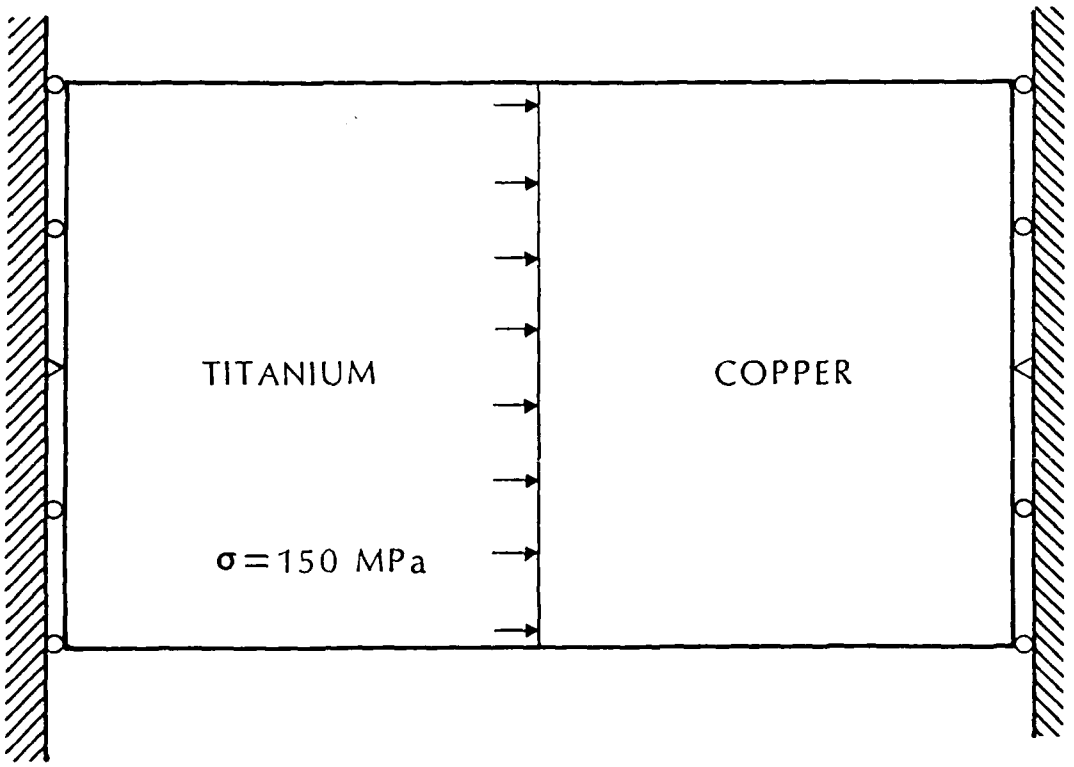

Figure 25 Composite Titanium-Copper Bar Loaded at the Material Interface.

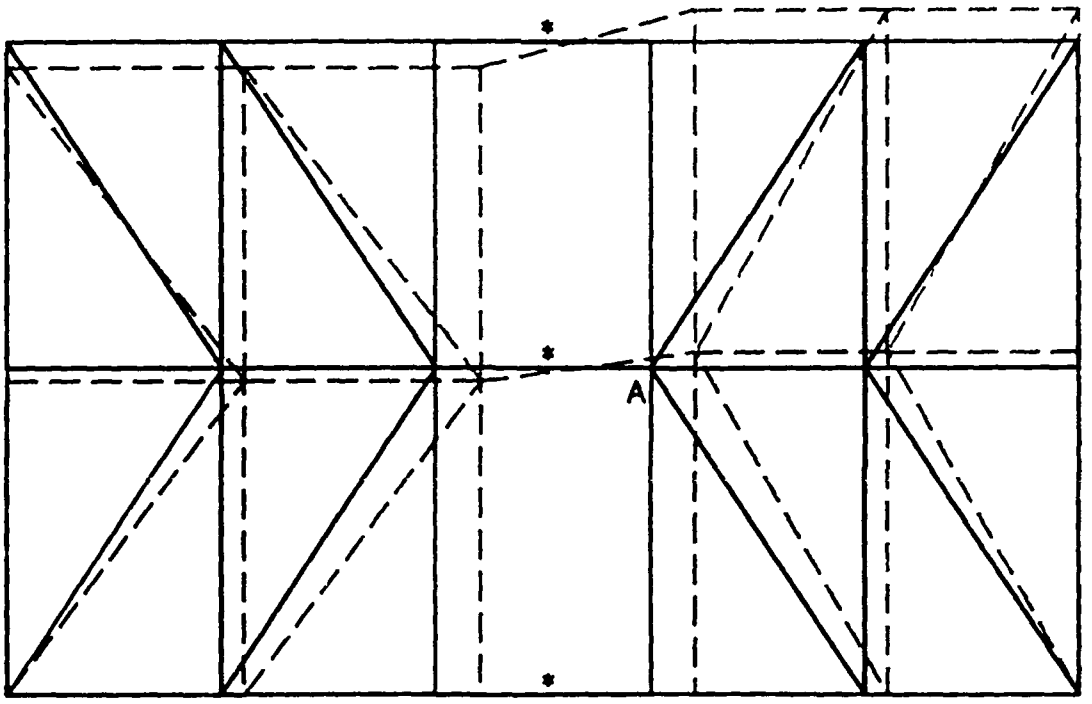

Figure 26 Original and Deformed Finite Element Mesh for a TI/Cu Composite Bar.

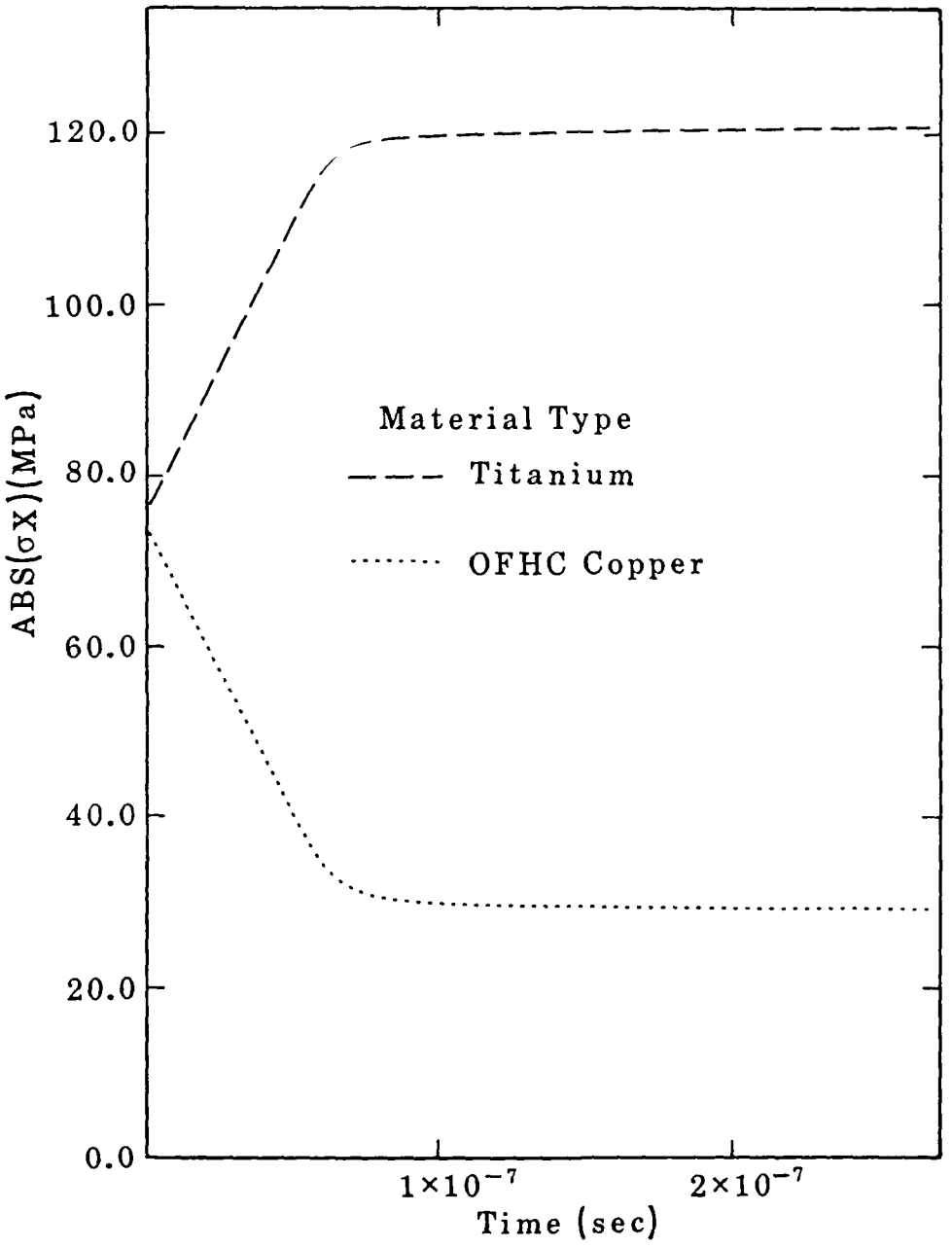

Figure 27 Stress Redistribution over Time for a TI/Cu Composite Bar.

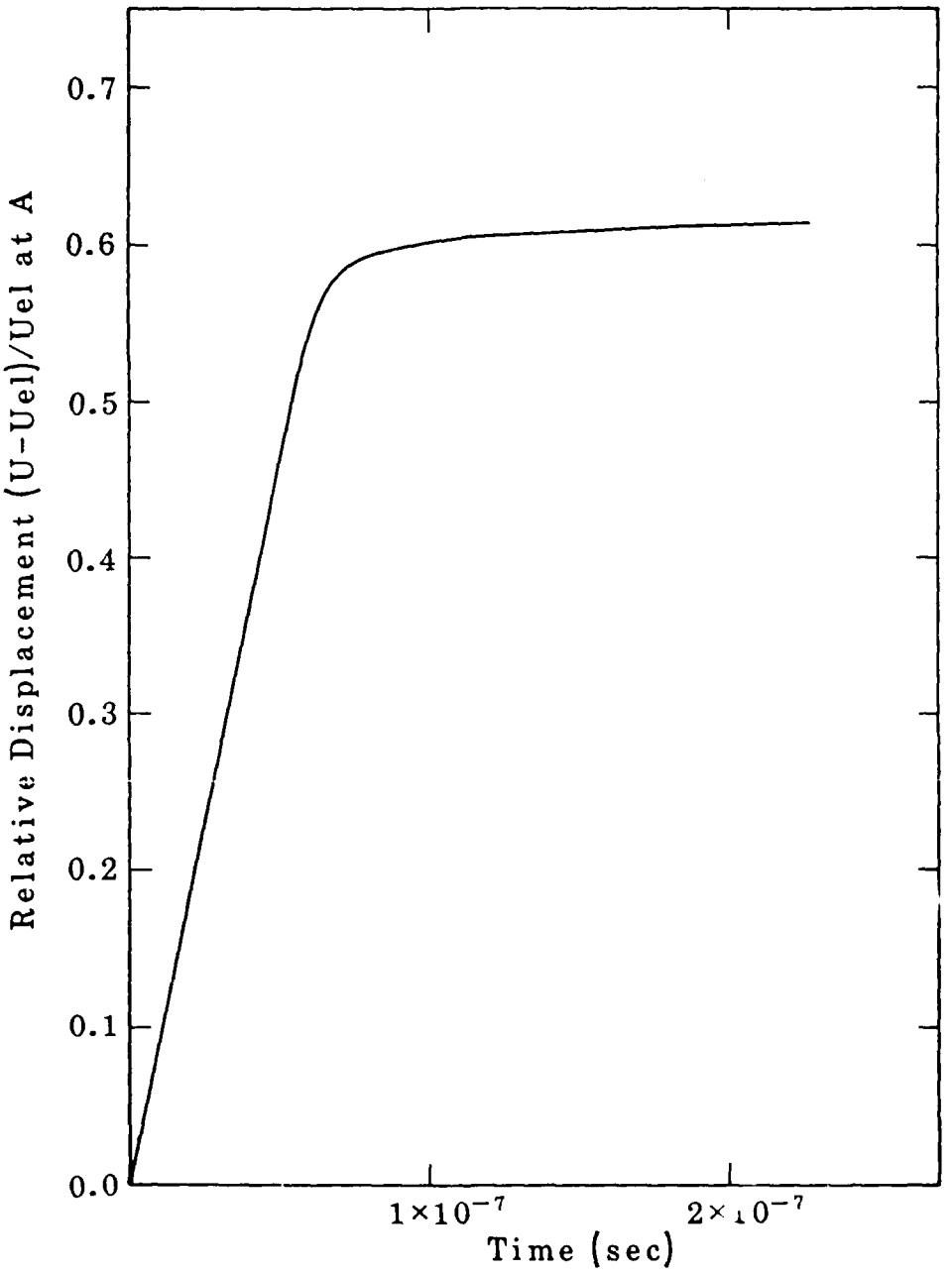

Figure 28 Relative Displacement over Time of the Material Interface for a TI/Cu Bar.

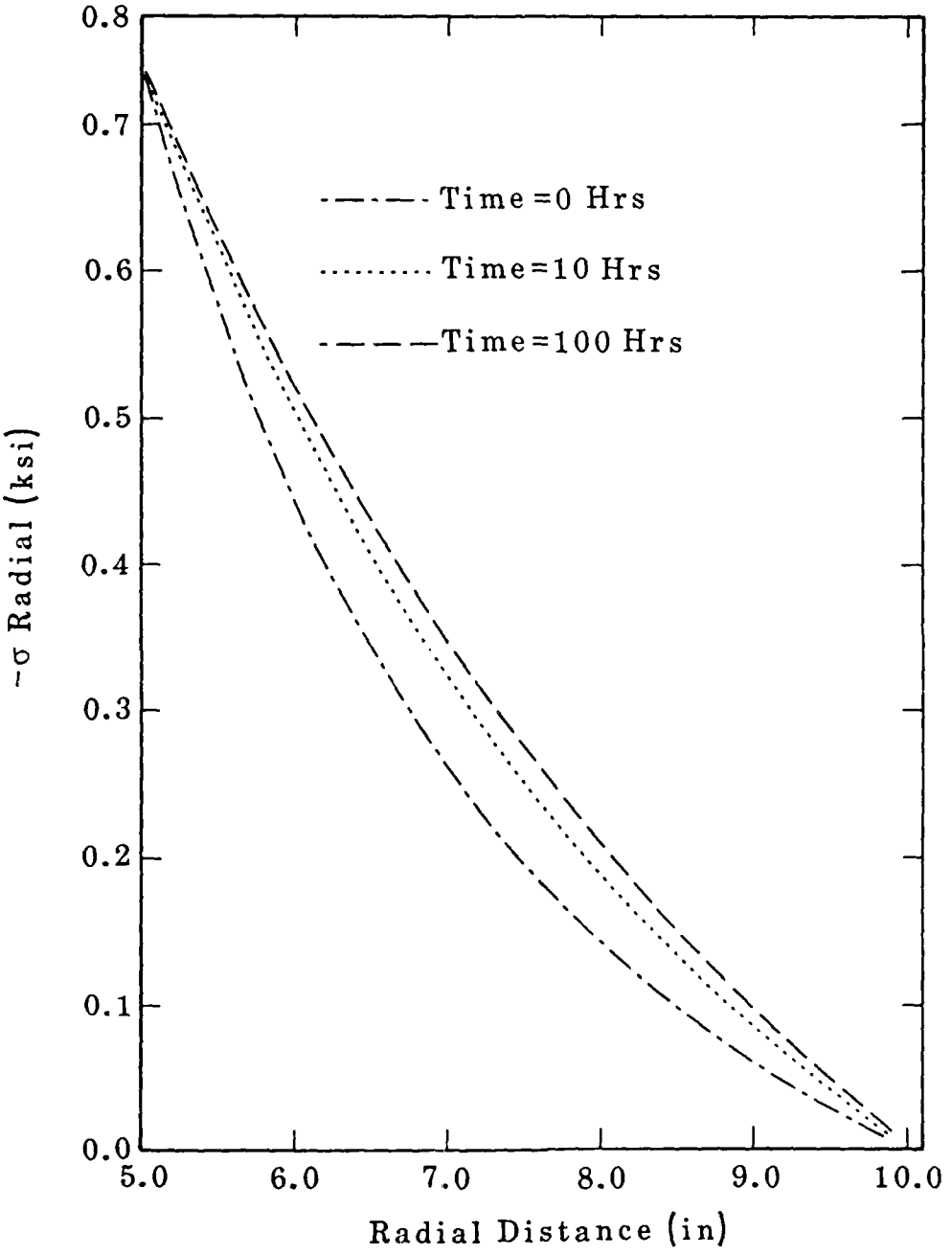

Figure 29 Variation of Radial Stress in a Creeping Cylinder in Plane Strain.

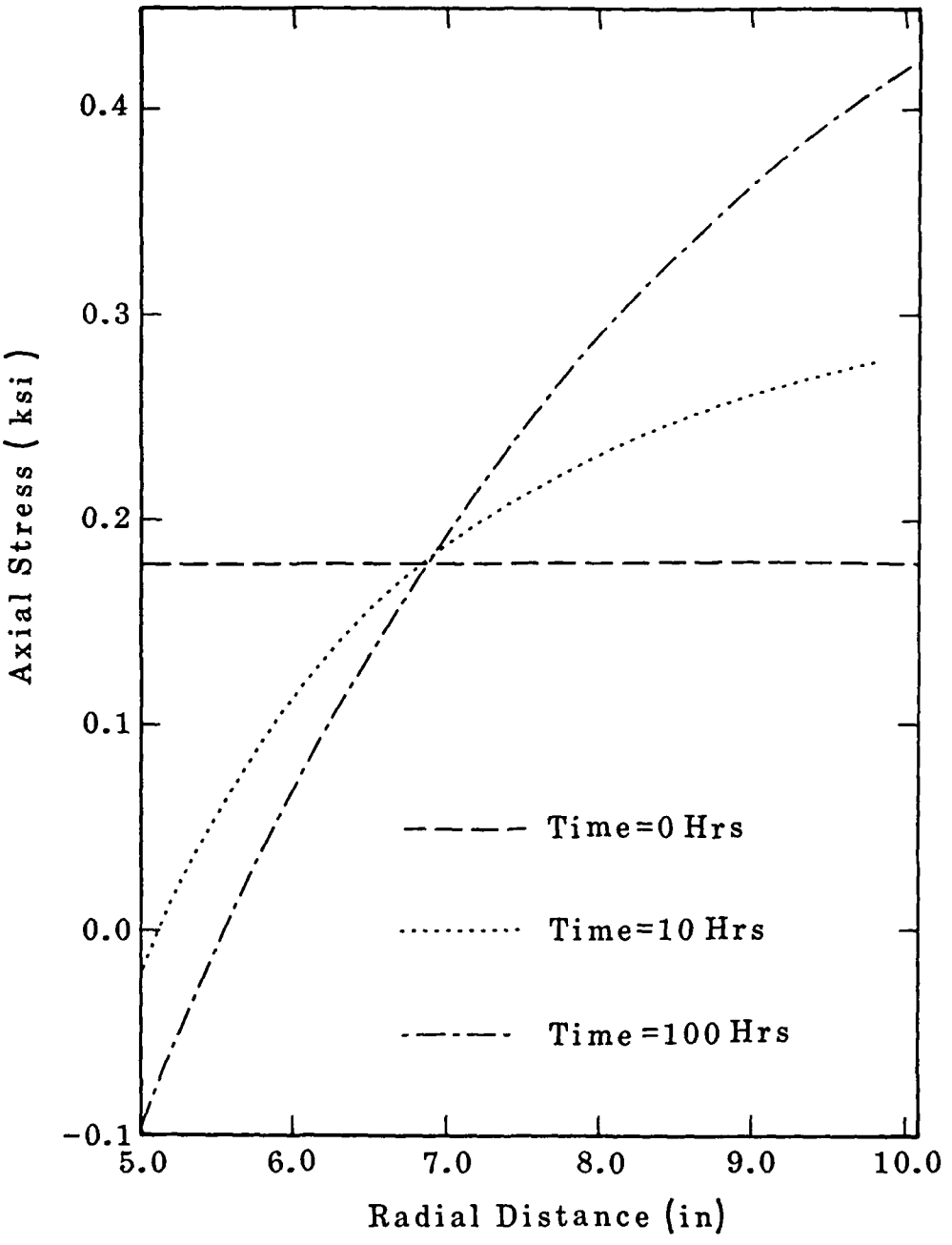

Figure 30 Variation of Axial Stress in a Creeping Cylinder in Plane Strain.

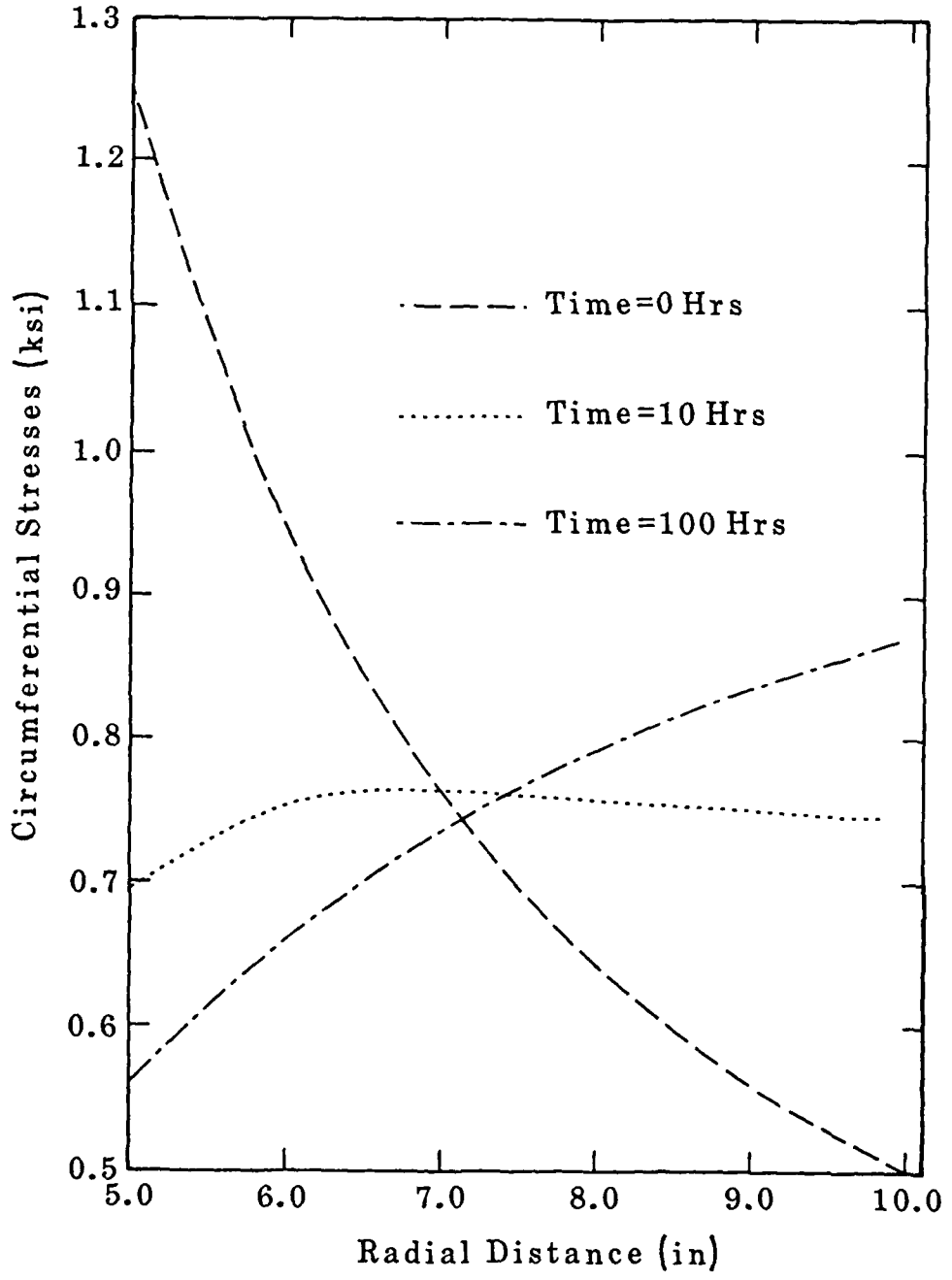

Figure 31 Variation of Circumferential Stress in a Creeping Cylinder in Plane Strain.

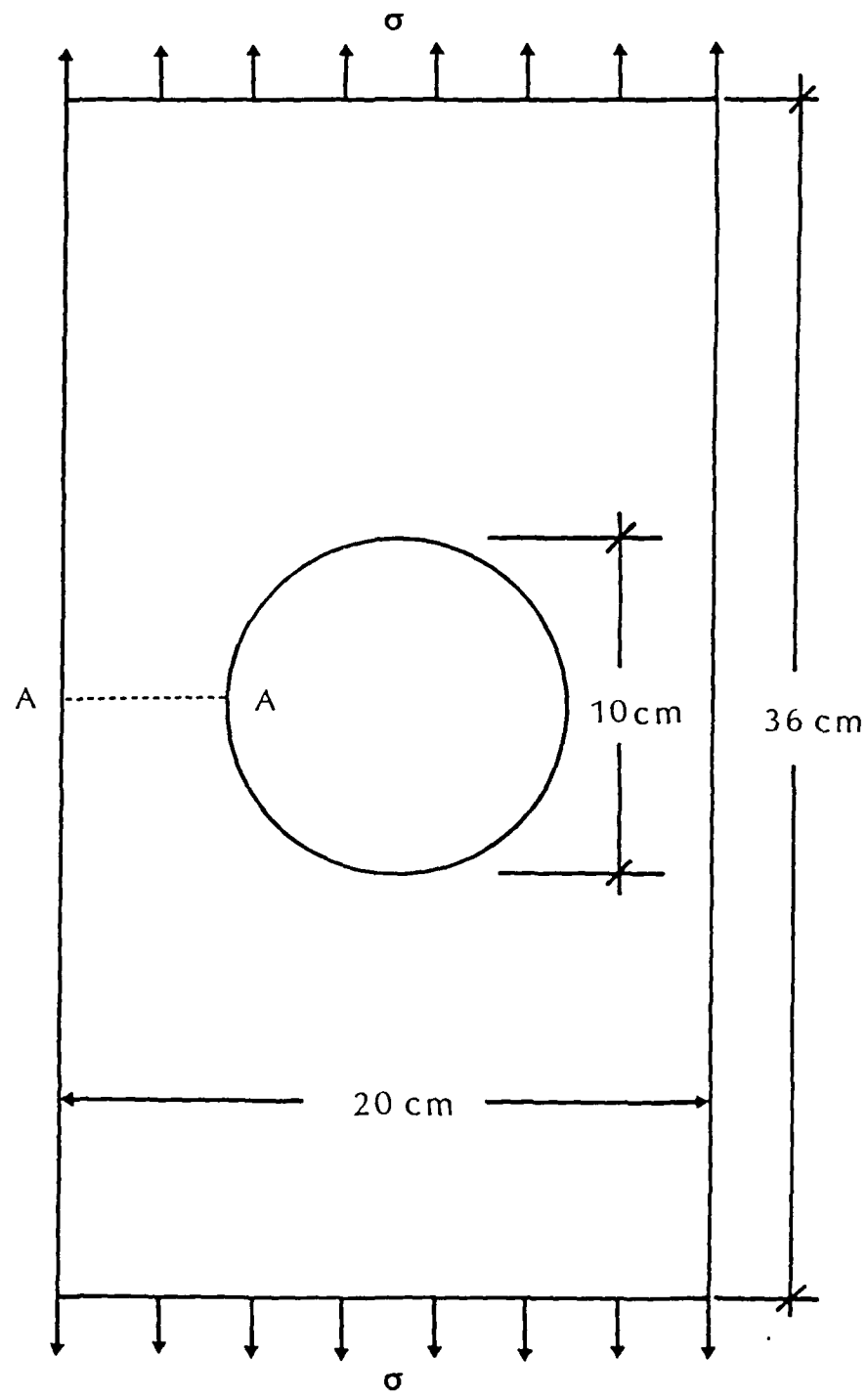

Figure 32 Perforated Tension Strip in Uniaxial Tension.

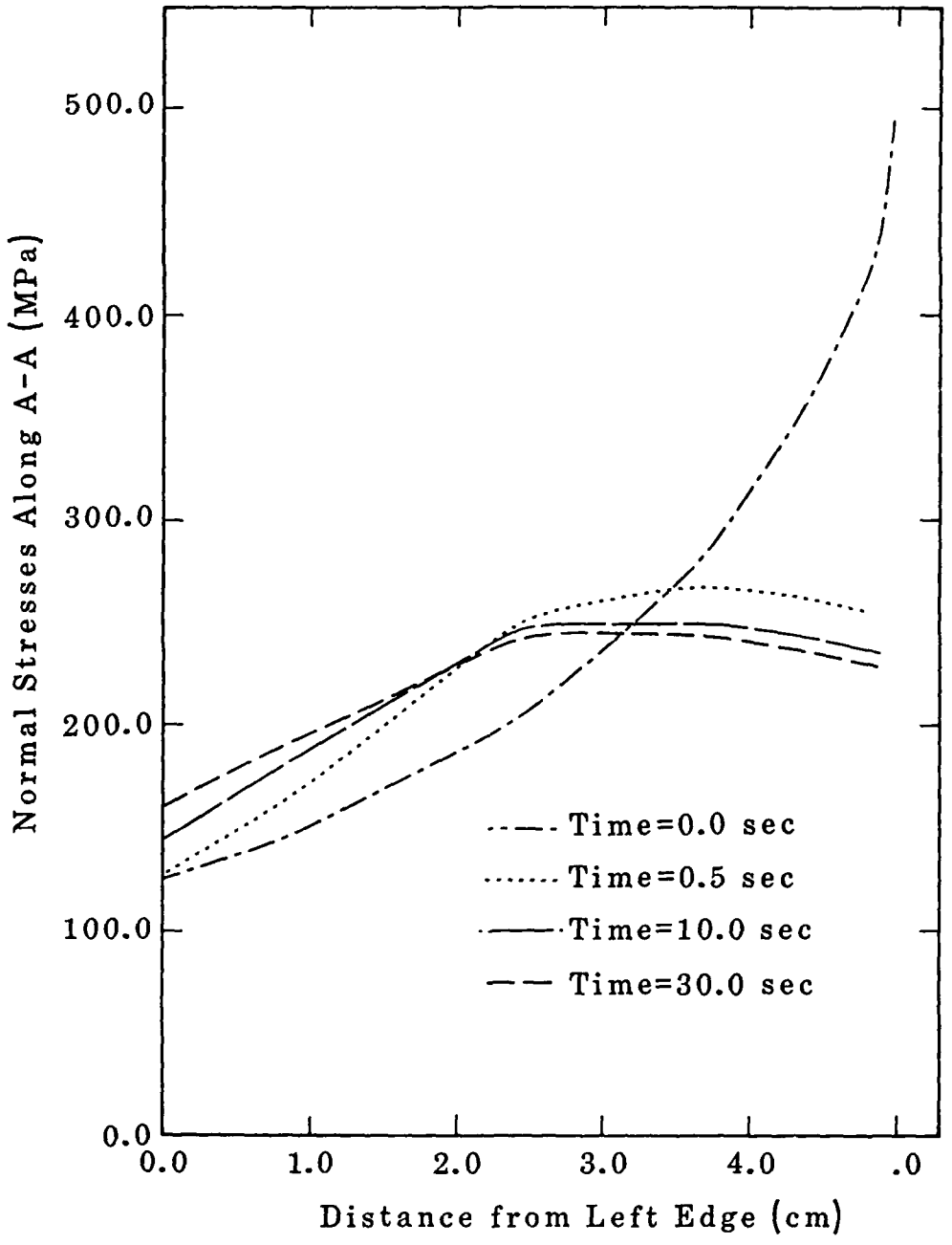

Figure 33 Normal Stress Distributions Along Section A-A in a Perforated Tension Strip.

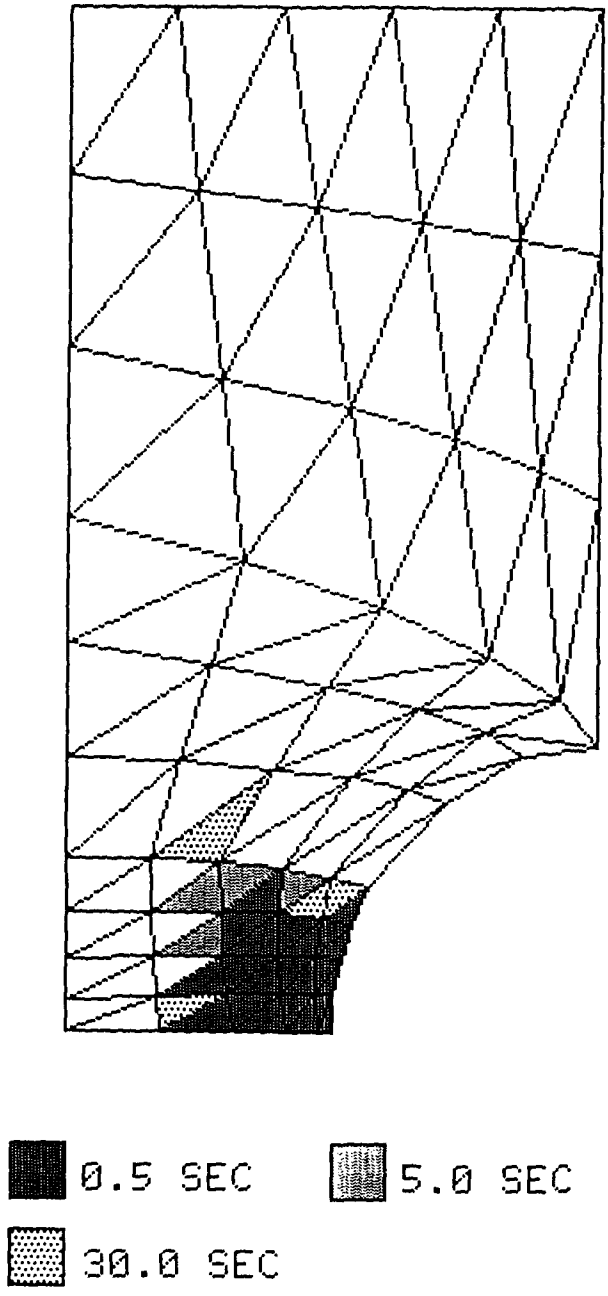

Figure 34 Time Dependent Regions of Nonelastic Deformation for a Perforated Tension Strip (Applied Stress = 100 Mpa).

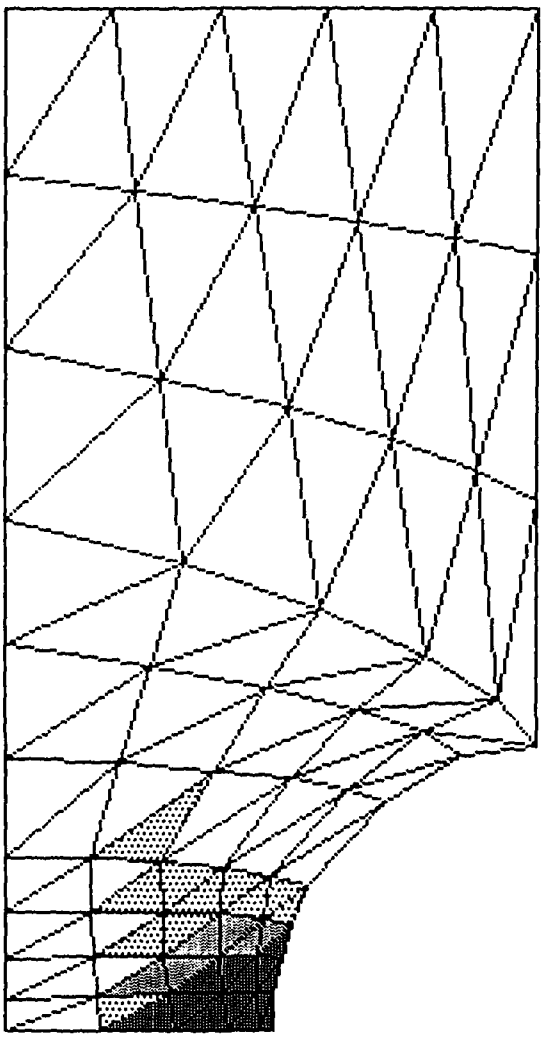

Figure 35 Regions of Equivalent Nonelastic Strain at 30 Seconds for a Perforated Tension Strip (Applied Stress = 100 Mpa).

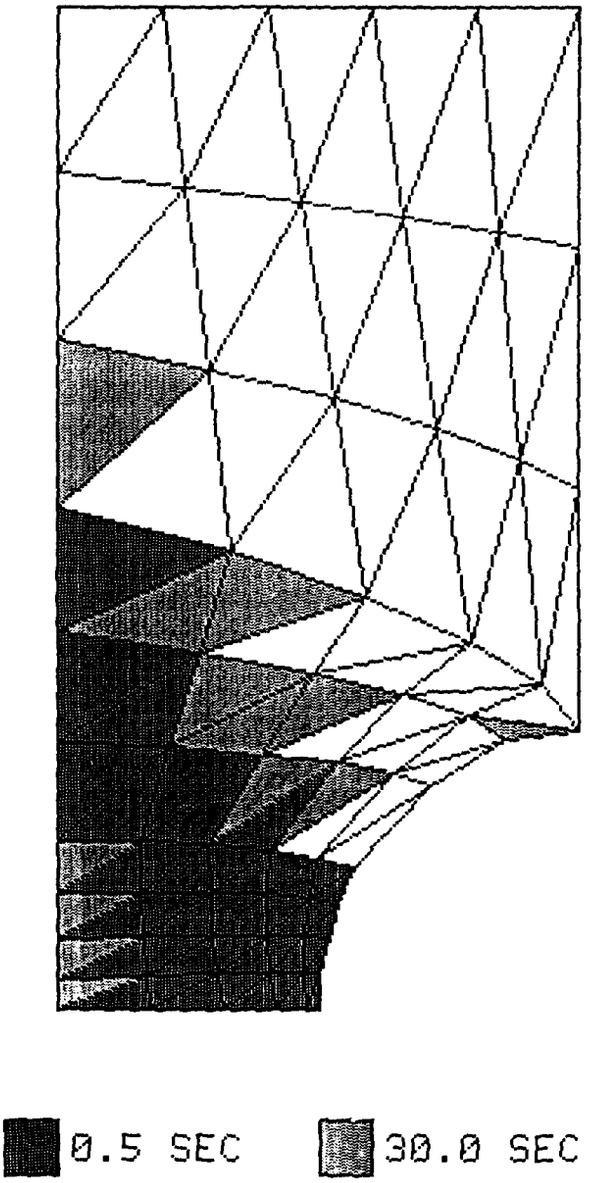

Figure 36 Time Dependent Regions of Nonelastic Deformation for a Perforated Tension Strip (Applied Stress = 125 Mpa).

REPORT DOCUMENTATION PAGE

READ INSTRUCTIONS BEFORE COMPLETING FORM

1. REPORT NUMBER	2. GOVT ACCESSION NO. NA; 3. RECIPIENT'S CATALOG NUMBER NA
4. TITLE (and Subtitle) NUMERICAL ANALYSIS OF A CLASS OF PROBLEMS IN THE MATHEMATICAL THEORY OF PLASTICITY AND DAMAGE	5. TYPE OF REPORT & PERIOD COVERED FINAL REPORT April 14, 1987-April 14,'89; 6. PERFORMING ORG. REPORT NUMBER
7. AUTHOR(s) J. Tinsley Oden	8. CONTRACT OR GRANT NUMBER(s) DAAL03-86-K-0043
9. PERFORMING ORGANIZATION NAME AND ADDRESS Texas Institute for Computational Mechanics, The University of Texas at Austin, Asutin, TX 78712-1085	10. PROGRAM ELEMENT, PROJECT, TASK AREA & WORK UNIT NUMBERS NA
11. CONTROLLING OFFICE NAME AND ADDRESS U. S. Army Research Office, P. O. Box 12211, Research Triangle Park, NC 27709-2211	12. REPORT DATE June 14, 1989; 13. NUMBER OF PAGES
14. MONITORING AGENCY NAME & ADDRESS(if different from Controlling Office)	15. SECURITY CLASS. (of this report) UNCLASSIFIED; 15a. DECLASSIFICATION/DOWNGRADING SCHEDULE

16. DISTRIBUTION STATEMENT (of this Report)

Approved for public release; distribution unlimited.

17. DISTRIBUTION STATEMENT (of the abstract entered in Block 20, if different from Report)

NA

18. SUPPLEMENTARY NOTES

The view, opinions and/or findings contained in this report are those of the author(s) and should not be construed as an official Department of the Army position, policy, or decision, unless so designated by other documentation.

19. KEY WORDS (Continue on reverse side if necessary and identify by block number)

Plasticity
Damage

20. ABSTRACT (Continue on reverse side if necessary and identify by block number)

A fairly detailed study of many existing theories of damage was conducted. One conclusion, perhaps not surprising, is that there is poor agreement among researchers in this field as to what constitutes a physically correct measure of damage in both brittle and ductile materials. For anisotropic damage, scalar-, vector-, and tensor-valued damage variables have been proposed for materials that undergo elastic and elastoplastic deformation. Numerous deficiencies and inconsistencies, both physical and mathematical, exist

20. ABSTRACT CONTINUED

in some of the more publicized theories. In general, the field is still quite immature and the general acceptance of basic principles and definition of terms have neither the experimental support nor the consensus of workers in the field to form the nucleus of a general mathematical theory.

The field of isotropic damage is in somewhat better shape. In the present study, a critical look at the subject was conducted and several new results were produced. In addition to providing arguments that some prevailing theories are based on mathematically-unsound assumptions, a consistent theory for isotropic damage was identified which with proper choices of parameters, could be used to produce results consistent with experimental data. An interesting and possibly new result of this study was the establishment of actual bounds on the moduli and Poisson's ration for damaged isotropic elastic solid.

In addition, existence and uniqueness theorems were proven for model boundary-value problems in isotropic damage theoery. These results were obtained using rather standard techniques. To extend them to more general theories of damage and plasticity appears to be far outside the reach of existing mathematical theories.

A second part of the study focused on developing numerical models of damage in elastic- and plastic materials and in developing test codes for numerical experimentation. In this phase of the work, finite element models of damage in two-dimensional structures were developed and several test problems were solved. The most challenging feature of this portion of the effort was the development of robust numerical schemes for integrating the evolution equations of damage and rate-dependency plasticity. Briefly, a new robust implicit scheme was developed which proved to be very effective in treating cyclic problems in damage simulations. Studies on error estimation and stability or these schemes for nonlinear problems remains a topic for future work.